

**Discovery of (10*R*)-7-amino-12-fluoro-2,10,16-trimethyl-15-oxo-10,15,16,17-tetrahydro-2*H*-8,4-(metheno)pyrazolo[4,3-*h*][2,5,11]benzoxadiazacyclotetradecine-3-carbonitrile (PF-06463922), a macrocyclic inhibitor of ALK/ROS1 with pre-clinical brain exposure and broad spectrum potency against ALK-resistant mutations**

Ted W Johnson, Paul F Richardson, Simon Bailey, Alexei Brooun, Benjamin J. Burke, Michael R. Collins, J Jean Cui, Judith G Deal, Ya-Li Deng, Dac M. Dinh, Lars D. Engstrom, Mingying He, Jacqui E. Hoffman, Robert L. Hoffman, Qinhua Huang, John Kath, Robert S Kania, Hieu Lam, Justine L. Lam, Phuong T. Le, Laura Lingardo, Wei Liu, Michele A McTigue, Cynthia L. Palmer, Neal W Sach, Tod Smeal, Graham L. Smith, Albert E. Stewart, Sergei L Timofeevski, Huichun Zhu, Jinjiang Zhu, Helen Y Zou, and Martin P. Edwards

*J. Med. Chem.*, **Just Accepted Manuscript** • Publication Date (Web): 13 May 2014

Downloaded from <http://pubs.acs.org> on May 25, 2014

**Just Accepted**

“Just Accepted” manuscripts have been peer-reviewed and accepted for publication. They are posted online prior to technical editing, formatting for publication and author proofing. The American Chemical Society provides “Just Accepted” as a free service to the research community to expedite the dissemination of scientific material as soon as possible after acceptance. “Just Accepted” manuscripts appear in full in PDF format accompanied by an HTML abstract. “Just Accepted” manuscripts have been fully peer reviewed, but should not be considered the official version of record. They are accessible to all readers and citable by the Digital Object Identifier (DOI®). “Just Accepted” is an optional service offered to authors. Therefore, the “Just Accepted” Web site may not include all articles that will be published in the journal. After a manuscript is technically edited and formatted, it will be removed from the “Just Accepted” Web site and published as an ASAP article. Note that technical editing may introduce minor changes to the manuscript text and/or graphics which could affect content, and all legal disclaimers and ethical guidelines that apply to the journal pertain. ACS cannot be held responsible for errors or consequences arising from the use of information contained in these “Just Accepted” manuscripts.

1  
2  
3  
4  
5  
6  
7  
8  
9  
10  
11  
12  
13  
14  
15  
16  
17  
18  
19  
20  
21  
22  
23  
24  
25  
26  
27  
28  
29  
30  
31  
32  
33  
34  
35  
36  
37  
38  
39  
40  
41  
42  
43  
44  
45  
46  
47  
48  
49  
50  
51  
52  
53  
54  
55  
56  
57  
58  
59  
60

|  |   |
|--|---|
|  | Zou, Helen; Pfizer,<br>Edwards, Martin; Pfizer, |
|  |   |

SCHOLARONE™  
Manuscripts

1  
2  
3  
4  
5  
6  
7  
8  
9  
10  
11  
12  
13  
14  
15  
16  
17  
18  
19  
20  
21  
22  
23  
24  
25  
26  
27  
28  
29  
30  
31  
32  
33  
34  
35  
36  
37  
38  
39  
40  
41  
42  
43  
44  
45  
46  
47  
48  
49  
50  
51  
52  
53  
54  
55  
56  
57  
58  
59  
60

Discovery of (10*R*)-7-amino-12-fluoro-2,10,16-trimethyl-15-oxo-10,15,16,17-tetrahydro-2*H*-8,4-(metheno)pyrazolo[4,3-*h*][2,5,11]benzoxadiazacyclotetradecine-3-carbonitrile (PF-06463922), a macrocyclic inhibitor of ALK/ROS1 with pre-clinical brain exposure and broad spectrum potency against ALK-resistant mutations

*Ted W. Johnson, \* Paul F. Richardson, \* Simon Bailey, Alexei Brooun, Benjamin J. Burke, Michael R. Collins, J. Jean Cui, Judith G. Deal, Ya-Li Deng, Dac Dinh, Lars D. Engstrom, Mingying He, Jacqui Hoffman, Robert L. Hoffman, Qinhua Huang, Robert S. Kania, John C. Kath, Hieu Lam, Justine L. Lam, Phuong T. Le, Laura Lingardo, Wei Liu, Michele McTigue, Cynthia L. Palmer, Neal W. Sach, Tod Smeal, Graham L. Smith, Albert E. Stewart, Sergei Timofeevski, Huichun Zhu, Jinjiang Zhu, Helen Y. Zou, Martin P. Edwards*

1  
2  
3  
4  
5 La Jolla Laboratories, Pfizer Worldwide Research and Development, 10770 Science Center  
6  
7 Drive, San Diego, California, 92121, United States.  
8  
9  
10

## 11 12 13 ABSTRACT

14  
15 Although crizotinib demonstrates robust efficacy in ALK positive NSCLC patients, progression  
16 during treatment eventually develops. Resistant patient samples revealed a variety of point  
17 mutations in the kinase domain of ALK, including the L1196M gatekeeper mutation. In addition,  
18 some patients progress due to cancer metastasis in the brain. Using structure based drug design,  
19 LipE, and physical property based optimization, highly potent macrocyclic ALK inhibitors were  
20 prepared with good ADME, low propensity for Pgp-mediated efflux and good passive  
21 permeability. These structurally unusual macrocyclic inhibitors were potent against wild-type  
22 ALK and clinically reported ALK kinase domain mutations. Significant synthetic challenges  
23 were overcome, utilizing novel transformations to enable the use of these macrocycles in drug  
24 discovery paradigms. This work led to the discovery of **8k** (PF-06463922), combining broad  
25 spectrum potency, CNS ADME and a high degree of kinase selectivity.  
26  
27  
28  
29  
30  
31  
32  
33  
34  
35  
36  
37  
38  
39  
40  
41  
42

## 43 44 INTRODUCTION

45  
46 Anaplastic lymphoma kinase (ALK) is a member of the insulin receptor (IR) sub-family of  
47 receptor tyrosine kinases. It is primarily expressed in adult brain tissue and plays an important  
48 role in the development and function of the nervous system.<sup>1</sup> ALK knockout mice live a full life-  
49 span without obvious abnormalities, but are described as having an “anti-depressive”  
50 phenotype.<sup>2</sup>  
51  
52  
53  
54  
55  
56  
57  
58  
59  
60

1  
2  
3 The ALK name was derived from the discovery of the driving role this kinase plays in  
4 anaplastic large cell lymphoma (ALCL), a subtype of non-Hodgkin lymphoma, in which the  
5 t(2;5)(p32;q35) chromosomal translocation involving the *ALK* gene was first described.<sup>3</sup> The  
6 finding that this translocation results in the fusion of nucleophosmin (NPM) to a truncated form  
7 of anaplastic lymphoma kinase (ALK) led to the first suggestion that this fusion could result in a  
8 constitutively active cytoplasmic tyrosine kinase that could be acting as an oncogenic driver.<sup>4</sup>  
9 Subsequently, other ALK-fusion proteins have been identified in diffuse large B-cell lymphoma  
10 (DLBCL),<sup>5</sup> inflammatory myofibroblastic tumors (IMT)<sup>6</sup> and non-small-cell lung carcinoma  
11 (NSCLC).<sup>7</sup> Over the last 20 years, more than a dozen fusion partners for ALK have been  
12 identified in a variety of cancer types (typically rare childhood cancers). Like NPM, the fusion  
13 partners replace the ALK protein domains responsible for ligand binding and crossing the  
14 membrane with a domain that results in constitutive dimerization/oligomerization activation of  
15 ALK tyrosine kinase in the cytoplasm. However, it was the discovery of a fusion of echinoderm  
16 microtubule associated protein-like 4 with ALK (EML4-ALK) in 3-7% of NSCLC patients that  
17 enabled the rapid clinical development and validation of ALK inhibitors as a viable, new cancer  
18 therapy.<sup>7c,7d</sup> In addition to chromosomal translocations leading to fusion-proteins, amplification  
19 of *ALK* and activating point mutations in full length protein have been described in  
20 neuroblastoma,<sup>8</sup> inflammatory breast cancer<sup>9</sup> and ovarian cancer patients.<sup>10</sup> Similar to *ALK*, c-ros  
21 oncogene 1 (*ROS1*) chromosomal translocations define a unique, albeit smaller, subset of non-  
22 small-cell lung cancers.<sup>11</sup>

23  
24  
25  
26  
27  
28  
29  
30  
31  
32  
33  
34  
35  
36  
37  
38  
39  
40  
41  
42  
43  
44  
45  
46  
47  
48  
49  
50  
51  
52  
53  
54  
55  
56  
57  
58  
59  
60  
Compound **1** (PF-02341066, crizotinib),<sup>12</sup> a MET, ALK and ROS1 kinase inhibitor at  
clinically relevant drug exposures, was in early clinical trials when the EML4-ALK translocation  
was identified.<sup>13</sup> The marked efficacies from two clinical trials led to US Food and Drug

1  
2  
3 Administration (FDA) approval in 2011 based on an objective response rate of approximately  
4  
5 60% and progression-free survival (PFS) times of approximately 10 months.<sup>14</sup> Xalkori was the  
6  
7 first ALK inhibitor approved by the US FDA as a first-line treatment for ALK-positive lung  
8  
9 cancer patients.  
10

11  
12 Although compound **1** demonstrates initial robust efficacy in ALK-positive tumors, patients  
13  
14 eventually develop resistance. Emerging data from the analysis of patient tumor tissue collected  
15  
16 after progression suggests that resistance develops through point mutations in the *ALK* gene,  
17  
18 which may be as frequent as that seen in the EGFR setting (gatekeeper mutation frequency over  
19  
20 40%).<sup>15</sup> Additionally, a common site of metastases in NSCLC patients is in the brain where  
21  
22 current standard of care (SOC) and recent experimental agents have only limited effectiveness,  
23  
24 thus identifying an area of unmet medical need. A sample taken at steady state from a single  
25  
26 patient at the recommended 250 mg BID dose of compound **1** showed a CSF to free plasma ratio  
27  
28 of 0.03.<sup>16</sup> The high level of asymmetric distribution indicates poor blood-brain barrier  
29  
30 penetration of the drug.  
31  
32  
33  
34  
35

36  
37 Approximately 200,000 brain metastases (BM) are diagnosed annually in the United States,  
38  
39 accounting for 20% of cancer mortality. Across tumor types, lung cancers and breast cancers  
40  
41 constitute the majority of brain metastases, with the next most prevalent being melanoma.<sup>17</sup>  
42  
43 Among the cohort of lung cancer patients with brain metastases, 10–25% of patients exhibit  
44  
45 brain metastases at diagnosis, another 40–50% during the course of disease, and more at  
46  
47 autopsy.<sup>18</sup> Overall, patients presenting metastatic brain cancer have a poor prognosis with a  
48  
49 median survival of 2.5 months,<sup>19</sup> which may be due partly to the poor blood-brain-barrier (BBB)  
50  
51 permeability of the drugs developed for treating systemic disease. Treatment of peripheral  
52  
53  
54  
55  
56  
57  
58  
59  
60

disease with CNS excluded drugs may extend progression free survival times, but could enhance the proportion of patient mortality due to uncontrolled brain metastases.

Recently, several inhibitors of ALK have become a new and promising class of therapeutics for treatment-naïve and relapsed ALK-positive NSCLC patients, highlighted by AP26113 (Ariad; undisclosed structure exemplified as **2**),<sup>20</sup> **3** (CH5424802, Roche/Chugai),<sup>21</sup> **4** (ASP3026, Astellas),<sup>22</sup> and **5** (LDK378, Novartis)<sup>23</sup> (Figure 1). The clinical impact on metastasis in the brain and relation to preclinical CNS exposure or brain tumor models are not well-established for these compounds.

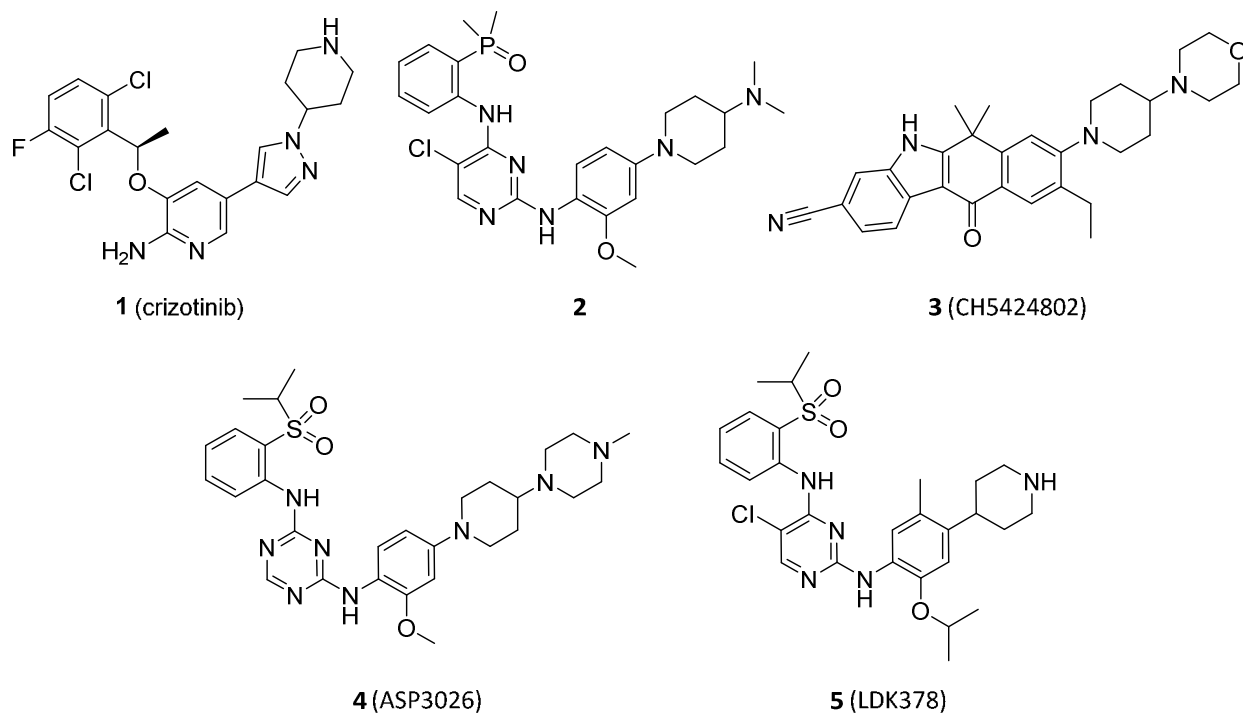


**Figure 1.** Structures of ALK inhibitors marketed or currently in the clinic.

## RESULTS AND DISCUSSION

**In vitro resistance.** Compound **1** phospho-ALK  $IC_{50}$  values in NIH-3T3 cell lines engineered with mutations reported from the clinic have been previously described.<sup>24</sup> The mutant cell  $IC_{50}$

1  
2  
3 data for compound **1** ranged from 165-3039 nM, which represented a 2 to 38-fold shift relative to  
4 wt potency (pALK cell IC<sub>50</sub> 80 nM) in the same engineered line.  
5  
6

7  
8 **Objectives.** The goal of this next generation ALK inhibitor program was to develop a small  
9 molecule inhibitor that combined CNS exposure with broad spectrum ALK potency. A  
10 compound with these properties has potential utility in the treatment of patients who exhibit  
11 tumor progression, overcoming both resistance mutations and brain metastases.  
12  
13  
14  
15

16  
17 By avoiding transporter-mediated efflux at the BBB and tumor cell surface, the increased CNS  
18 availability of this next generation inhibitor could provide significant efficacy benefits. The  
19 benefits include higher free brain and tumor intracellular concentrations for better target  
20 modulation, critical for patients who relapse due to brain metastases or over-expression of efflux  
21 transporters in tumor cells. To mitigate cell toxicity associated with off-target activities and  
22 improve therapeutic indices, a high degree of kinase selectivity was required to avoid potential  
23 liabilities associated with the inhibition of closely related kinases.  
24  
25  
26  
27  
28  
29  
30  
31  
32

33  
34 **Critical parameters to meet objectives: LipE and MW.** Ligand interactions with most  
35 proteins are substantially influenced by lipophilicity.<sup>25</sup> To monitor the progress of optimization,  
36 lipophilic efficiency (LipE = pKi (or pIC<sub>50</sub>) – log D) was used as a numerical index of binding  
37 effectiveness per unit lipophilicity.<sup>26</sup> Drug design aimed at improving LipE results in parallel  
38 optimization for desirable ADME and greater likelihood of safe drug profiles by increasing the  
39 ratio of potency to lipophilicity. Since log D within a series also tends to correlate with oxidative  
40 clearance,<sup>27</sup> increasing LipE will raise the chance for a lower dose through improvements in IC<sub>50</sub>  
41 and clearance, assuming the introduction of structural features do not impart greater metabolic  
42 liabilities.<sup>28</sup>  
43  
44  
45  
46  
47  
48  
49  
50  
51  
52  
53  
54  
55  
56  
57  
58  
59  
60

1  
2  
3 Since molecular weight is inversely correlated with permeability within a series,<sup>27,29</sup> reducing  
4 ligand size was crucial to provide the smallest, most potent ligands with the greatest chance of  
5 possessing desired drug-like properties, including CNS exposure.  
6  
7

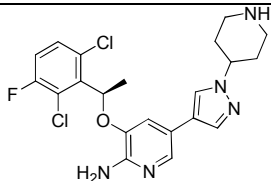
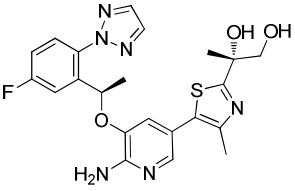
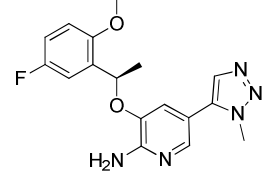
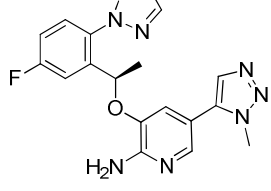
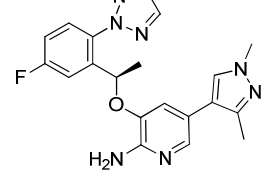
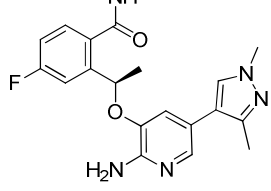
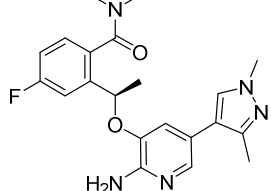
8  
9  
10 **Acyclic aminopyridine/aminopyrazine ALK inhibitors.** Optimization to address emerging  
11 resistance to compound **1** was previously described.<sup>24a,30</sup> Table 1 highlights some key  
12 compounds from the first- and second-generation ALK inhibitor programs. Compound **1** lacks  
13 sufficient potency against resistant clinical mutants and shows high P-glycoprotein 1 (Pgp) efflux  
14 as measured by the MDR BA/AB ratio (>2.5), consistent with CNS exclusion.<sup>31</sup> Structure-based,  
15 property-based, and efficiency-focused drug design efforts culminated in broadly potent,  
16 permeable, and metabolically stable second-generation ALK inhibitors, highlighted by  
17 compound **6a** (PF-06439015).<sup>24a</sup> This compound improved wild-type and gatekeeper (L1196M)  
18 mutant potencies by 105- and 128-fold relative to compound **1** and showed robust *in vivo*  
19 efficacy in the same gatekeeper-mutant cell line. While significant improvements in potency  
20 were achieved, the overall higher lipophilicity required introduction of polar groups to lower the  
21 lipophilicity of the whole molecule for acceptable LipE and good metabolic stability. This added  
22 polarity and molecular weight resulted in high efflux potential and very low rat CSF drug levels.  
23  
24 Other analogues were pursued that lacked excess hydrogen bond donors and polarity. Compound  
25 **6b** and **6c** both had improved *in vitro* clearance and permeability relative to compound **1**. The  
26 MDR efflux ratios for both compounds are less than or equal to 2.5 and consistent with good  
27 predicted brain availability in humans. Unfortunately, both wild-type and L1196M ALK cellular  
28 IC<sub>50</sub> values suffered. Compound **6d** also displayed a desirable, low MDR efflux ratio, but lacked  
29 the required potency and *in vitro* clearance.  
30  
31  
32  
33  
34  
35  
36  
37  
38  
39  
40  
41  
42  
43  
44  
45  
46  
47  
48  
49  
50  
51  
52  
53  
54  
55  
56  
57  
58  
59  
60

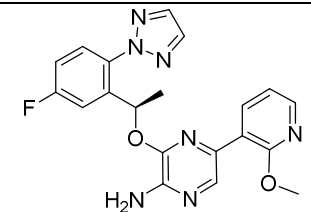
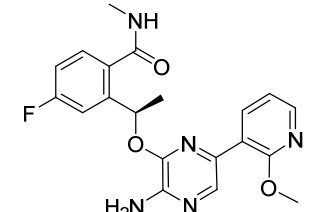
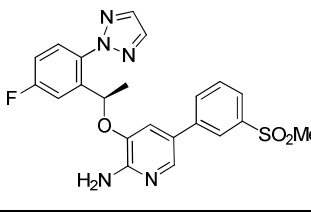
The amide substituents on the phenyl ring of compounds **6e**, **6f** and **6h** were designed to lower lipophilicity and improve efficiency. Indeed, the amide group in **6e** and **6f** lowered the lipophilicity significantly relative to the triazole **6d**. Insights into the impact of the amide on potency and efficiency were gained by highlighting matched molecular pairs. The secondary amide **6e** showed roughly a 10-fold reduction in cellular potencies against both wild-type and mutant ALK and a slight improvement in LipE compared to the aminopyridine 1,2,3-triazole **6d**. Addition of a methyl group provided the tertiary amide analogue **6f**, which lost more than 100-fold potency relative to the triazole analogue **6d**, presumably due to steric clash of the pyrazole and *N,N*-dimethylamide in the preferred bound conformation. The aminopyrazine matched molecular pair demonstrated a similar trend. *N*-methyl amide **6h** showed a 6-fold loss in mutant cell potency but a modest gain in LipE relative to the triazole analogue **6g**. Although acyclic phenyl sulfone analogue **6i** came the closest to meeting our lab objectives, it lacked the required potency and selectivity (data not shown).

These acyclic compounds represented the difficulty in overlapping potency (L1196M IC<sub>50</sub> <25 nM) and low MDR BA/AB ratios (<2.5) to afford the highest probability of reaching efficacious exposures in the CNS. To overlap the required properties, new design efforts targeted neutral inhibitors with improved lipophilic efficiency that fell within property space commensurate with low efflux. This strategy required a novel approach, which is the focus of this manuscript.

**Table 1.** Potency and ADME of compound **1** and other key acyclic leads

| Compound # | Structure | ALK Ki (nM)        | pALK cell IC <sub>50</sub> (nM)   | Log D <sup>a</sup> | LipE <sup>b</sup> | HLM Cl (mL/min/kg) <sup>c</sup> | MDR BA/AB (ratio) <sup>d</sup> |
|------------|-----------|--------------------|-----------------------------------|--------------------|-------------------|---------------------------------|--------------------------------|
|            |           | ALK-L1196M Ki (nM) | pALK-L1196M cell IC <sub>50</sub> |                    |                   |                                 |                                |

|                            |   | (nM) |       |     |     |     |                     |
|----------------------------|---|------|-------|-----|-----|-----|---------------------|
| <b>1</b>                   |    | 0.74 | 80    | 2.0 | 4.1 | 44  | 12.5/0.28<br>(44.5) |
|                            |   | 8.2  | 843   |     |     |     |                     |
| <b>6a</b><br>(PF-06439015) |    | <0.1 | 0.76  | 2.9 | 5.3 | 13  | 30.6/2.8<br>(10.9)  |
|                            |   | 0.2  | 6.6   |     |     |     |                     |
| <b>6b</b>                  |    | 4.0  | 95    | 2.4 | 3.1 | 25  | 16.3/20.0<br>(0.82) |
|                            |   | 38   | 3,200 |     |     |     |                     |
| <b>6c</b>                  |   | 9.0  | 249   | 2.4 | 3.2 | 8.0 | 27.5/11.0<br>(2.5)  |
|                            |   | 70   | 2,650 |     |     |     |                     |
| <b>6d</b>                  |  | <0.2 | 14    | 3.4 | 3.4 | 66  | 16.5/10.9<br>(1.5)  |
|                            |   | 2.6  | 176   |     |     |     |                     |
| <b>6e</b>                  |  | 2.8  | 116   | 2.1 | 3.7 | 28  | 12.6/0.74<br>(17.0) |
|                            |   | 35   | 1,665 |     |     |     |                     |
| <b>6f</b>                  |  | 22   | --    | 2.1 | --  | 58  | 18.8/2.5<br>(7.6)   |
|                            |   | 310  |       |     |     |     |                     |

|    |           |   |      |     |     |     |    |           |
|----|-----------|---|------|-----|-----|-----|----|-----------|
| 1  |           |   |      |     |     |     |    |           |
| 2  |           |   |      |     |     |     |    |           |
| 3  |           |   |      |     |     |     |    |           |
| 4  |           |   |      |     |     |     |    |           |
| 5  |           |   |      |     |     |     |    |           |
| 6  | <b>6g</b> |  | <0.2 | 9.7 | 4.0 | 3.3 | 41 | 5.1/3.2   |
| 7  |           |   | 0.7  | 53  |     |     |    | (1.6)     |
| 8  |           |   |      |     |     |     |    |           |
| 9  |           |   |      |     |     |     |    |           |
| 10 |           |   |      |     |     |     |    |           |
| 11 |           |   |      |     |     |     |    |           |
| 12 |           |   |      |     |     |     |    |           |
| 13 | <b>6h</b> |  | 0.85 | 16  | 3.0 | 3.5 | 76 | 33.8/7.7  |
| 14 |           |   | 8.2  | 312 |     |     |    | (4.4)     |
| 15 |           |   |      |     |     |     |    |           |
| 16 |           |   |      |     |     |     |    |           |
| 17 |           |   |      |     |     |     |    |           |
| 18 |           |   |      |     |     |     |    |           |
| 19 |           |   |      |     |     |     |    |           |
| 20 | <b>6i</b> |  | <0.2 | 4.6 | 3.4 | 3.9 | 10 | 15.6/11.4 |
| 21 |           |   | 1.4  | 54  |     |     |    | (1.4)     |
| 22 |           |   |      |     |     |     |    |           |
| 23 |           |   |      |     |     |     |    |           |
| 24 |           |   |      |     |     |     |    |           |

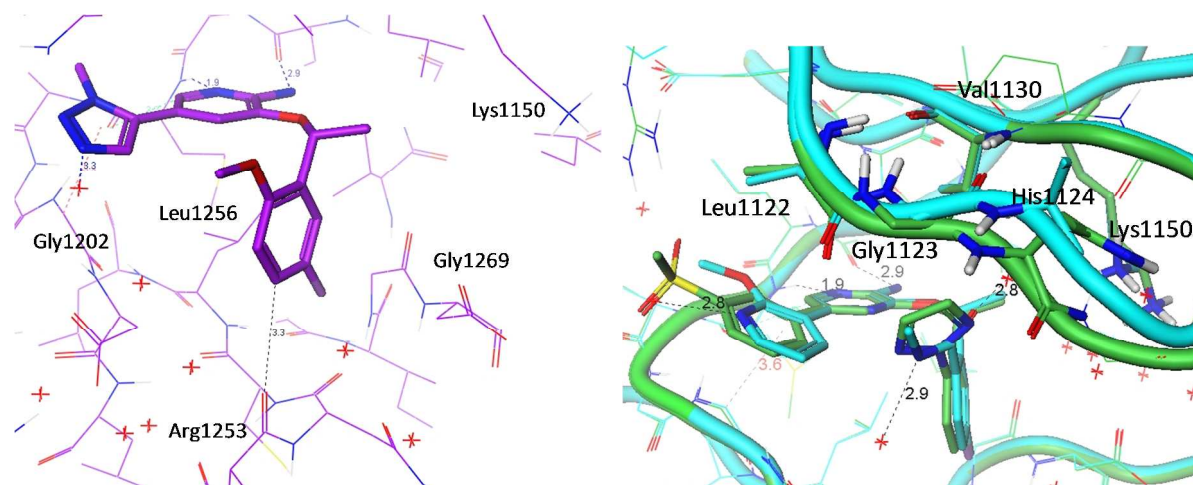
<sup>a</sup>Log D was measured at pH 7.4. <sup>b</sup>LipE =  $-\log(\text{pALK L1196M cell IC}_{50}) - \log D$ . <sup>c</sup>Cl<sub>int,app</sub> refers to the total intrinsic clearance obtained from scaling *in vitro* half-lives in human liver microsomes. <sup>d</sup>MDCK-MDR1 BA/AB efflux at 2 μM substrate concentration and pH 7.4.

Acyclic ligands bound to the ALK kinase domain provided key structural information which revealed protein ligand interactions and facilitated the design of ligands with improved binding affinity and efficiency. Methyl ether **6b** was one of the earliest co-crystal structures obtained in the wild-type kinase domain of ALK (Figure 2, left panel). The aminopyridine core interacted with the hinge portion of the protein *via* an acceptor-donor motif. The benzylic fragment adopted a conformation with the benzylic hydrogen coplanar to the methoxy substituent that minimized A-1,3 strain. Both the benzylic methyl and fluorophenyl filled lipophilic pockets. In addition, the aryl fluoride polarized the *ortho* aryl C-H groups, which provided close contact and electrostatic complementarity with backbone carbonyls at Gly1269 and Arg1253. The orientation of the triazole ring was at a 30 degree torsion with a close contact to the CH of the Gly1202 residue, approximating a C-H donor-pi interaction. Finally, the Leu1256 residue beneath the ligand filled the hydrophobic pocket created by the U-shaped structure of the inhibitor.

1  
2  
3 The co-crystal structure of the ALK kinase domain with amide **6h** (Figure 2, right panel, cyan  
4 structure) revealed that the amide N-H formed a hydrogen bond to water and the carbonyl group  
5 of the secondary amide interacted with the carbonyl group of His1124 *via* a water molecule. The  
6 amide carbonyl did not seem optimal for interaction with structural waters to Lys1150, which  
7 would have required a more perpendicular dihedral angle. Overlay of **6h** with **6i** (a similar  
8 analog having the 2-triazol-2-yl head group – green structure) illustrated the orientation of the  
9 amide away from the surface of the triazole group (Figure 2, right panel). The dihedral angle of  
10 the amide (CCCO) was 45 degrees while the angle for the triazole (CCNN) was 64 degrees,  
11 representing an approximate 20 degree rotation difference. Consequently, the methyl group did  
12 not point to the desired direction for a stronger hydrophobic interaction with Val1130, Gly1123  
13 and Leu1122 in the G-loop. Overall, the G-loop backbone was displaced away from the *N*-  
14 methyl amide **6h** relative to triazole **6i**.

15  
16  
17  
18  
19  
20  
21  
22  
23  
24  
25  
26  
27  
28  
29  
30  
31  
32 Structural data in Figure 2 showcased specific interactions driving binding, but also presented  
33 opportunities to enhance lipophilic efficiency. The bound structures of these U-shaped binders  
34 underscored the proximity of the substituted fluorophenyl head group to the hetero-aromatic tail,  
35 which was directly linked to the aminopyridine or aminopyrazine hinge-binding motif. Two  
36 general designs were pursued to provide novel macrocyclic<sup>33,34</sup> templates and a means to control  
37 conformations for further optimization. Specifically, macrocycles were formed by linking the  
38 two groups from the triazole 4-carbon to the methoxy carbon of **6b** or the pyrazole carbon and  
39 amide nitrogen of **6e** and **6f**. These templates were expected to reinforce the binding  
40 conformation and provide additional protein ligand interactions in the linker region.  
41 Additionally, they significantly reduced the number of rotatable bonds and were more compact  
42 with increased buried surface area than acyclic analogues, which we postulated would provide  
43  
44  
45  
46  
47  
48  
49  
50  
51  
52  
53  
54  
55  
56  
57  
58  
59  
60

1  
2  
3 permeability advantages. Furthermore, we envisioned that designing macrocyclic based  
4  
5 inhibitors driven by LipE and MW optimization would provide the highest probability to achieve  
6  
7 desirable CNS ADME properties without sacrificing potency.  
8  
9



10  
11  
12  
13  
14  
15  
16  
17  
18  
19  
20  
21  
22  
23  
24  
25  
26  
27  
28  
29  
30  
31  
32  
33  
34  
35  
36  
37  
38  
39  
40  
41  
42  
43  
44  
45  
46  
47  
48  
49  
50  
51  
52  
53  
54  
55  
56  
57  
58  
59  
60  
Figure 2. Left panel: Compound **6b** co-crystal structure in ALK kinase domain (purple, PDB 4CNH) highlighting Type I U-shaped binding conformation and proximity of methoxy-fluorophenyl head group and triazole tail group. Right panel: ALK co-xtl of **6h** (cyan, PDB 4CMO) overlaid with **6i** (green, PDB 4CMT) showing triazole, amide and G-loop conformations.

**Macrocyclic ALK Inhibitors.** To evaluate the macrocycle design concept, a variety of 12- to 14-membered ether-linked macrocycles were prepared based on the co-crystal structure analysis of acyclic methyl ether **6b** and the data is summarized in Table 2. According to matched molecular pairs, the smaller ring sizes consistently provided the most lipophilic efficient macrocycles. For example, cyclic ethers **7a**, **7c** and **7e** had higher LipE than their corresponding larger-ring matched molecular pairs **7b**, **7d** and **7f**. The 12-membered macrocycle **7e** displayed the highest LipE (4.4) with picomolar binding affinities and good cellular potencies (ALK IC<sub>50</sub> 1.0 nM; ALK-L1196M IC<sub>50</sub> 20 nM). Although some of the more efficient analogues provided improved potency and lipophilic efficiency relatively to the acyclic analogue **6b**, the macrocyclic

ethers were generally too lipophilic and still lacked the required efficiency for more facile overlap of potency, ADME and CNS availability.

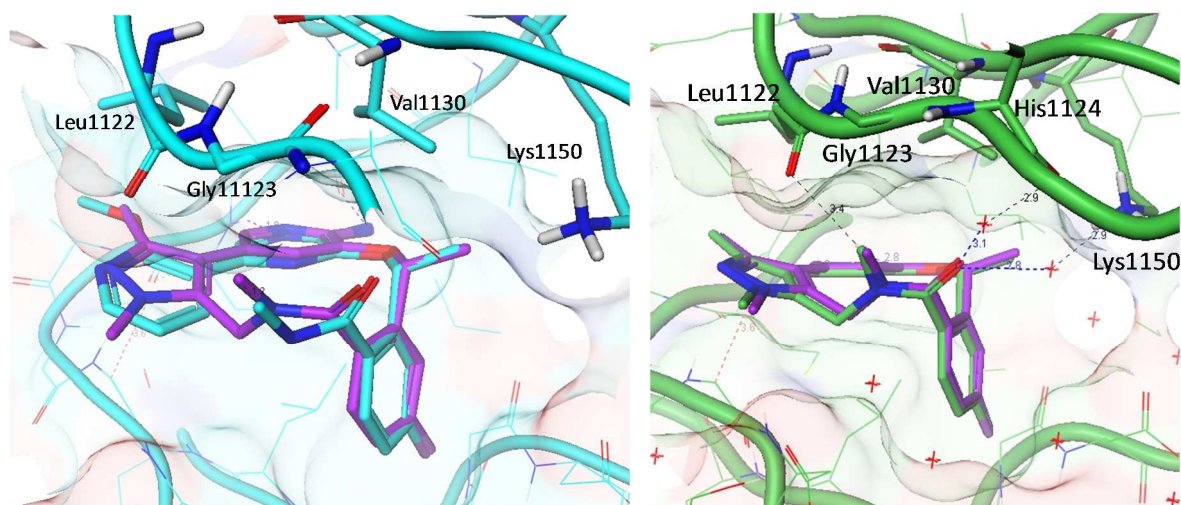
**Table 2.** Ether-linked macrocycles

| Compound # | Structure | ALK Ki (nM)        |                    | pALK cell IC <sub>50</sub> (nM)        |  |                    |                   |
|------------|-----------|--------------------|--------------------|--|--|--------------------|-------------------|
|            |           | ALK-L1196M Ki (nM) | ALK-L1196M Ki (nM) | pALK-L1196M cell IC <sub>50</sub> (nM) | pALK-L1196M cell IC <sub>50</sub> (nM) | Log D <sup>a</sup> | LipE <sup>b</sup> |
| 7a         |           | 0.36               | 1.6                | 22                                     | 101                                    | 3.0                | 4.0               |
|            |           |                    |                    |  |  |                    |                   |
| 7b         |           | 0.22               | <0.1               | 15                                     | 112                                    | 3.6                | 3.4               |
|            |           |                    |                    |  |  |                    |                   |
| 7c         |           | 3.8                | 29                 | 86                                     | 654                                    | 3.4                | 2.8               |
|            |           |                    |                    |  |  |                    |                   |
| 7d         |           | 5                  | 36                 | 524                                    | 3,655                                  | 3.1                | 2.3               |
|            |           |                    |                    |  |  |                    |                   |
| 7e         |           | <0.1               | 0.57               | 1.0                                    | 20                                     | 3.3                | 4.4               |
|            |           |                    |                    |  |  |                    |                   |
| 7f         |           | <0.1               | 0.62               | 0.9                                    | 21                                     | 3.8                | 3.9               |
|            |           |                    |                    |  |  |                    |                   |

1  
2  
3 <sup>a</sup>Log D was measured at pH 7.4. <sup>b</sup>LipE = -log(pALK L1196M cell IC<sub>50</sub>) – log D.  
4  
5  
6

7 The second template followed a design strategy to harness the increased LipE of the 12-  
8 membered ether macrocycles while lowering lipophilicity with a lactam linker. Modeling (Figure  
9 3) suggested a single carbon atom linking the amide with the proximal pyrazole moiety leading  
10 to a proposed 12-membered lactam that would have minimal binding strain (see modeling  
11 methods section). In addition, the *N*-methyl group may provide close contact with Val1130,  
12 Leu1122, and Gly1123 of the G-loop and the lactam carbonyl oxygen may act through a  
13 structural water to stabilize Lys1150 (Figure 3). Importantly, the amide macrocycles would  
14 significantly lower lipophilicity, placing them in optimal log D space.  
15  
16  
17  
18  
19  
20  
21  
22  
23  
24

25 A set of amide-linked macrocycles was prepared to test the hypothesis. The co-crystal structure  
26 of the ALK kinase domain with the cyclic amide **8a** supported the design hypothesis and  
27 molecular modeling, superimposing well with the original docking result (Figure 3, right panel).  
28 As expected, the *N*-methyl group in **8a** was pulled tighter toward the G-loop by 1.2 Å from the  
29 open amide position, and therefore had a closer contact with the carbonyl group of Leu1122 (3.4  
30 Å) and nearby side chains of Leu1122 (4.1 Å), Gly1123 (4.7 Å), and Val1130 (4.7 Å). The  
31 amide carbonyl of macrocycle **8a** formed a water bridge with Lys1150, and a second water  
32 bridge to His1124. It was expected that interaction of the lactam carbonyl oxygen with waters in  
33 the bound state may effectively lower binding desolvation penalties.  
34  
35  
36  
37  
38  
39  
40  
41  
42  
43  
44  
45  
46  
47  
48  
49  
50  
51  
52  
53  
54  
55  
56  
57  
58  
59  
60

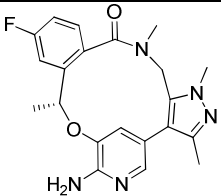
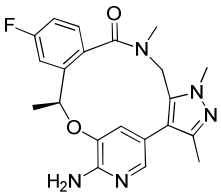
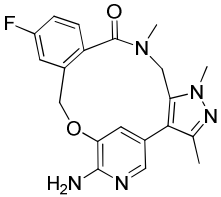
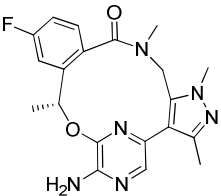
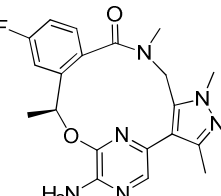


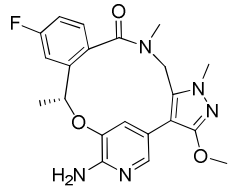
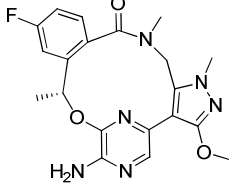
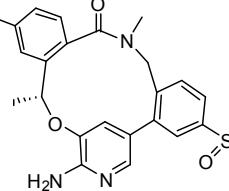
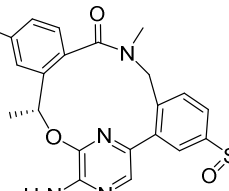
**Figure 3.** Left panel: Acyclic amide **6h** co-crystal structure in ALK (cyan, PDB 4CMO) overlaid with modeled macrocycle **8a** (purple) in ALK (see modeling methods section). Right panel: **8a** co-crystal structure in ALK-kinase domain (green, PDB 4CMU) overlaid with modeled ligand (purple).

Improvement in key parameters was realized upon cyclization to the amide macrocycle **8a** (Table 3) from acyclic analogues **6d-f** (Table 1). Compound **8a** improved cellular potencies against ALK and L1196M ALK by 10-fold relative to compound **6d** and also lowered lipophilicity by one unit, without additional molecular weight. As a result, macrocycle **8a** had more than two units higher LipE. Relative to **6e**, compound **8a** improved cellular potency against the gatekeeper mutant protein by 119-fold while maintaining log D, which also translated to a two unit increase in LipE. In addition, molecular weight was low. Improvements in potency and efficiency were even more pronounced relative to the closest matched pair **6f**. A reduction of the *in vitro* clearance from 56 mL/min/kg (high) to the lower limit of detection for this assay demonstrated the inherent metabolic stability of the cyclic structure. Finally, the permeability of **8a**, measured by Pgp efflux potential, was superior to the acyclic analogue **6f**. Overall, there was a dramatic and compelling improvement in overall properties for **8a** relative to **6f**. These results clearly positioned the macrocyclic amides as an attractive series for the generation of ALK

inhibitors capable of brain penetration. The higher LipE and lower MW allowed navigation to desired CNS ADME space without sacrificing potency and safety.

**Table 3.** Impact of macrocyclization, benzylic methyl, aminopyrazine vs. pyridine and different tail groups on potency and efficiency

| Compound # | Structure   | ALK Ki (nM)        | pALK cell IC <sub>50</sub> (nM)        | Log D <sup>a</sup> | LipE <sup>b</sup> | HLM Cl (mL/min/kg) <sup>c</sup> | MDR BA/AB (ratio) <sup>d</sup> |
|------------|---|--------------------|--|--------------------|-------------------|---------------------------------|--------------------------------|
|            |   | ALK-L1196M Ki (nM) | pALK-L1196M cell IC <sub>50</sub> (nM) |                    |                   |                                 |                                |
| <b>8a</b>  |    | <0.2<br>0.29       | 0.70<br>14                             | 2.2                | 5.7               | 8.6                             | 28.3/8.1<br>(4.2)              |
| <b>8b</b>  |  | 17<br>61           | --<br>--                               | 2.2                | --                | 8.0                             | 34.6/5.8<br>(6.0)              |
| <b>8c</b>  |  | <0.2<br>1.9        | 6.4<br>97                              | 2.0                | 5.0               | 8.4                             | 25.4/4.6<br>(5.5)              |
| <b>8d</b>  |  | <0.2<br>0.10       | 0.21<br>1.4                            | 2.5                | 6.4               | 8.0                             | 26.5/11.9<br>(2.2)             |
| <b>8e</b>  |  | 17<br>61           | 156<br>1,230                           | 2.5                | 3.4               | 9.7                             | 29.6/9.6<br>(3.1)              |

|    |           |  |       |      |     |     |           |
|----|-----------|--|-------|------|-----|-----|-----------|
| 1  |           |  |       |      |     |     |           |
| 2  |           |  |       |      |     |     |           |
| 3  |           |  |       |      |     |     |           |
| 4  |           |  |       |      |     |     |           |
| 5  | <b>8f</b> |   | <0.2  | 0.18 |     |     | 19.9/7.2  |
| 6  |           |  | 0.10  | 2.1  | 2.4 | 6.3 | 8.3       |
| 7  |           |  |       |      |     |     | (2.8)     |
| 8  |           |  |       |      |     |     |           |
| 9  |           |  |       |      |     |     |           |
| 10 |           |  |       |      |     |     |           |
| 11 | <b>8g</b> |   | <0.08 | 0.11 |     |     | 40.3/20.1 |
| 12 |           |  | <0.02 | 0.75 | 2.7 | 6.4 | 23.5      |
| 13 |           |  |       |      |     |     | (2.0)     |
| 14 |           |  |       |      |     |     |           |
| 15 |           |  |       |      |     |     |           |
| 16 |           |  |       |      |     |     |           |
| 17 |           |  |       |      |     |     |           |
| 18 | <b>8h</b> |   | <0.07 | 1.3  |     |     | 22.1/2.4  |
| 19 |           |  | 0.40  | 21   | 1.8 | 5.9 | 9.1       |
| 20 |           |  |       |      |     |     | (9.2)     |
| 21 |           |  |       |      |     |     |           |
| 22 |           |  |       |      |     |     |           |
| 23 |           |  |       |      |     |     |           |
| 24 |           |  |       |      |     |     |           |
| 25 |           |  |       |      |     |     |           |
| 26 | <b>8i</b> |  | <0.1  | 0.34 |     |     | 8.0/1.2   |
| 27 |           |  | 0.12  | 1.9  | 2.2 | 6.5 | 8.0       |
| 28 |           |  |       |      |     |     | (6.7)     |
| 29 |           |  |       |      |     |     |           |
| 30 |           |  |       |      |     |     |           |

<sup>a</sup>Log D was measured at pH 7.4. <sup>b</sup>LipE =  $-\log(\text{pALK L1196M cell IC}_{50}) - \log D$ . <sup>c</sup>Cl<sub>int,app</sub> refers to the total intrinsic clearance obtained from scaling *in vitro* half-lives in human liver microsomes. <sup>d</sup>MDCK-MDR1 BA/AB efflux at 2 μM substrate concentration and pH 7.4.

Table 3 highlights important ALK protein sensitivities to subtle structural changes within the amide macrocycle series. The stereochemical sensitivity was determined by the eutomer distomer ratio. Both **8a** and **8d** improved potency relative to their enantiomeric pairs **8b** and **8e** by 210 and 610-fold, respectively, based on gatekeeper mutant biochemical potencies. The desmethyl analogue, **8c**, lost potency and LipE relative to the more potent methyl analogue **8a**. Three matched molecular pairs highlighted the tolerance of the aminopyrazine core. Several examples (**8a/8d** and **8f/8g** and **8h/8i**) showed an improvement in potency for the aminopyrazine analogues, but the LipE improvement was attenuated as this change was accompanied by an increase, rather than a decrease, in lipophilicity. The additional buried nitrogen atom was not

1  
2  
3 well-solvated and also decreased the basicity of the aminopyrazine leading to an increase in  
4 lipophilicity. Table 3 also highlights the tolerability of both substituted 5- and 6-membered  
5 aromatics adjacent to the aminopyridine or aminopyrazine cores. The methanesulfonyl-benzene  
6 substituent on the aminopyrazine inhibitor **8i** was one of the most lipophilic efficient analogues  
7 (L1196M cell IC<sub>50</sub> LipE 6.5). A comparison of sulfones **8h** and **8i** with the dimethylpyrazoles **8a**  
8 and **8d** revealed that both inhibitors possess almost identical potencies. The increased LipE of  
9 the sulfone is partly due to the polarity of the sulfone exposed to solvent, which maintained  
10 potency and lowered log D without incurring additional desolvation penalties.  
11  
12  
13  
14  
15  
16  
17  
18  
19  
20  
21

22 In addition to providing potent inhibitors of ALK within the desired range of log D (2-3), the  
23 amide macrocycles generally displayed low clearance and low MDR BA/AB efflux ratios. With  
24 the initial encouraging results, lead optimization on the macrocyclic amide 2-  
25 aminopyridine/pyrazine series was carried out to achieve the best overall balance of potency,  
26 CNS availability, ADME *and* selectivity in a *single* compound.  
27  
28  
29  
30  
31  
32  
33

34 **Designing for selectivity.** There are 27 residues in the ATP binding pocket of ALK and to  
35 gain selectivity against other kinases, residues were targeted that differed from ALK. The ALK  
36 Leu1198 residue is conserved in 26% of the kinome at this position and is most often Phe or Tyr  
37 in other kinases (Figure 4). This smaller Leu residue is potentially an avenue to gain selectivity  
38 against a majority of kinases (60%) by building into this pocket to bump into the larger Phe and  
39 Tyr residues.  
40  
41  
42  
43  
44  
45  
46  
47

48 As a surrogate for kinases containing a Phe/Tyr residue at the position corresponding to ALK  
49 Leu1198, TrkB (PDB 4AT3)<sup>34</sup> and ALK proteins were aligned by superposition based on a set of  
50 residues in the active site. Several macrocyclic amides were prepared and ALK co-crystal x-ray  
51 structures were solved for **8a**, **8j**, **8k** and **8m** (Figure 4). The closest distance between ALK co-  
52  
53  
54  
55  
56  
57  
58  
59  
60

crystallized compounds and the Tyr635 atoms of TrkB was measured. Sub-van der Waals distances reflect the need for protein or ligand movement to accommodate the ALK compounds in kinases with Phe/Tyr residues at this selectivity position.

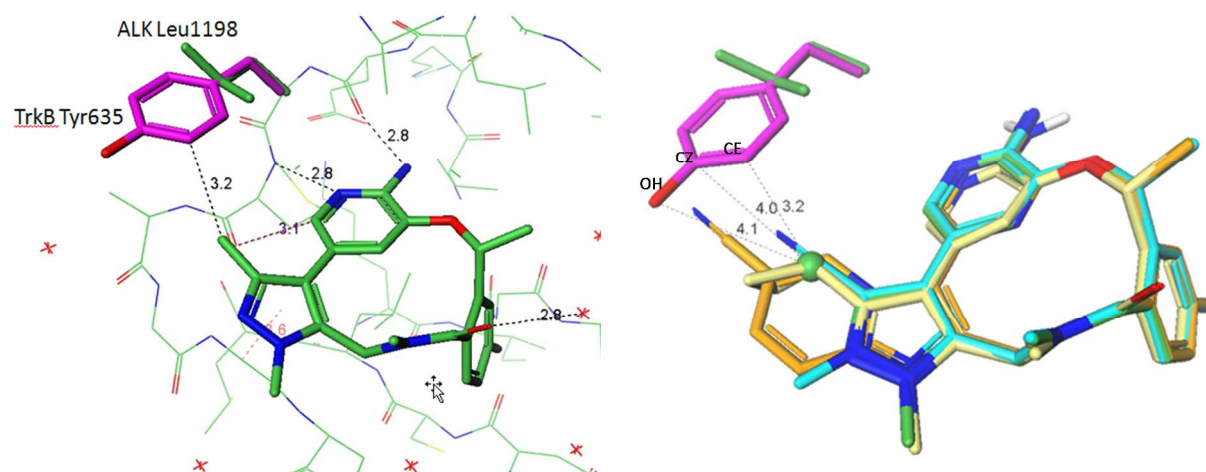


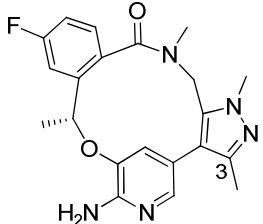
**Figure 4.** Left panel: **8a** and ALK bound structure (green, PDB 4CMU) and TrkB (purple, PDB 4AT3) with selectivity residues highlighted. Right panel: Ligands from ALK co-crystal structures aligned with TrkB demonstrated the potential for clash between ligand and Tyr635; **8a** (Me, green, PDB 4CMU), **8j** (cyPr, yellow, PDB 4CTC), **8k** (CN, cyan, PDB 4CLI), **8m** (orange, PDB 4CTB). Distances shown are between **8a** methyl carbon (shown as a ball) and TrkB Tyr635. PDB atom names for the terminal atoms are shown on Tyr635 (OH, CZ, CE).

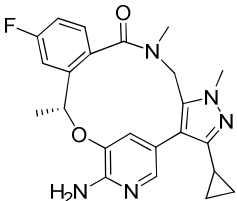
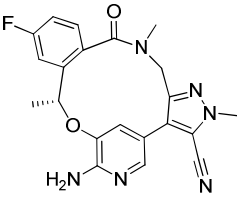
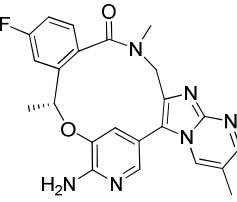
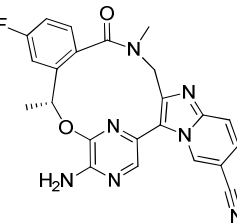
Substituents at the *ortho* position of the pyrazole in ALK structures can approach atoms in the TrkB Tyr635 residue at distances below the sum of van der Waals radii for the pair of atoms. The methyl on the pyrazole group of **8a** in the ALK structure begins to reach the contact distance to TrkB Tyr635 since it is 3.2-4.1 Å away from the three terminal atoms of the Tyr (terminal OH group (OH), terminal carbon (CZ), and adjacent carbon (CE), see Figure 4, right panel) in the aligned TrkB structure. The cyclopropyl group on **8j** had similar distances ranging from 3.2 to 3.7 Å away. The cyano group on **8k** pointed toward the terminal carbon (CZ) of Tyr635 and was

2.1-3.1 Å from the three terminal Tyr atoms. The carbon of the cyano group in **8m** would approximate the position of the terminal methyl of **8l** which is estimated to be 2.0-2.3 Å from Tyr635. The nitrile of compound **8m** was measured to be 1.0-1.8 Å from the terminal two atoms indicating a greater potential clash than with smaller substituents. Further, the macrocycle restricts rotation and the groups are unable to rotate away from the Tyr/Phe residues as might be hypothesized with acyclic compounds.

Macrocyclic amides **8a** and **8j-m** were tested against TrkB (Table 4). Both the pyrazoles substituted at C3 with methyl and cyclopropyl (**8a** and **8j**, respectively) retained picomolar enzymatic potencies against TrkB and provided little to no selectivity based on ALK-L1196M Ki (approximately 2-fold). However, the cyano-pyrazole **8k** and the methyl substituted imidazopyrimidine **8l** displayed significantly attenuated potency in TrkB and provided reasonable selectivity ratios (approximately 40-fold). Finally, the cyano-imidazopyrimidine **8m** afforded the most robust selectivity ratio (93-fold). This selectivity data was consistent with our previous modeling analysis.

**Table 4.** Potency, ADME and selectivity of macrocyclic analogues

| Compound # | Structure   | ALK-L1196M Ki (nM) | pALK-L1196M cell IC <sub>50</sub> (nM) | Log D <sup>a</sup> | HLM Cl <sub>int,app</sub> <sup>b</sup> | MDR BA/AB (ratio) <sup>c</sup> | TrkB Ki (nM) (selectivity) <sup>d</sup> |
|------------|---|--------------------|--|--------------------|--|--------------------------------|---|
| <b>8a</b>  |  | 0.29               | 14                                     | 2.2                | 8.6                                    | 28.3/8.1<br>(4.2)              | 0.5<br>(1.7x)                           |

|    |                      |  |      |     |     |      |                                 |               |
|----|----------------------|--|------|-----|-----|------|---------------------------------|---------------|
| 1  |                      |  |      |     |     |      |                                 |               |
| 2  |                      |  |      |     |     |      |                                 |               |
| 3  |                      |  |      |     |     |      |                                 |               |
| 4  |                      |  |      |     |     |      |                                 |               |
| 5  |                      |  |      |     |     |      |                                 |               |
| 6  | <b>8j</b>            |   | <0.1 | 5.8 | 2.9 | 14.6 | 16.3/8.0<br>(2.0)               | 0.4<br>(2.0x) |
| 7  |                      |  |      |     |     |      |                                 |               |
| 8  |                      |  |      |     |     |      |                                 |               |
| 9  |                      |  |      |     |     |      |                                 |               |
| 10 |                      |  |      |     |     |      |                                 |               |
| 11 | <b>8k</b>            |   | 0.70 | 21  | 2.3 | <8   | 28.0/19.3<br>(1.5) <sup>e</sup> | 23<br>(38x)   |
| 12 | <b>(PF-06463922)</b> |  |      |     |     |      |                                 |               |
| 13 |                      |  |      |     |     |      |                                 |               |
| 14 |                      |  |      |     |     |      |                                 |               |
| 15 |                      |  |      |     |     |      |                                 |               |
| 16 |                      |  |      |     |     |      |                                 |               |
| 17 |                      |  |      |     |     |      |                                 |               |
| 18 |                      |  |      |     |     |      |                                 |               |
| 19 |                      |  |      |     |     |      |                                 |               |
| 20 | <b>8l</b>            |   | 2.0  | 365 | 1.7 | <8   | 32.4/1.74<br>(20.2)             | 77<br>(39x)   |
| 21 |                      |  |      |     |     |      |                                 |               |
| 22 |                      |  |      |     |     |      |                                 |               |
| 23 |                      |  |      |     |     |      |                                 |               |
| 24 |                      |  |      |     |     |      |                                 |               |
| 25 |                      |  |      |     |     |      |                                 |               |
| 26 |                      |  |      |     |     |      |                                 |               |
| 27 | <b>8m</b>            |  | 0.56 | 45  | 2.4 | <8   | 22.1/3.8<br>(5.8)               | 65<br>(93x)   |
| 28 |                      |  |      |     |     |      |                                 |               |
| 29 |                      |  |      |     |     |      |                                 |               |
| 30 |                      |  |      |     |     |      |                                 |               |
| 31 |                      |  |      |     |     |      |                                 |               |

<sup>a</sup>Log D was measured at pH 7.4. <sup>b</sup>Cl<sub>int,app</sub> refers to the total intrinsic clearance obtained from scaling *in vitro* half-lives in human liver microsomes. <sup>c</sup>MDCK-MDR1 BA/AB efflux at 2 μM substrate concentration and pH 7.4. <sup>d</sup>TrkB Ki and ratio relative to ALK-L1196M Ki. <sup>e</sup>RRCK-BCRP BA/AB is 37/28 (1.8); determined at 2 μM substrate concentration and pH 7.4.

The pyrazole cyano moiety in **8k** was efficient for obtaining selectivity because the cyano contains only one more heavy atom than the unselective methyl analogue (**8a**) and gains >35x selectivity, similar to the bulkier methyl-substituted imidazo-pyrimidine (**8l**). It is hypothesized that the nitrile makes an unfavorable contact with the CE atom of the Tyr635 in TrkB, closer to the mid-point of the side chain rather than at the terminus (Figure 4, right panel). Unfavorable desolvation penalties or electrostatics due to the proximity of the electron-rich nitrile nitrogen atom and tyrosine may further enhance selectivity.

**Designing for CNS availability.** Previous publications highlighted the importance of minimizing efflux in Pgp over-expressing cell lines (MDCK-MDR1) to maximize both CSF to

1  
2  
3 free plasma ratios and free brain to free plasma ratios.<sup>35</sup> Compounds that exhibited MDR BA/AB  
4  
5  
6 efflux ratios (ER) of less than 2.5 did not demonstrate significant BBB efflux *in vivo* and have  
7  
8  
9 higher probability for achieving pharmacologically relevant brain to plasma ratios. To elucidate  
10  
11 the physicochemical properties that provide low MDR efflux, we performed an analysis of the  
12  
13 Pfizer MDR data set that contains greater than 115,000 compounds evaluated in the same MDR  
14  
15 permeability model.<sup>36</sup> A combination of experimental HPLC-based and shake-flask methods  
16  
17 were used to measure log D. Figure 5 depicts a sub-set of this data that focuses within a range of  
18  
19 molecular weight and lipophilicity values to encompass the majority of the inhibitors in our ALK  
20  
21 program. Often authors discuss the influence of a single physicochemical descriptor in the  
22  
23 analysis of efflux and permeability. However, similar to the CNS MPO<sup>37</sup> algorithm, the  
24  
25 dependence of a given ADME property is multidimensional and it is more appropriate to  
26  
27 consider several factors simultaneously.<sup>27</sup>  
28  
29  
30

31  
32 Along with plotting binned values for molecular weight on the y-axis and lipophilicity on the  
33  
34 x-axis, we also examined further segmentation by hydrogen bond donor (HBD) count. The  
35  
36 independent influence of molecular weight, lipophilicity and hydrogen bond donor count was  
37  
38 clearly demonstrated in the outcome of binned MDR ratios performance, confirming these as  
39  
40 first principles. The chance of increased efflux was observed with elevated molecular weight or  
41  
42 HBD counts, and the chance of decreased efflux was seen with increased lipophilicity. This type  
43  
44 of data visualization also provided the opportunity to readily evaluate the influence of multiple  
45  
46 first-principle operators and determine the trade-offs that can be utilized in compound design.  
47  
48 For example, the impact of increased HBD count on efflux within defined molecular weight and  
49  
50 lipophilicity bins was clearly demonstrated by the comparison of binned efflux ratios. Trade-offs  
51  
52 between physicochemical properties were observed as with the comparison of areas A and B  
53  
54  
55  
56  
57  
58  
59  
60

(Figure 5) where for molecules with 2 HBD counts, similar distributions of binned efflux were observed between groups of compounds with higher molecular weight and log D (A) and lower molecular weight and log D (B). This, and other property-based analyses, reinforced the importance of molecular weight and lipophilicity efficiency indices as a means to drive to the design of small molecule inhibitors within a focused log D range of 2-3 and with minimal introduction of hydrogen bond donors.



**Figure 5.** Effect of log D, HBD count and MW on MDR BA/AB ratio (blue <2.5; red >2.5). Percent of each sector shown and total count per bin highlighted in center of pie.

The selection of the aminopyridine as a kinase hinge binding motif provides a minimum requirement of two HBDs and a constraint for inhibitor design. As outlined earlier, one of the NH<sub>2</sub> group hydrogen atoms provides a key interaction with the carbonyl of hinge-residue Glu1197 within the protein-ligand complex.<sup>24a</sup> However, the potential for the second NH<sub>2</sub>

1  
2  
3 hydrogen to participate in an intramolecular hydrogen bond (IMHB) with the adjacent ether  
4 oxygen may provide lower MDR ratios than other molecules with two HBDs and similar  
5 physicochemical properties.<sup>38</sup> In this program, it was observed that the presence of even a  
6 moderately basic nitrogen when combined with elevated molecular weight and HBD count can  
7 increase MDR ratios and limit CNS exposure, as observed with compound **1**.  
8  
9  
10  
11  
12  
13  
14

15 While the analysis of large data sets against physicochemical properties is a valuable method  
16 to assess general probabilistic odds for defined outcomes, it can also furnish comparison sets for  
17 new hypothesis generation. The pie charts of Figure 6 illustrate that macrocyclic inhibitors  
18 display lower levels of binned MDR efflux when compared to acyclic molecules with similar  
19 molecular weight, measured log D and HBD count. The macrocycles may afford the potential  
20 benefits for permeability and efflux by reducing rotatable bonds and achieving a highly compact  
21 shape for a given molecular weight. The box & whisker plots of Figure 6 illustrate that, on  
22 average, solvent accessible surface areas (SASA)<sup>39</sup> for macrocyclic molecules are almost 10%  
23 smaller than non-macrocycles within defined molecular weight ranges. Replacing molecular  
24 weight with SASA may provide a more accurate descriptor for molecular size and increase the  
25 probabilistic assessment in the future design of macrocyclic inhibitors.  
26  
27  
28  
29  
30  
31  
32  
33  
34  
35  
36  
37  
38  
39  
40  
41  
42  
43  
44  
45  
46  
47  
48  
49  
50  
51  
52  
53  
54  
55  
56  
57  
58  
59  
60

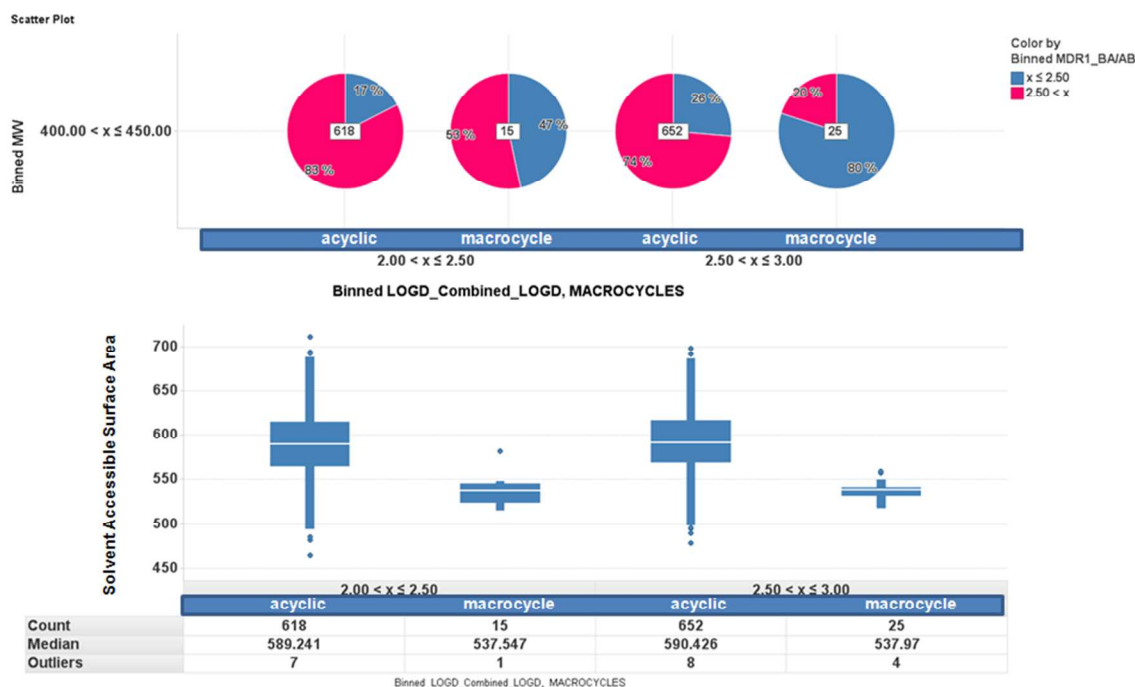


**Figure 6.** Top panel: Comparison of acyclic and macrocyclic compounds binned MDR ratios (blue  $<2.5$ ; red  $>2.5$ ) for compounds within the same MW, log D and HBD count (2) bins. Percent of each sector shown and total count per bin highlighted in center of pie. Bottom panel: Acyclic and macrocyclic compound SASA differences within the same MW, log D, and HBD count (2) bins.

The cohort of potent and low clearance compounds shown in Table 4 were also tested *in vitro* for their Pgp-mediated efflux potential. Compounds **8a**, **8l** and **8m** showed MDR BA/AB ratios significantly above 2.5 and are predicted to be substrates of Pgp with the inability to adequately cross the BBB. Both compounds **8j** and **8k** displayed MDR BA/AB ratios less than 2.5, and are predicted to access the CNS. This data was consistent with the Pfizer comprehensive dataset analysis describing the impact of MW (or SASA), log D, and HBD count on binned MDR ratios (Figure 5).

To appreciate the efficiency differences between macrocyclic and acyclic analogues, two plots were constructed. The LipE plot (Figure 7, left panel), with log D on the x-axis and potency on the y-axis, showed that many of the macrocyclic compounds (colored aqua), some that display

LipE values of greater than 6, out-performed the acyclics in both potency and LipE. Importantly, many macrocycles were able to access optimal log D space (2-3) coupled with improvements in potency. Evaluation of both LipE and HACNT on the same plot (Figure 7, right panel) clearly demonstrated that the macrocycles were able to achieve the highest lipophilic efficiency measures in heavy atom count cohorts, indicating the economical use of each atom in exploiting complementarity to the binding pocket of the kinase with minimal ligand strain. Consequently, property overlap was made more facile.

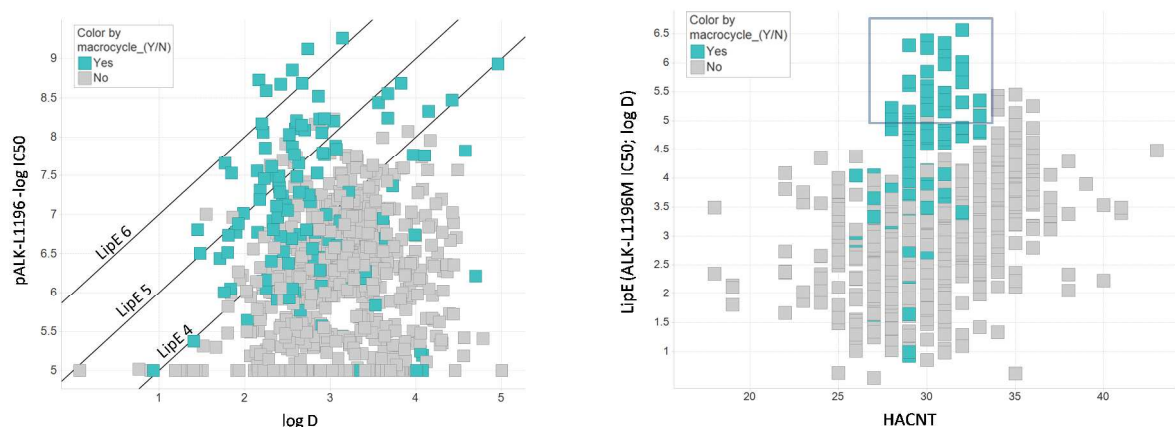


**Figure 7.** Left panel: LipE plot comparing macrocyclic (aqua) and acyclic (light gray) analogues. Right panel: LipE vs. HACNT plot with macrocyclic and acyclic analogues.

**Potency, selectivity and PK of 8k (PF-06463922).** Based on outstanding potency, low *in vitro* clearance, good selectivity and low efflux potential, macrocycle **8k** (Table 4) emerged as a candidate for further profiling. As revealed in Table 5, **8k** demonstrated significantly improved cell activity against ALK and a large set of ALK clinical mutations compared to compound **1**. In the engineered NIH-3T3 ALK wild-type phosphorylation assay, the potency of **8k** was improved 62-fold (from 80 nM IC<sub>50</sub> vs. wt ALK for compound **1** to 1.3 nM for **8k**). In addition, it was

1  
2  
3 potent against all available clinical ALK mutants showing a 40- to 825-fold potency  
4  
5 improvement compared to compound **1**.  
6  
7  
8  
9

10 **Table 5.** pALK inhibition ( $IC_{50}$ ) values for compounds **1** and **8k** against ALK and clinical  
11 mutants of ALK  
12

| pALK $IC_{50}$ (nM) in 3T3-EML4-ALK Engineered cell lines |     |        |        |        |        |        |        |        |          |
|---|-----|--------|--------|--------|--------|--------|--------|--------|----------|
| Compound #  | ALK | F1174L | C1156Y | G1269A | S1206Y | L1196M | L1152R | G1202R | 1151Tins |
| <b>1</b>  | 80  | 165    | 478    | 605    | 626    | 843    | 1026   | 1148   | 3039     |
| <b>8k</b>   | 1.3 | 0.2    | 1.6    | 15     | 4.2    | 21     | 9.0    | 77     | 38       |

13  
14  
15  
16  
17  
18  
19  
20  
21  
22  
23  
24  
25  
26  
27 To investigate kinase selectivity of **8k** relative to its target kinases ALK and ROS1, it was  
28 evaluated in biochemical kinase screening assays against a panel of 206 recombinant kinases. In  
29 these preliminary biochemical kinase selectivity screens, only 10 off-target kinases were  
30 identified that exhibited enzyme-based activity and showed selectivity margins less than 100-  
31 fold compared to the ALK-L1196M gatekeeper mutant (Table 6).  
32  
33  
34  
35  
36  
37  
38  
39  
40

41 **Table 6.** Enzyme-based selectivity of **8k**  
42

| Enzyme     | $IC_{50}^a$ or $K_i^b$ , nM | fold shift vs. ALK-L1196M |
|------------|-----------------------------|---------------------------|
| ROS1       | <0.02 <sup>b</sup>          | <0.03                     |
| ALK        | <0.07 <sup>b</sup>          | <0.10                     |
| ALK-L1196M | 0.7 <sup>b</sup>            | 1.0                       |
| LTK (TYK1) | 2.7                         | 3.9                       |
| FER        | 3.3                         | 4.7                       |
| FES (FPS)  | 6.0                         | 8.6                       |

|              |                 |    |
|--------------|-----------------|----|
| PTK2B (FAK2) | 14              | 20 |
| TNK2 (ACK)   | 17              | 24 |
| PTK2 (FAK)   | 17              | 24 |
| NTRK2 (TRKB) | 23 <sup>b</sup> | 33 |
| NTRK1 (TRKA) | 24              | 34 |
| NTRK3 (TRKC) | 46              | 66 |
| FRK (PTK5)   | 53              | 76 |

<sup>a</sup>IC<sub>50</sub> values by Invitrogen Z'-LYTE™ assays using K<sub>M</sub>-levels of ATP, unless specified otherwise. <sup>b</sup>Ki by off-chip mobility shift assays conducted in-house.

Table 7 summarizes rat pharmacokinetic data. Compound **8k** displayed low plasma clearance, a moderate volume of distribution, reasonable half-life and bioavailability of 100%. This very good preclinical PK and low protein binding provided high free plasma exposures. In addition, CNS penetration of **8k** was evaluated in rats. After a single 10 mg/kg oral dose, samples of CSF, brain and plasma were collected at 1, 4, 7, 12 and 24 h with the PK parameters shown in Table 8. AUC ratios of CSF/free plasma (0.31) and free brain/free plasma<sup>40</sup> (0.21) suggest **8k** distributes into the CNS. The rat *in vivo* data was further supported by *in vitro* data in Table 4, which indicated a lack of transporter-mediated efflux in both Pgp and breast cancer resistance protein (BCRP) over-expressing cell lines.

*In vivo* efficacy data on **8k** was generated in a variety of wild-type and resistant ALK and ROS1 engineered cell lines, and was disclosed previously.<sup>24b-d</sup> Additionally, a detailed pharmacology manuscript is currently in preparation.

**Table 7.** Preclinical rat PK of **8k**

| Route <sup>a,b</sup> | C <sub>max</sub><br>(ng/mL) | Free <sup>c</sup><br>C <sub>max</sub><br>(nM) | T <sub>max</sub> (hr) | AUC <sub>inf</sub> /AUC <sub>(0-24)</sub><br>(ng*hr/mL) | Free<br>C <sub>ave</sub><br>(nM) | CL <sub>p</sub><br>(mL/min/kg) | V <sub>ss</sub><br>(L/kg) | T <sub>1/2</sub> (h) | F (%) |
|----------------------|-----------------------------|---|-----------------------|---|----------------------------------|--------------------------------|---------------------------|----------------------|-------|
|----------------------|-----------------------------|---|-----------------------|---|----------------------------------|--------------------------------|---------------------------|----------------------|-------|

|      |       |       |     |        |     |      |     |     |     |
|------|-------|-------|-----|--------|-----|------|-----|-----|-----|
| i.v. | --    | --    | --  | 1,150  | -   | 15.5 | 2.7 | 2.7 | --  |
| p.o. | 1,727 | 1,530 | 1.3 | 14,933 | 551 | --   | --  | --  | 100 |

<sup>a</sup>Formulation for the i.v. and p.o. routes was ethanol:PEG200:water (10:40:50) in solution. <sup>b</sup>Dose: po 10 mg/kg QD; iv 1 mg/kg QD. <sup>c</sup>Rat plasma protein binding fraction unbound of 0.36 (determined at 2.4  $\mu$ M).

**Table 8.** Preclinical *in vivo* CNS availability data of **8k**

|                  | Matrices | AUC (nM*hr) | Free AUC (nM*hr) <sup>b</sup> |
|------------------|----------|-------------|-------------------------------|
|                  | CSF      | 3,475       | 3,475                         |
| rat <sup>a</sup> | Brain    | 19,621      | 2,355 <sup>a</sup>            |
|                  | Plasma   | 30,700      | 11,052                        |

<sup>a</sup>Dose: po 10 mg/kg. <sup>b</sup>Free brain AUC was calculated using brain ( $f_u$ ) of 0.12 and free plasma AUC was calculated using PPB ( $f_u$ ) of 0.36.

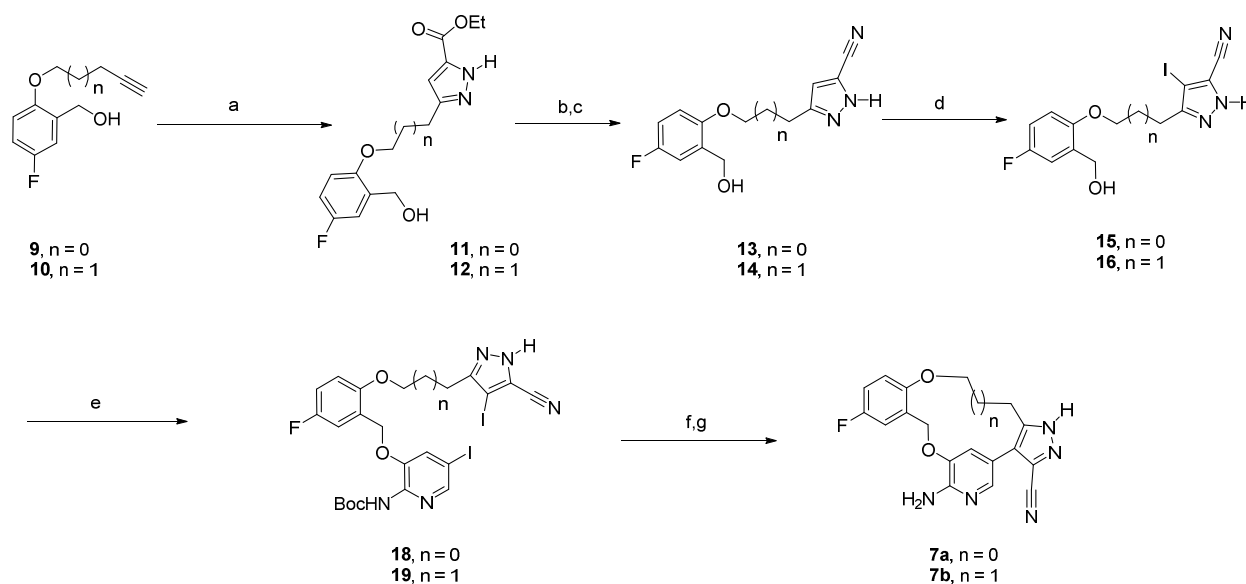
## CHEMISTRY

Ring closure presents a unique synthetic challenge in devising routes to access macrocycles.<sup>41</sup> Eight to eleven-membered rings are typically the most challenging to prepare with a modest increase in intramolecular rate of ring closure for rings  $\geq 12$  members. As well as ring size, other factors influence the intramolecular ring closure such as the strain present in preferred pre-cyclization conformations<sup>42</sup> and the reaction conditions employed. Given the structural diversity and highly engineered nature of the macrocyclic inhibitors described herein, a range of ring closure methods were evaluated for each series to ensure efficient access to the desired target.

**Ether-linked macrocycles.** The route to compounds **7a** and **7b** is shown in Scheme 1 (described herein for **7a**,  $n = 0$ ). The starting materials (**9**, **10**) were prepared from 5-fluoro-2-hydroxybenzoic acid *via* a three step esterification, alkylation and reduction sequence. Treatment of the alkyne **9** with ethyl diazoacetate in a sealed tube afforded the pyrazole **11** as a 4:1 mixture of regioisomers favoring the desired C3 ethyl ester.<sup>43</sup> The ester was converted to the nitrile through a two step amidation-dehydration process to afford compound **13**.<sup>44</sup> Iodination of the 4-

position of the pyrazole proceeded cleanly to give alcohol **15** followed by a Mitsunobu reaction<sup>45</sup> with the Boc-protected 2-amino-3-hydroxy-5-iodo-pyridine **17** to provide **18**. The ring closure was achieved by a one-pot Suzuki coupling<sup>46</sup> with the boronate being generated *in situ* using bispinacolatodiboron ( $B_2pin_2$ ) to give the intermediate protected macrocycle (not shown). Removal of the Boc group under standard acid-mediated conditions<sup>47</sup> afforded the desired macrocycle **7a**. Compound **7b** was prepared *via* an identical sequence starting with the alkyne **10**.

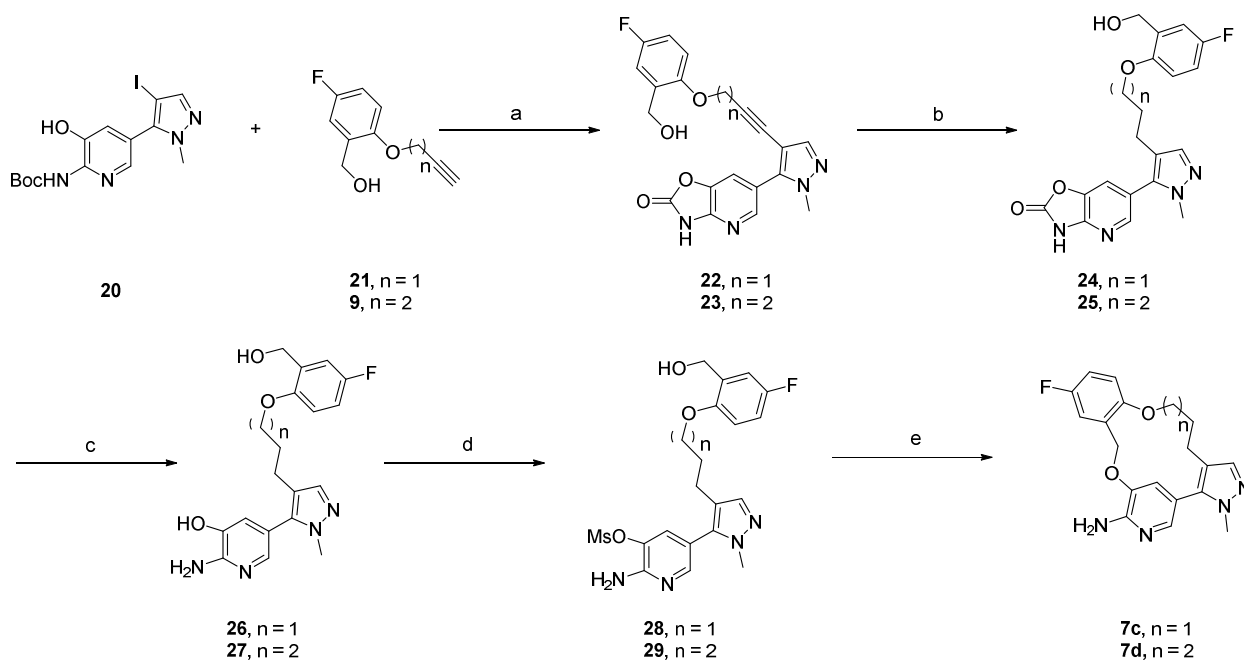
**Scheme 1. Synthesis of Ether-Linked Macrocycles 7a and 7b**



Reagents and conditions (yields for n = 0): (a) 1.1 eq ethyl diazoacetate, 100 °C, sealed tube, 18 h, 49%; (b)  $NH_4OH$ , MeOH, 60 °C, 12 h; (c) 4 eq TFAA, pyridine, 0 °C, 1 h, 81% over 2 steps; (d) 0.70 eq  $I_2$ , 0.70 eq CAN, MeCN, 60 °C, 2 h, 66%; (e) 1.25 eq  $Ph_3P$ , 1.25 eq DIAD, 1 eq Boc-2-amino-3-hydroxy-5-iodopyridine **17**, THF, 1 h, 16%; (f) 5 eq  $B_2pin_2$ , 5 eq CsF, 6 mol%  $Pd(amphos)Cl_2$ , MeOH,  $H_2O$ , 60 °C, 1 h; (g) 25 eq HCl (4 M in dioxane),  $CH_2Cl_2$ , 12 h, rt, 29% over two steps.

Compounds **7c** and **7d** were synthesized in an alternative manner with the ring closure being achieved through ether bond formation as shown in Scheme 2 (described herein for **7c**,  $n = 1$ ). The pyrazole **20** was obtained from Suzuki coupling of the 5-substituted boronic acid of methylpyrazole with Boc-protected 2-amino-3-hydroxy-5-bromopyridine, followed by regioselective iodination at the 4-position of the pyrazole. The iodide **20** was coupled with the alkyne **21** under standard Sonagashira conditions<sup>48</sup> with concomitant cyclization between the Boc moiety and the adjacent alcohol to afford the cyclic carbamate **22**. Hydrogenation of **22** to give **24** followed by hydrolysis provided **26**. Activation of **26** gave mesylate **28**, which was then cyclized *via* a mesyl-transfer<sup>49</sup> process to afford the desired macrocycle **7c**. Compound **7d** was prepared *via* an identical sequence starting with the alkyne **9**.

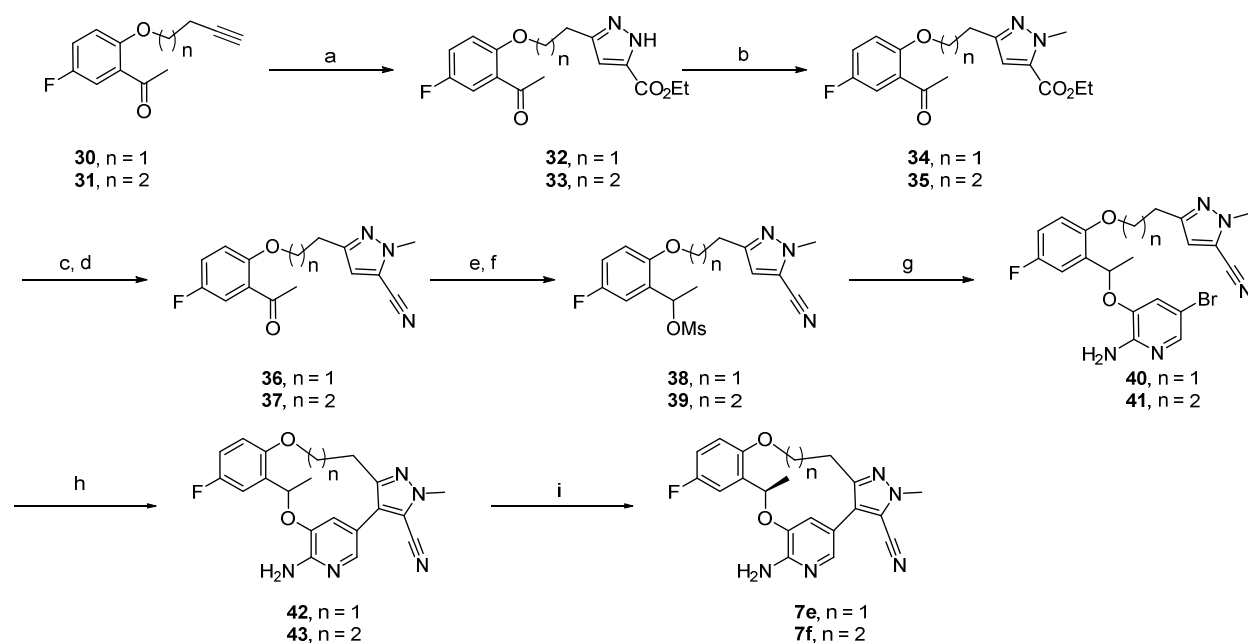
**Scheme 2.** Synthesis of Ether-Linked Macrocycles **7c** and **7d**



1  
2  
3 Reagents and conditions (yields for n = 1): (a) 1 eq Ph<sub>3</sub>P, 20 mol% CuI, 20 mol% PdCl<sub>2</sub>(PPh<sub>3</sub>)<sub>2</sub>,  
4 piperidine, 90 °C, 5 h; (b) 10 wt% Pd(OH)<sub>2</sub> (20% on carbon), EtOH, 50 °C, 4 bar H<sub>2</sub>, 18 h; (c)  
5 15% aq NaOH, EtOH, 85 °C, 12 h, 34% over 3 steps; (d) 10 eq pyridine, 1 eq MsCl, cat. DMAP,  
6 CH<sub>2</sub>Cl<sub>2</sub>, 1 h; (e) 1 eq NaH (60 wt%), DMF, 50 °C, 2 h, 37% over 2 steps.  
7  
8  
9

10  
11 The methyl-substituted macrocycles **7e** and **7f** incorporated a similar strategy shown in Scheme  
12 3 but utilized a direct arylation<sup>50</sup> ring closing process (described herein for **7e**, n = 1). Initial  
13 [3+2] condensation of the alkyne **30** with ethyl diazoacetate formed the pyrazole **32**,<sup>43</sup> followed  
14 by methylation, and ester group elaboration through an amidation-dehydration sequence<sup>44</sup> that  
15 resulted in the nitrile group in **36**. Reduction and activation of the alcohol followed by reaction  
16 with 2-amino-3-hydroxy-5-bromo-pyridine allowed access to the cyclization precursor **40**. Direct  
17 arylation was achieved under Pd-catalyzed conditions to give **42** as a mixture of enantiomers,  
18 which were separated by chiral SFC to afford **7e**. Compound **7f** was prepared *via* an identical  
19 sequence starting with the alkyne **31**.  
20  
21  
22  
23  
24  
25  
26  
27  
28  
29  
30  
31  
32  
33  
34  
35  
36

37 **Scheme 3.** Synthesis of Ether-Linked Macrocycles **7e** and **7f**  
38  
39  
40  
41  
42  
43  
44  
45  
46  
47  
48  
49  
50  
51  
52  
53  
54  
55  
56  
57  
58  
59  
60

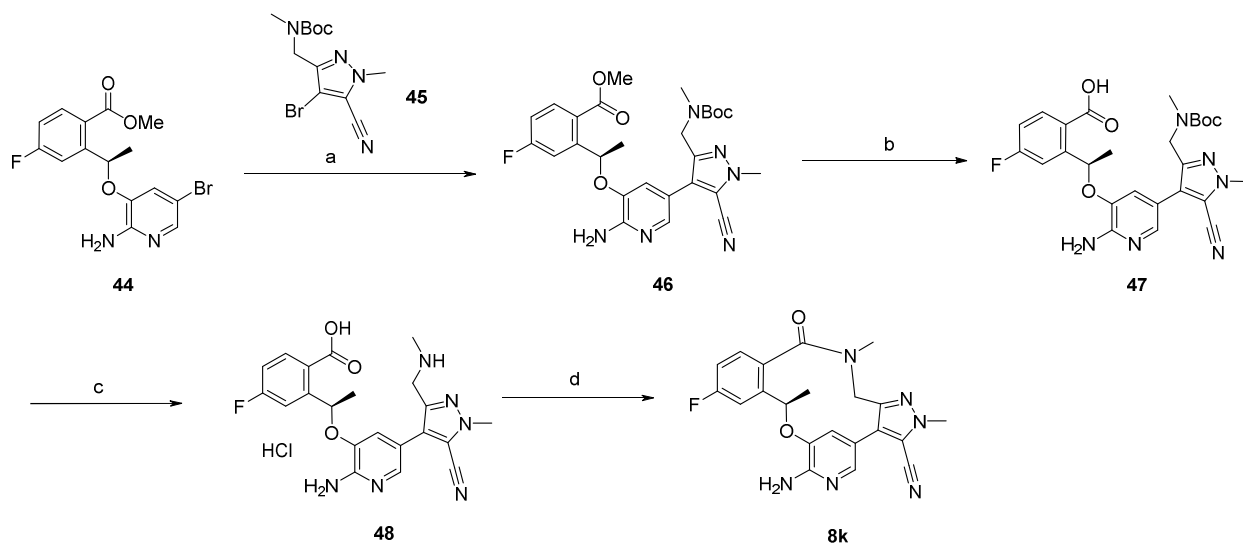


Reagents and conditions (yields for  $n = 1$ ): (a) 1.1 eq ethyl diazoacetate, sealed tube, 100 °C, 18 h, 76%; (b) 1.2 eq  $\text{Me}_2\text{SO}_4$ , toluene, 80 °C, 12 h, 46%; (c)  $\text{NH}_4\text{OH}$ , MeOH, 60 °C, 18 h, 74%; (d) 2 eq TFAA, 4 eq pyridine,  $\text{CH}_2\text{Cl}_2$ , 0 °C, 1 h, 94%; (e) 1.1 eq  $\text{NaBH}_4$ , MeOH, 0 °C, 1 h; (f) 1.1 eq  $\text{MsCl}$ , 1.5 eq TEA,  $\text{CH}_2\text{Cl}_2$ , 0 °C, 1 h, 94% over two steps; (g) 1.2 eq 2-amino-3-hydroxy-5-bromopyridine, 2 eq  $\text{Cs}_2\text{CO}_3$ , DMF, 80 °C, 40 h, 18%; (h) 20 mol% cataCXium A, 20 mol%  $\text{Pd}(\text{OAc})_2$ , 5 eq KOAc, *t*-AmOH, 140 °C, 2 h, 24%; (i) Chiral SFC, Whelk-O1 (R,R) 30% MeOH @ 120 bar, 4 mL/min.

**Amide-linked macrocycles.** The approach to the amide-based macrocycles featuring the aminopyridine hinge-binding motif (**8a-c**, **8f**, **8h**, **8j-l**) is shown for **8k** and illustrated in Scheme 4. A Suzuki coupling between **44** and the heteroaryl halide **45** provided **46**. Subsequent studies on this coupling reaction indicated that optimal yields were obtained carrying out the borylation and coupling as separate processes using different palladium-ligand combinations. Ester hydrolysis gave **47**, which underwent acid-mediated Boc deprotection to provide the macrocycle precursor **48**. The ring closure to form **8k** was achieved by a HATU-mediated macrolactamization reaction in DMF.<sup>51</sup> In general, high dilution conditions were employed with the slow addition of a solution of the hydrochloride salt of **48** and base in DMF being added to a solution of HATU in the same solvent at 0 °C. The reaction was observed to be complete by the

end of the addition, and yields ranged from 2 - 45% across the analogues prepared with higher yields being obtained for compounds featuring the chiral benzylic methyl.

#### Scheme 4. Synthesis of Pyridine Amide Macrocycle, **8k**



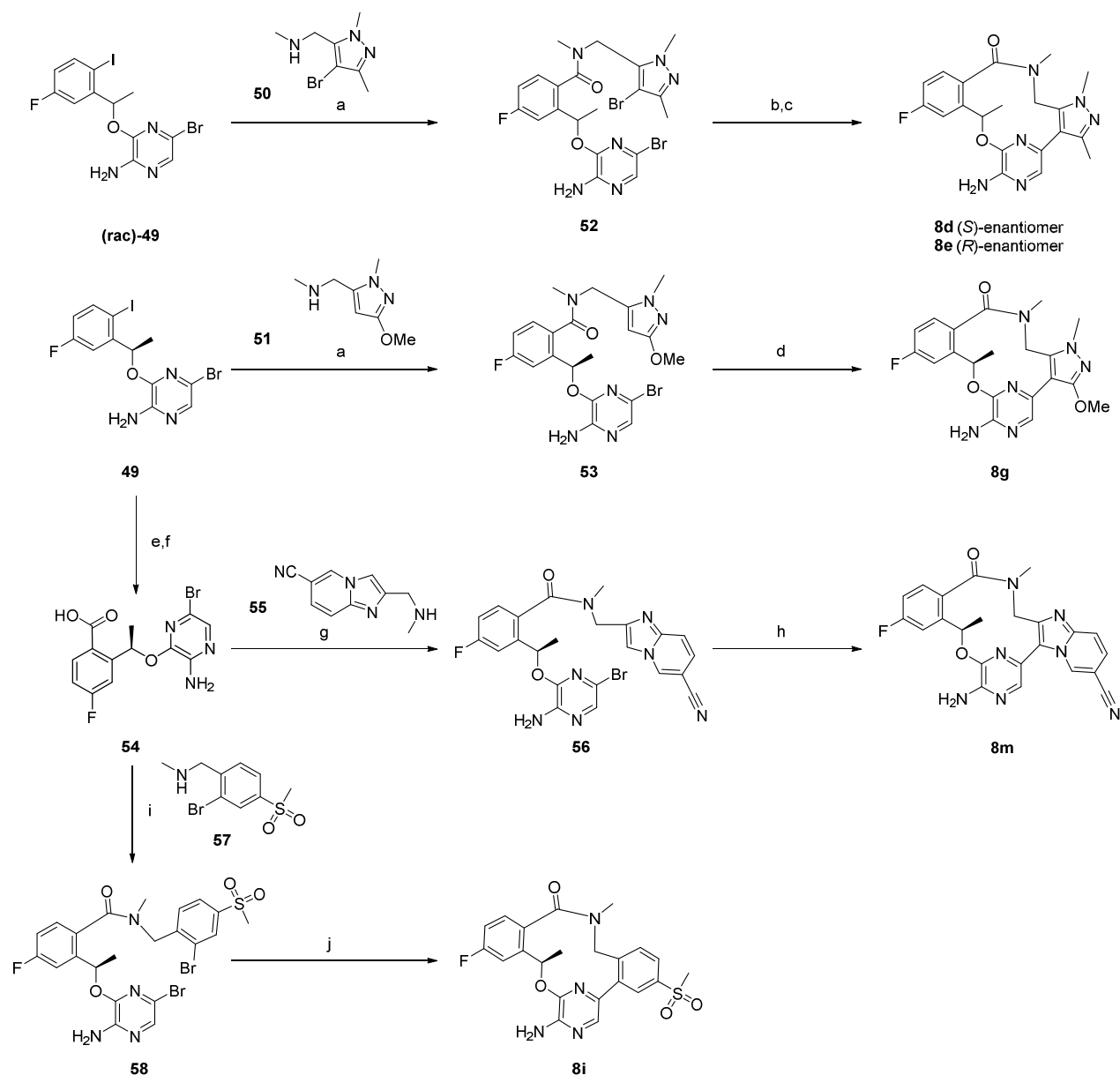
Reagents and conditions: (a) 20 mol% CataCXium A, 10 mol% Pd(OAc)<sub>2</sub>, 1.24 eq **45**, 1.5 eq B<sub>2</sub>pin<sub>2</sub>, 5 eq CsF, MeOH, H<sub>2</sub>O, 60 °C, 3 h, 43%; (b) NaOH, MeOH, H<sub>2</sub>O, 40 °C, 3.5 h, 87%; (c) 4 M HCl in dioxane, MeOH, 40 °C, 2.5 h, 87%; (d) for compound **8k**, 1.4 eq HATU, 10 eq DIPEA, DMF, 0 °C, 30 min, slow reverse addition, 29%. Macrocycles **8a-c**, **8f**, **8h**, **8j** and **8l** were prepared in an analogous manner.

The importance of the conformation of the precursor to cyclization in the overall success of the macrocyclization is illustrated in the case of **8a** and **8c** (Table 3). The presence of the chiral methyl in compound **8a** provided a 10-fold improvement in yield of the cyclization (22% vs. 2%), and this is observed as a trend throughout the series. Preliminary conformational studies on these two molecules indicate that the benzylic chiral center methyl substituent enables a preferred conformation by A-1,3 strain,<sup>52</sup> which allows the acid and amine termini of the molecule to be in close proximity for cyclization to take place. Interestingly, **8c** exists as a pair of

1  
2  
3 atropisomers<sup>53</sup> in this case, which can be separated by chiral SFC. The atropisomerism is  
4  
5 observed by <sup>1</sup>H NMR, but after SFC separation the distinct atropisomers convert back to an  
6  
7 equilibrium 50/50 mixture upon standing for several weeks at room temperature.  
8  
9

10 An alternative approach was developed to the amide-macrocycles featuring the aminopyrazine  
11 hinge-binding motif (**8d**, **8e**, **8g**, **8i**, **8m**). For these molecules, the critical ring closure step is  
12 hinge-binding motif (**8d**, **8e**, **8g**, **8i**, **8m**). For these molecules, the critical ring closure step is  
13 achieved through formation of the aryl-aryl bond as shown in Scheme 5 either *via* an  
14  
15 intramolecular Suzuki coupling<sup>54</sup> or a direct arylation type process.<sup>50</sup> Selective amino-  
16  
17 carbonylation<sup>55</sup> of (**rac**)-**49** with pyrazole **50** afforded amide **52**. Ring closure *via* an *in situ*  
18  
19 Suzuki coupling approach lead to the racemic product, which after chiral separation gave  
20  
21 compounds **8d** and **8e**. A similar amino-carbonylation of **49** with **51** gave intermediate amide **53**,  
22  
23 which was subjected to a direct arylation type process to afford **8g**. From reaction screening  
24  
25 studies, it was determined that cataCXium A was crucial to enable this reaction to take place in  
26  
27 DMF. Subsequent optimization indicated that solvent played a crucial role and that *t*-AmOH as  
28  
29 solvent<sup>56</sup> with the reaction performed in a pressure vessel avoided the need for high dilution  
30  
31 conditions. The yields within the program varied depending on the substrate employed with the  
32  
33 best yields being observed with substrates possessing an adjacent C3 substituent capable of  
34  
35 directing C-H activation.<sup>57</sup> Carbonylation of the iodide **49** in the presence of methanol followed  
36  
37 by hydrolysis provided the intermediate **54**. Condensation of **54** with **55** under standard amide  
38  
39 coupling conditions provided amide **56**, which was converted to compound **8m** by a direct  
40  
41 arylation process. In a similar manner, condensation of **54** with **57** provided amide **58**, which was  
42  
43 converted to compound **8i** by an *in situ* Suzuki coupling.  
44  
45  
46  
47  
48  
49  
50  
51  
52  
53  
54

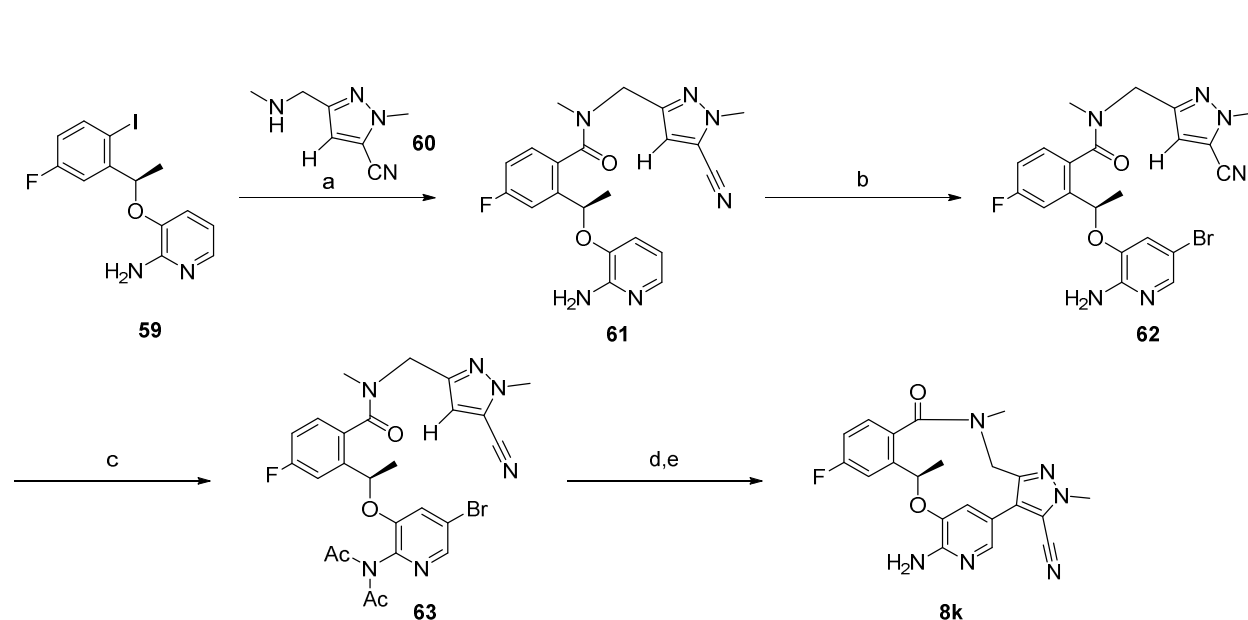
55 **Scheme 5.** Synthesis of the Pyrazine Amide Macrocycles **8d**, **8e**, **8g**, **8i** and **8m**  
56  
57  
58  
59  
60



Reagents and conditions: (a) for synthesis of **52**, 1.25 eq **50**, 10 mol% Pd(P<sup>t</sup>Bu<sub>3</sub>)<sub>2</sub>, 5 eq DIPEA, toluene, 85 °C, 4 bar CO, 18 h, 21%; (b) 20 mol% cataCXium A, 10 mol% Pd(OAc)<sub>2</sub>, 5 eq B<sub>2</sub>pin<sub>2</sub>, 5 eq CsF, MeOH, H<sub>2</sub>O, 90 °C, 6 h, 11%; (c) Chiral SFC, Chiralcel OD-H 25% MeOH @ 140 bar, 3 mL/min; (d) 20 mol% cataCXium A, 10 mol% Pd(OAc)<sub>2</sub>, 5 eq KOAc, 0.25 eq PivOH, DMF, 150 °C, 1 h, 8%; (e) 5 mol% Pd(OAc)<sub>2</sub>, 10 mol% DPE-Phos, 5 eq DIPEA, MeOH, 50 °C, 4 bar CO, 3 h, 77%; (f) 5 eq NaOH, MeOH/THF/H<sub>2</sub>O (5 : 2 : 1), rt, 15 h, 89%; (g) 1.1 eq **55**, 1.5 eq EDCl, 1.5 eq HOBT, 5 eq DIPEA, DMF, -30 °C to rt, 15 h, 46%; (h) 20 mol% cataCXium A, 10 mol% Pd(OAc)<sub>2</sub>, 10 mol% *t*-AmOH, 5 eq KOAc, DMA, 110 °C, 12 h, 12%; (i) 1.1 eq **57**, 1.1 eq HATU, 4 eq DIPEA, DMF, rt 12 h, 94%; (j) 20 mol% cataCXium A, 10 mol% Pd(OAc)<sub>2</sub>, 3 eq B<sub>2</sub>pin<sub>2</sub>, 5 eq K<sub>2</sub>CO<sub>3</sub>, THF, 80 °C, 6 h, 8%.

1  
2  
3 This methodology has also been extended to the analogous pyridine-based macrocycles (such  
4 as **8k**) though judicious protection of the aminopyridine is required in order to effect the directed  
5 arylation as shown in Scheme 6. The iodide **59** can be accessed in three steps from readily  
6 available starting materials. Amino-carbonylation in the presence of **60**, under similar conditions  
7 to those employed for the transformation of **49** to **53** (Scheme 5), allowed access to **61**.  
8 Bromination using a slight excess of NBS at -10 °C formed the desired cyclization precursor **62**  
9 in a regioselective fashion. Attempts to directly cyclize **62** led to only minor amounts of the  
10 desired product **8k** with the major product resulting from des-halogenation. To overcome this  
11 unproductive reaction pathway, the aminopyridine was protected as the *bis*-acetamide derivative.  
12 Heating **62** with acetic anhydride as solvent allowed **63** to be obtained after solvent evaporation  
13 and azeotropic distillation with toluene. The optimal conditions for the direct arylation described  
14 previously utilized *t*-AmOH as the solvent (0.1 M concentration) with no additive being  
15 required.<sup>58</sup> The reaction went to completion in a sealed vessel on heating overnight with a  
16 mixture of **8k**, and the corresponding mono- and bis-protected derivatives of the desired product  
17 were obtained. The crude mixture of products was subjected to exhaustive acid-mediated  
18 deprotection to provide **8k** in a 42% yield over two steps.  
19  
20  
21  
22  
23  
24  
25  
26  
27  
28  
29  
30  
31  
32  
33  
34  
35  
36  
37  
38  
39  
40  
41  
42  
43  
44

45 **Scheme 6.** Synthesis of **8k** by Directed Arylation.  
46  
47  
48  
49  
50  
51  
52  
53  
54  
55  
56  
57  
58  
59  
60



Reagents and conditions: (a) 5 mol% Pd(P<sup>t</sup>Bu<sub>3</sub>)<sub>2</sub>, 3 eq DIPEA, 1.1 eq **60**, toluene, 80 °C, 4 bar CO, 18 h, 70%; (b) 1.1 eq NBS, THF, -10 °C, 2 h, 86%; (c) Acetic anhydride, 100 °C, 8 h, quant.; (d) 20 mol% cataCXium A, 10 mol% Pd(OAc)<sub>2</sub>, 5 eq KOAc, *t*-AmOH, 130 °C, 14 h; (e) 10 eq 4 N HCl in dioxane, MeOH, 60 °C, 14 h, 42% over 2 steps.

## CONCLUSION

The challenges associated with overlapping potency against resistant mutants of ALK and CNS exposure in kinase inhibitor chemical space required a special approach. Utilizing structure based drug design, a unique macrocyclic template was discovered leading to the development of amido-linked 12-membered macrocycles possessing significantly increased lipophilic efficiencies relative to acyclic analogues. This increase in efficiency was the foundation for overlapping broad spectrum potency and desirable ADME, including CNS availability. Diverse synthetic approaches were adopted to access the novel macrocycles, and reactivity trends emerged which guided efforts toward optimal methods to close the ring. In addition, we believe this to be the first report of a macrocyclic ring closure achieved by a palladium-catalyzed direct arylation. This work culminated in **8k**, a novel macrocyclic ALK inhibitor with excellent

1  
2  
3 potency, selectivity, ADME and CNS availability. Compound **8k** is currently in Phase 1/2  
4 clinical trials (<http://clinicaltrials.gov/ct2/show/NCT01970865>).  
5  
6  
7  
8  
9

## 10 EXPERIMENTAL METHODS

11  
12 Starting materials and other reagents were purchased from commercial suppliers and were  
13 used without further purification unless otherwise indicated. Compound **6a** (PF-06439015) is  
14 now commercially available from Sigma Aldrich. The syntheses of **6a**, **6b**, **6c**, **6d**, **6g** and **6i**  
15 have been reported in the literature.<sup>24a,30</sup> The syntheses of **6e**, **6f** and **6h** and the intermediates  
16 utilized here (**9**, **10**, **17**, **20**, **21**, **30**, **31**, **44**, **45**, **49**, **50**, **51**, **55**, **57**, **59**, **60**, **69** – **75**) are described in  
17 the Supporting Information. All reactions were performed under a positive pressure of nitrogen,  
18 argon, or with a drying tube, at ambient temperature (unless otherwise stated), in anhydrous  
19 solvents, unless otherwise indicated. Analytical thin-layer chromatography was performed on  
20 glass-backed Silica Gel 60\_F 254 plates (Analtech (0.25 mm)) and eluted with the appropriate  
21 solvent ratios (v/v). The reactions were assayed by high-performance liquid chromatography  
22 (HPLC) or thin-layer chromatography (TLC) and terminated as judged by the consumption of  
23 starting material. The TLC plates were visualized by UV, phosphomolybdic acid stain, or iodine  
24 stain. Microwave assisted reactions were run in a Biotage Initiator. <sup>1</sup>H NMR spectra were  
25 recorded on a Bruker instrument operating at 400 MHz unless otherwise indicated. <sup>1</sup>H NMR  
26 spectra are obtained as DMSO-*d*<sub>6</sub> or CDCl<sub>3</sub> solutions as indicated (reported in ppm), using  
27 chloroform as the reference standard (7.25 ppm) or DMSO-*d*<sub>6</sub> (2.50 ppm). Other NMR solvents  
28 were used as needed. When peak multiplicities are reported, the following abbreviations are  
29 used: s = singlet, d = doublet, t = triplet, m = multiplet, br = broadened, dd = doublet of doublets,  
30 dt = doublet of triplets. Coupling constants, when given, are reported in hertz. The mass spectra  
31  
32  
33  
34  
35  
36  
37  
38  
39  
40  
41  
42  
43  
44  
45  
46  
47  
48  
49  
50  
51  
52  
53  
54  
55  
56  
57  
58  
59  
60

1  
2  
3 were obtained using liquid chromatography mass spectrometry (LC-MS) on an Agilent  
4 instrument using atmospheric pressure chemical ionization (APCI) or electrospray ionization  
5 (ESI). High resolution mass measurements were carried out on an Agilent TOF 6200 series with  
6  
7  
8  
9  
10  
11  
12  
13  
14  
15  
16  
17  
18  
19  
20  
21  
22  
23  
24  
25  
26  
27  
28  
29  
30  
31  
32  
33  
34  
35  
36  
37  
38  
39  
40  
41  
42  
43  
44  
45  
46  
47  
48  
49  
50  
51  
52  
53  
54  
55  
56  
57  
58  
59  
60  
were obtained using liquid chromatography mass spectrometry (LC-MS) on an Agilent instrument using atmospheric pressure chemical ionization (APCI) or electrospray ionization (ESI). High resolution mass measurements were carried out on an Agilent TOF 6200 series with ESI. All test compounds showed > 95% purity as determined by combustion analysis or by high-performance liquid chromatography (HPLC). HPLC conditions were as follows: XBridge C18 column @ 80 °C, 4.6 mm x 150 mm, 5 µm, 5%-95% MeOH/H<sub>2</sub>O buffered with 0.2% formic acid/0.4% ammonium formate, 3 min run, flow rate 1.2 mL/min, UV detection (λ = 254, 224 nm). Combustion analyses were performed by Atlantic Microlab, Inc. (Norcross, Georgia).

*Ethyl-3-{2-[4-fluoro-2-(hydroxymethyl)phenoxy]ethyl}-1H-pyrazole-5-carboxylate (11)*. Ethyl diazoacetate (1.18 mL, 11.1 mmol) and **9** (2 g, 10.3 mmol – see Supporting Information) were heated at 100 °C in a sealed tube for 18 h. The crude product was purified by flash chromatography on silica gel eluting with EtOAc/heptanes (0 - 80%) to give **11** (1.56 g, 49% yield) as a cream solid, with a second fraction being eluted as a yellow gum (451 mg) containing 40% of the desired regioisomer. <sup>1</sup>H NMR (400 MHz, DMSO-*d*<sub>6</sub>) δ 13.29 (br s, 1 H), 7.13 (dd, *J* = 9.4, 2.6 Hz, 1 H), 7.06 - 6.89 (m, 2 H), 6.63 (br s, 1 H), 5.34 - 4.95 (m, 1 H), 4.40 (s, 2 H), 4.25 (d, *J* = 6.6 Hz, 2 H), 4.22 - 4.13 (m, 2 H), 3.07 (br s, 2 H), 1.28 (t, *J* = 7.0 Hz, 3 H).

*Ethyl 3-{3-[4-fluoro-2-(hydroxymethyl)phenoxy]propyl}-1H-pyrazole-5-carboxylate (12)*. The procedure used to prepare compound **11** was used to prepare compound **12** as a 4:1 regioisomeric mixture of pyrazoles from compound **10** (see Supporting Information), which was used without further purification.

*3-{3-[4-Fluoro-2-(hydroxymethyl)phenoxy]ethyl}-1H-pyrazole-5-carbonitrile (13)*. In a sealed tube, a solution of **11** (1.55 g, 5.0 mmol) in MeOH (20 mL) was heated at 60 °C for 1 h. Ammonium hydroxide (10 mL) was added and the solution was heated at 60 °C overnight. The

1  
2  
3 reaction mixture was concentrated, cooled to 0 °C and the solids collected by vacuum filtration  
4  
5 to give the intermediate primary amide (933 mg, 67% yield). To a cooled (0 °C) mixture of the  
6  
7 intermediate primary amide (930 mg, 3.33 mmol) in pyridine (16.6 mL) was added TFAA (1.87  
8  
9 mL, 13.3 mmol) in a drop-wise manner. After 1 h at 0 °C the solution was diluted with EtOAc  
10  
11 (100 mL), washed with saturated NaHCO<sub>3</sub> (2 x 25 mL), 1 N HCl (2 x 25 mL), brine (25 mL),  
12  
13 dried (Na<sub>2</sub>SO<sub>4</sub>), filtered and concentrated under reduced pressure. The resulting solid was  
14  
15 slurried in 50% EtOAc/heptanes, and filtered to afford **13** (703 mg, 81% yield) as a cream solid.  
16  
17  
18  
19  
20 <sup>1</sup>H NMR (400 MHz, DMSO-*d*<sub>6</sub>) δ 13.77 (br s, 1 H), 7.13 (dd, *J* = 9.6, 3.0 Hz, 1 H), 7.05 – 6.91  
21  
22 (m, 2 H), 6.82 (s, 1 H), 4.37 (s, 2 H), 4.19 (t, *J* = 6.3 Hz, 2 H), 3.10 (t, *J* = 6.2 Hz, 2 H).  
23

24  
25 *3-{3-[4-Fluoro-2-(hydroxymethyl)phenoxy]propyl}-1H-pyrazole-5-carbonitrile* (**14**). The  
26  
27 procedure used to prepare compound **13** was used to prepare compound **14**. <sup>1</sup>H NMR (400 MHz,  
28  
29 DMSO-*d*<sub>6</sub>) δ 13.71 (br s, 1 H), 7.14 (dd, *J* = 9.4, 3.1 Hz, 1 H), 7.03 - 6.94 (m, 1 H), 6.94 - 6.88  
30  
31 (m, 1 H), 6.76 (s, 1 H), 4.48 (s, 2 H), 3.96 (t, *J* = 6.0 Hz, 2 H), 2.82 (t, *J* = 7.7 Hz, 2 H), 2.12 -  
32  
33 1.96 (m, 2 H).  
34  
35

36  
37 *3-{3-[4-Fluoro-2-(hydroxymethyl)phenoxy]ethyl}-4-iodo-1H-pyrazole-5-carbonitrile* (**15**). To  
38  
39 a solution of **13** (650 mg, 2.5 mmol) and cerium ammonium nitrate (954 mg, 1.74 mmol) in  
40  
41 MeCN (25 mL) was added a solution of iodine (442 mg, 1.74 mmol) in MeCN (5 mL). The  
42  
43 reaction was heated at 60 °C and stirred for 2 h. The reaction mixture was diluted with EtOAc  
44  
45 (100 mL), washed with saturated Na<sub>2</sub>S<sub>2</sub>O<sub>3</sub> (2 x 25 mL) and brine (25 mL), dried (Na<sub>2</sub>SO<sub>4</sub>),  
46  
47 filtered and concentrated. The resulting solids were triturated with 30% EtOAc/heptanes to  
48  
49 afford **15** (632 mg, 66% yield) as a cream solid, which contained ~5% of the aldehyde. <sup>1</sup>H NMR  
50  
51 (400 MHz, DMSO-*d*<sub>6</sub>) δ 7.13 (dd, *J* = 9.4, 3.2 Hz, 1 H), 7.05 - 6.91 (m, 2 H), 4.34 (s, 2 H), 4.20  
52  
53 (t, *J* = 6.2 Hz, 2 H), 3.10 (t, *J* = 6.2 Hz, 2 H).  
54  
55  
56  
57  
58  
59  
60

1  
2  
3  
4  
5  
6  
7  
8  
9  
10  
11  
12  
13  
14  
15  
16  
17  
18  
19  
20  
21  
22  
23  
24  
25  
26  
27  
28  
29  
30  
31  
32  
33  
34  
35  
36  
37  
38  
39  
40  
41  
42  
43  
44  
45  
46  
47  
48  
49  
50  
51  
52  
53  
54  
55  
56  
57  
58  
59  
60

*3-{3-[4-Fluoro-2-(hydroxymethyl)phenoxy]propyl}-4-iodo-1H-pyrazole-5-carbonitrile* (**16**).

The procedure used to prepare compound **15** was used to prepare compound **16**. <sup>1</sup>H NMR (400 MHz, DMSO-*d*<sub>6</sub>) δ 7.15 (dd, *J* = 9.4, 3.1 Hz, 1 H), 7.02 - 6.94 (m, 1 H), 6.91 - 6.87 (m, 1 H), 4.50 (s, 2 H), 3.94 (t, *J* = 5.9 Hz, 2 H), 2.81 (t, *J* = 7.6 Hz, 2 H), 2.08 - 1.99 (m, 2 H).

*tert-Butyl [3-({2-[3-(5-cyano-4-iodo-1H-pyrazol-3-yl)ethoxy]-5-fluorobenzyl}oxy)-5-iodopyridin-2-yl]carbamate* (**18**). To a solution of **15** (625 mg, 1.65 mmol), *tert*-butyl (3-hydroxy-5-iodopyridin-2-yl)carbamate **17** (624 mg, 1.86 mmol) and triphenylphosphine (635 mg, 2.42 mmol) in THF (6.7 mL) was added DIAD (494 μL, 2.42 mmol) drop-wise over 1 h. Once the reaction was complete by LC-MS, the solution was concentrated and purified by flash chromatography eluting with EtOAc/heptanes (0 - 50%). The fractions containing the desired product were concentrated and the solids were triturated with Et<sub>2</sub>O to give **18** (181 mg, 16% yield) as a white solid. <sup>1</sup>H NMR (400 MHz, DMSO-*d*<sub>6</sub>) δ 14.23 (br s, 1 H), 9.03 (s, 1 H), 8.17 (d, *J* = 1.8 Hz, 1 H), 7.74 (d, *J* = 1.8 Hz, 1 H), 7.33 (dd, *J* = 9.3, 3.0 Hz, 1 H), 7.19 - 6.96 (m, 2 H), 5.00 (s, 2 H), 4.25 (t, *J* = 6.3 Hz, 2 H), 3.16 (t, *J* = 6.2 Hz, 2 H), 1.41 (s, 9 H).

*tert-Butyl [3-({2-[3-(5-cyano-4-iodo-1H-pyrazol-3-yl)propoxy]-5-fluorobenzyl}oxy)-5-iodopyridin-2-yl]carbamate* (**19**). The procedure used to prepare compound **18** was used to prepare compound **19**. <sup>1</sup>H NMR (400 MHz, DMSO-*d*<sub>6</sub>) δ 14.14 (br s, 1 H), 9.00 (s, 1 H), 8.15 (d, *J* = 1.5 Hz, 1 H), 7.80 (d, *J* = 1.5 Hz, 1 H), 7.35 (dd, *J* = 9.2, 3.2 Hz, 1 H), 7.13 (td, *J* = 8.8, 3.2 Hz, 1 H), 7.02 (dd, *J* = 9.2, 4.4 Hz, 1 H), 5.12 (s, 2 H), 4.02 (t, *J* = 5.7 Hz, 2 H), 2.85 (t, *J* = 7.4 Hz, 2 H), 2.15 - 1.99 (m, 2 H), 1.40 (s, 9 H).

*7-Amino-12-fluoro-16,17-dihydro-1H,10H-8,4-(metheno)pyrazolo-[3,4-d][1,11,8]benzodioxacyclotetradecine-3-carbonitrile* (**7a**). To a sealed vial was added **18** (175 mg, 0.25 mmol), B<sub>2</sub>pin<sub>2</sub> (315 mg, 1.24 mmol), and CsF (188 mg, 1.24 mmol) in MeOH (12 mL)

1  
2  
3 and water (1.2 mL), and the mixture was bubbled with nitrogen. A solution of *bis*(di-*tert*-butyl(4-  
4 dimethylaminophenyl)phosphine)dichloropalladium (II) (26 mg, 0.037 mmol) in toluene (0.8  
5 mL) was added. The mixture was heated at 60 °C for 1 h then diluted with EtOAc (100 mL),  
6 washed with brine (2 x 25 mL), dried (Na<sub>2</sub>SO<sub>4</sub>), filtered, and concentrated. The residue was  
7 dissolved in CH<sub>2</sub>Cl<sub>2</sub> (2 mL) and HCl was added (4 N in dioxane, 2 mL, 4.2 mmol). After stirring  
8 at room temperature overnight, the reaction was concentrated and purified by flash  
9 chromatography on silica gel eluting with 7 N NH<sub>3</sub> MeOH/ CH<sub>2</sub>Cl<sub>2</sub> (0 - 10%). The fractions  
10 containing the desired product were concentrated and the resultant solids were triturated with  
11 Et<sub>2</sub>O to give **7a** (25 mg, 29% yield) as a yellow solid. LC-MS (ESI), *m/z* 352 [M+H]<sup>+</sup>; <sup>1</sup>H NMR  
12 (400 MHz, DMSO-*d*<sub>6</sub>) δ 13.46 (s, 1 H), 7.86 (d, *J* = 1.8 Hz, 1 H), 7.67 (d, *J* = 1.8 Hz, 1 H), 7.37  
13 (dd, *J* = 9.1, 3.0 Hz, 1 H), 7.19 – 7.02 (m, 2 H), 5.54 (br s, 2 H), 5.19 (br s, 2 H), 4.51 (br s, 2 H),  
14 3.17 - 3.06 (m, 2 H).  
15  
16  
17  
18  
19  
20  
21  
22  
23  
24  
25  
26  
27  
28  
29  
30  
31

32 *7-Amino-12-fluoro-1,16,17,18-tetrahydro-10H-8,4-(metheno)pyrazolo[3,4-*  
33 *e][1,12,9]benzodioxazacyclopentadecine-3-carbonitrile (7b)*. The procedure used to prepare  
34 compound **7a** was used to prepare compound **7b** from **19**. LC-MS (APCI) *m/z* 366 [M+H]<sup>+</sup>; <sup>1</sup>H  
35 NMR (400 MHz, DMSO-*d*<sub>6</sub>) δ 13.88 (br s, 1 H), 7.75 (d, *J* = 1.8 Hz, 1 H), 7.38 (d, *J* = 2.0 Hz, 1  
36 H), 7.30 (dd, *J* = 8.9, 2.4 Hz, 1 H), 7.16 - 7.04 (m, 2 H), 5.90 (s, 2 H), 5.21 (br s, 2 H), 4.55 -  
37 3.55 (m, 2 H), 3.03 (br s, 2 H), 2.23 (br s, 2 H).  
38  
39  
40  
41  
42  
43  
44  
45

46 *6-(4-{4-[4-Fluoro-2-(hydroxymethyl)phenoxy]prop-1-yn-1-yl}-1-methyl-1H-pyrazol-5-*  
47 *yl)[1,3]oxazolo[4,5-b]pyridin-2(3H)-one (22)*. A mixture of **20** (270 mg, 0.65 mmol - see  
48 Supporting Information), **21** (176 mg, 0.97 mmol - see Supporting Information), cuprous iodide  
49 (6 mg, 0.032 mmol), triphenyl phosphine (17 mg, 0.065 mmol) and PdCl<sub>2</sub>(PPh<sub>3</sub>)<sub>2</sub> (23 mg, 0.032  
50 mmol) in piperidine (4.3 mL) was bubbled with nitrogen, and then heated in an oil bath to 90 °C.  
51  
52  
53  
54  
55  
56  
57  
58  
59  
60

1  
2  
3 After 5 h, the reaction was allowed to cool, and diluted with EtOAc (100 mL). The solution was  
4  
5 washed with saturated aqueous NH<sub>4</sub>Cl (2 x 50 mL), brine (25 mL) and the organics dried over  
6  
7 MgSO<sub>4</sub>. The solution was filtered, concentrated, and the residue subjected to column  
8  
9 chromatography over silica gel (0 - 5% MeOH/ CH<sub>2</sub>Cl<sub>2</sub>) to afford **22** as a gummy solid  
10  
11 contaminated with excess piperidine. This material was used without further purification in the  
12  
13 following step.  
14  
15

16  
17 *6-(4-{4-[4-Fluoro-2-(hydroxymethyl)phenoxy]but-1-yn-1-yl}-1-methyl-1H-pyrazol-5-*  
18  
19 *yl)[1,3]oxazolo[4,5-b]pyridin-2(3H)-one (23)*. The procedure used to prepare compound **22** was  
20  
21 used to prepare compound **23** from **9** (see Supporting Information). LC-MS (APCI), *m/z* 409  
22  
23 [M+H]<sup>+</sup>; <sup>1</sup>H NMR (400 MHz, DMSO-*d*<sub>6</sub>) δ 9.22 (s, 1 H), 8.06 (d, *J* = 2.01 Hz, 1 H), 7.64 (s, 1  
24  
25 H) 7.45 (d, *J* = 1.76 Hz, 1 H), 7.13 (dd, *J* = 9.32, 2.77 Hz, 1 H), 7.01 – 6.92 (m, 2 H), 5.13 (br s,  
26  
27 1 H), 4.48 (d, *J* = 2.27 Hz, 2 H), 4.06 (t, *J* = 6.67 Hz, 2 H), 3.82 (s, 3 H), 2.78 (t, *J* = 6.55 Hz, 2  
28  
29 H), 4.48 (d, *J* = 2.27 Hz, 2 H), 4.06 (t, *J* = 6.67 Hz, 2 H), 3.82 (s, 3 H), 2.78 (t, *J* = 6.55 Hz, 2  
30  
31 H).  
32  
33

34  
35 *6-(4-{3-[4-Fluoro-2-(hydroxymethyl)phenoxy]propyl}-1-methyl-1H-pyrazol-5-*  
36  
37 *yl)[1,3]oxazolo[4,5-b]pyridin-2(3H)-one (24)*. Compound **22** (256 mg, 0.65 mmol) was  
38  
39 dissolved in ethanol (50 mL), and palladium hydroxide (50 mg, 20% on carbon) added. The  
40  
41 mixture was flushed with nitrogen, followed by being pressurized under 3-4 bar of hydrogen gas.  
42  
43 The reaction was agitated, and heated at 50 °C for 18 h. The reaction vessel was allowed to cool,  
44  
45 and LC-MS indicated that the major product was the desired **24** accompanied by minor amounts  
46  
47 of the ethyl carbamate. The reaction was filtered through a Celite cartridge to remove the  
48  
49 catalyst, and washed with MeOH. The filtrate was concentrated to afford crude **24**, which was  
50  
51 used without further purification.  
52  
53  
54  
55  
56  
57  
58  
59  
60

1  
2  
3  
4  
5  
6  
7  
8  
9  
10  
11  
12  
13  
14  
15  
16  
17  
18  
19  
20  
21  
22  
23  
24  
25  
26  
27  
28  
29  
30  
31  
32  
33  
34  
35  
36  
37  
38  
39  
40  
41  
42  
43  
44  
45  
46  
47  
48  
49  
50  
51  
52  
53  
54  
55  
56  
57  
58  
59  
60

6-(4-{3-[4-Fluoro-2-(hydroxymethyl)phenoxy]butyl}-1-methyl-1H-pyrazol-5-yl)[1,3]oxazolo[4,5-b]pyridin-2(3H)-one (**25**). The procedure used to prepare compound **24** was used to prepare compound **25**, which was used without further purification.

2-Amino-5-(4-{4-[4-fluoro-2-(hydroxymethyl)phenoxy]propyl}-1-methyl-1H-pyrazol-5-yl)pyridin-3-ol (**26**). Compound **24** was dissolved in ethanol (5 mL), and 15% aqueous NaOH (5 mL) was added. The reaction was heated at 85 °C for 12 h, and allowed to cool. The mixture was neutralized with 1 N aqueous HCl, and extracted with EtOAc (3 x 100 mL). The organics were dried over MgSO<sub>4</sub>, concentrated, and purified by column chromatography over silica gel (0 - 10% MeOH/CH<sub>2</sub>Cl<sub>2</sub>) to afford **26** (82 mg, 34% yield over 3 steps) as a colorless solid. LC-MS (APCI), *m/z* 372.2 [M+H]<sup>+</sup>; <sup>1</sup>H NMR (400 MHz, DMSO-*d*<sub>6</sub>) δ 9.72 (br s, 1 H), 7.41 (s, 1 H), 7.33 (s, 1 H), 7.12 (dd, *J* = 9.6, 3.0 Hz, 1 H), 7.00 - 6.89 (m, 1 H), 6.83 (dd, *J* = 9.1, 4.5 Hz, 1 H), 6.80 (d, *J* = 1.5 Hz, 1 H), 5.75 (s, 2 H), 5.11 (br. s, 1 H), 4.43 (br s, 2 H), 3.87 (t, *J* = 6.2 Hz, 2 H), 3.64 (s, 3 H), 2.49 - 2.42 (m, 2 H), 1.85 (q, *J* = 6.9 Hz, 2 H).

2-Amino-5-(4-{4-[4-fluoro-2-(hydroxymethyl)phenoxy]butyl}-1-methyl-1H-pyrazol-5-yl)pyridin-3-ol (**27**). The procedure used to prepare compound **26** was used to prepare compound **27**. LC-MS (APCI), *m/z* 387 [M+H]<sup>+</sup>; <sup>1</sup>H NMR (400 MHz, DMSO-*d*<sub>6</sub>) δ 9.72 (br s, 1 H), 7.41 (d, *J* = 1.76 Hz, 1 H), 7.33 (s, 1 H), 7.12 (dd, *J* = 9.44, 3.15 Hz, 1 H), 7.02 - 6.91 (m, 1 H), 6.85 (dd, *J* = 8.81, 4.53 Hz, 1 H), 6.79 (d, *J* = 2.01 Hz, 1 H), 5.75 (s, 2 H), 5.13 (br s, 1 H), 4.45 (s, 2 H), 3.87 (t, *J* = 6.04 Hz, 2 H), 3.64 (s, 3 H), 2.35 (t, *J* = 7.30 Hz, 2 H), 1.74 - 1.47 (m, 4 H).

2-Amino-5-(4-{4-[4-fluoro-2-(hydroxymethyl)phenoxy]propyl}-1-methyl-1H-pyrazol-5-yl)pyridin-3-yl methanesulfonate (**28**). To a cooled (0 °C) solution of **26** (80 mg, 0.22 mmol) in CH<sub>2</sub>Cl<sub>2</sub> (1.4 mL) was added pyridine (200 μL, 2.5 mmol), and a catalytic amount of DMAP (2-3 mg), followed by a solution of MsCl (17 μL, 0.22 mmol) in CH<sub>2</sub>Cl<sub>2</sub> (0.5 mL). The reaction was

1  
2  
3 allowed to slowly warm to room temperature. After 2 h, the reaction was diluted with EtOAc (10  
4 mL), and washed with saturated aqueous NH<sub>4</sub>Cl (5 mL) and brine (5 mL). The organics were  
5  
6 dried (MgSO<sub>4</sub>), filtered and concentrated. After being dried overnight under high vacuum, **28** (96  
7  
8 mg) was isolated as a slightly yellow gum, which was used without purification in the cyclization  
9  
10 step.  
11  
12

13  
14  
15 *2-Amino-5-(4-{4-[4-fluoro-2-(hydroxymethyl)phenoxy]butyl}-1-methyl-1H-pyrazol-5-*  
16  
17 *yl)pyridin-3-yl methanesulfonate (29)*. The procedure used to prepare compound **28** was used to  
18  
19 prepare compound **29**, which was used without purification in the cyclization step.  
20  
21

22  
23 *12-Fluoro-3-methyl-3,16,17,18-tetrahydro-10H-8,4-(metheno)pyrazolo[4,3-*  
24  
25 *e][1,12,9]benzodioxazacyclopentadecin-7-amine (7c)*. To a solution of **28** (96 mg, 0.21 mmol) in  
26  
27 DMF (4.1 mL) was added NaH (9.1 mg, 60% dispersion in mineral oil, 0.23 mmol). The reaction  
28  
29 was heated at 50 °C for 30 min. The reaction was diluted with EtOAc (10 mL), washed with  
30  
31 saturated aqueous NH<sub>4</sub>Cl/water mixture (1 : 1, 5 mL), brine (5 mL), dried (MgSO<sub>4</sub>), filtered and  
32  
33 concentrated. The residue was purified by column chromatography over silica gel (0 - 10%  
34  
35 MeOH/CH<sub>2</sub>Cl<sub>2</sub>) to afford **7c** (27 mg, 37% yield over 2 steps) as a cream solid. LC-MS (APCI),  
36  
37 *m/z* 355 [M+H]<sup>+</sup>; <sup>1</sup>H NMR (400 MHz, DMSO-*d*<sub>6</sub>) δ 7.65 (d, *J* = 1.5 Hz, 1 H), 7.38 (s, 1 H), 7.36  
38  
39 - 7.25 (m, 2 H), 7.16 – 6.99 (m, 2 H), 5.68 (br s, 2 H), 5.22 (s, 2 H), 4.14 - 3.97 (m, 2 H), 3.78 (s,  
40  
41 3 H), 2.65 (t, *J* = 6.8 Hz, 2 H), 2.20 - 2.04 (m, 2 H).  
42  
43  
44  
45

46  
47 *12-Fluoro-3-methyl-16,17,18,19-tetrahydro-3H,10H-8,4-(metheno)-pyrazolo[4,3-*  
48  
49 *ff][1,13,10]benzodioxazacyclohexadecin-7-amine (7d)*. The procedure used to prepare compound  
50  
51 **7c** was used to prepare compound **7d** from **29**. LC-MS (APCI), *m/z* 369 [M+H]<sup>+</sup>; <sup>1</sup>H NMR (400  
52  
53 MHz, 80 °C, DMSO-*d*<sub>6</sub>) δ 7.57 - 7.50 (m, 2 H), 7.33 - 7.29 (m, 2 H), 7.09 - 7.00 (m, 1 H), 7.00 -  
54  
55  
56  
57  
58  
59  
60

6.92 (m, 1 H), 5.77 (br s, 2 H), 5.28 (s, 2 H), 4.02 (t,  $J = 5.54$  Hz, 2 H), 3.69 (s, 3 H), 2.34 - 2.18 (m, 2 H), 1.89 - 1.71 (m, 4 H).

*Ethyl 3-[2-(2-acetyl-4-fluorophenoxy)ethyl]-1H-pyrazole-5-carboxylate (32)*. 1-[2-(But-3-yn-1-yloxy)-5-fluorophenyl]ethanone **30** (1.43 g, 6.94 mmol - see Supporting Information) and ethyl diazoacetate (0.87 g, 7.63 mmol) were combined in a sealed tube, and heated at 100 °C for 36 h. The reaction was allowed to cool, and the mixture purified by column chromatography on silica gel (0 - 50% EtOAc/heptanes) to afford **32** (2.22 g, 76% yield) as an amber gum. LC-MS (APCI),  $m/z$  321.1  $[M + H]^+$ ;  $^1H$  NMR (400 MHz, DMSO- $d_6$ )  $\delta$  13.43 (br s, 1 H), 7.45 - 7.36 (m, 1 H), 7.32 (dd,  $J = 9.1, 3.3$  Hz, 1 H), 7.24 (dd,  $J = 9.2, 4.4$  Hz, 1 H), 6.69 (s, 1 H), 4.38 (t,  $J = 6.5$  Hz, 2 H), 4.30 - 4.17 (m, 2 H), 3.15 (t,  $J = 6.4$  Hz, 2 H), 2.38 (s, 3 H), 1.32 - 1.23 (m, 5 H).

*Ethyl 3-[2-(2-acetyl-4-fluorophenoxy)propyl]-1H-pyrazole-5-carboxylate (33)*. The procedure used to prepare compound **32** was used to prepare compound **33** from **31** (see Supporting Information). LC-MS (APCI),  $m/z$  335.1  $[M + H]^+$ ;  $^1H$  NMR (400 MHz, DMSO- $d_6$ )  $\delta$  13.23 (br s, 1 H), 7.43 - 7.28 (m, 2 H), 7.17 (dd,  $J = 8.8, 4.3$  Hz, 1 H), 6.55 (s, 1 H), 4.34 - 4.17 (m, 2 H), 4.16 - 4.04 (m, 2 H), 2.82 (t,  $J = 7.6$  Hz, 2 H), 2.58 (s, 3 H), 2.12 (t,  $J = 7.2$  Hz, 2 H), 1.33 - 1.21 (m, 3 H).

*Ethyl 3-[2-(2-acetyl-4-fluorophenoxy)ethyl]-1-methyl-1H-pyrazole-5-carboxylate (34)*. Dimethyl sulfate (1.35 mL, 14.2 mmol) was added in a drop-wise manner to a solution of **32** (3.8 g, 11.9 mmol) in toluene (47.5 mL). Upon completion of addition, the reaction was heated at 80 °C for 12 h. The reaction was allowed to cool, concentrated *in vacuo*, and purified by column chromatography on silica gel (0 - 25% EtOAc/heptanes) to afford **34** (1.83 g, 46% yield) as a colorless gum, which solidified on standing. LC-MS (APCI)  $m/z$  335.1  $[M + H]^+$ ;  $^1H$  NMR (400 MHz, DMSO- $d_6$ )  $\delta$  7.40 - 7.35 (m, 1 H), 7.30 (dd,  $J = 9.2, 3.4$  Hz, 1 H), 7.23 (dd,  $J = 9.1, 4.3$

1  
2  
3 Hz, 1 H), 6.81 (s, 1 H), 4.36 (t,  $J = 6.5$  Hz, 2 H), 4.28 (q,  $J = 8$  Hz, 2 H), 4.02 (s, 3 H), 3.06 (t,  $J$   
4 = 6.4 Hz, 2 H), 2.41 (s, 3 H), 1.29 (t,  $J = 8$  Hz, 3 H).  
5  
6

7  
8 *Ethyl 3-[2-(2-acetyl-4-fluorophenoxy)propyl]-1-methyl-1H-pyrazole-5-carboxylate (35)*. The  
9 procedure used to prepare compound **34** was used to prepare compound **35**. LC-MS (APCI)  $m/z$   
10 349.1  $[M + H]^+$ ;  $^1H$  NMR (400 MHz, DMSO- $d_6$ )  $\delta$  7.42 - 7.30 (m, 2 H), 7.22 - 7.12 (m, 1 H),  
11 6.71 (s, 1H), 4.27 (q,  $J = 7.1$  Hz, 2 H), 4.11 (t,  $J = 6.3$  Hz, 2 H), 4.01 (s, 3 H), 2.73 (t,  $J = 7.6$  Hz,  
12 2 H), 2.56 (s, 3 H), 2.17 - 2.03 (m, 2 H), 1.29 (t,  $J = 7.1$  Hz, 3 H).  
13  
14  
15  
16  
17  
18  
19

20 *3-[2-(2-Acetyl-4-fluorophenoxy)ethyl]-1-methyl-1H-pyrazole-5-carbonitrile (36)*. A solution  
21 of **34** (2.65 g, 7.93 mmol) in MeOH (20 mL) was heated in a sealed tube for 1 h at 60 °C before  
22 being allowed to cool. Aqueous 33% ammonium hydroxide (10 mL, 260 mmol) was added, and  
23 the tube was re-sealed and heated for 18 h at 60 °C. The reaction was cooled, and concentrated *in*  
24 *vacuo*. The residue was slurried in water, and the solids collected by filtration to afford the  
25 primary amide (1.79 g) as a colorless solid. The amide (1.74 g, 5.7 mmol) was taken up in  
26 CH<sub>2</sub>Cl<sub>2</sub> (38 mL), pyridine (1.84 mL, 22.8 mmol) was added, and the mixture cooled to 0 °C  
27 using an ice-water bath. Trifluoroacetic anhydride (1.60 mL, 11.4 mmol) was added in a drop-  
28 wise manner leading to the formation of a clear solution. The reaction was stirred for 1 h before  
29 being diluted with EtOAc (100 mL). The organic solution was washed with 1 M aqueous  
30 Na<sub>2</sub>CO<sub>3</sub> (2 x 25 mL), brine (25 mL), 1 M HCl (2 x 25 mL), brine (25 mL), dried over MgSO<sub>4</sub>,  
31 and concentrated to afford **36** (1.54 g, 70% yield over two steps) as a yellow solid. LC-MS  
32 (APCI),  $m/z$  288.2  $[M + H]^+$ ;  $^1H$  NMR (400 MHz, DMSO- $d_6$ )  $\delta$  7.41 - 7.36 (m, 1 H), 7.32 (dd,  $J$   
33 = 9.1, 3.3 Hz, 1 H), 7.22 (dd,  $J = 9.1, 4.3$  Hz, 1 H), 7.07 (s, 1 H), 4.36 (t,  $J = 6.3$  Hz, 2 H), 3.95  
34 (s, 3 H), 3.11 (t,  $J = 6.3$  Hz, 2 H), 2.41 (s, 3 H).  
35  
36  
37  
38  
39  
40  
41  
42  
43  
44  
45  
46  
47  
48  
49  
50  
51  
52  
53  
54  
55  
56  
57  
58  
59  
60

1  
2  
3  
4  
5  
6  
7  
8  
9  
10  
11  
12  
13  
14  
15  
16  
17  
18  
19  
20  
21  
22  
23  
24  
25  
26  
27  
28  
29  
30  
31  
32  
33  
34  
35  
36  
37  
38  
39  
40  
41  
42  
43  
44  
45  
46  
47  
48  
49  
50  
51  
52  
53  
54  
55  
56  
57  
58  
59  
60

3-[2-(2-Acetyl-4-fluorophenoxy)propyl]-1-methyl-1H-pyrazole-5-carbonitrile (**37**). The procedure used to prepare compound **36** was used to prepare compound **37**. LC-MS (APCI),  $m/z$  302.1  $[M + H]^+$ ;  $^1H$  NMR (400 MHz, DMSO- $d_6$ )  $\delta$  7.42 - 7.30 (m, 2 H), 7.18 (dd,  $J = 9.1, 4.3$  Hz, 1 H), 6.99 (s, 1 H), 4.12 (t,  $J = 6.3$  Hz, 2 H), 3.94 (s, 3 H), 2.77 (t,  $J = 7.6$  Hz, 2 H), 2.56 (s, 3 H), 2.16 - 2.00 (m, 2 H).

1- $\{2-[2-(5-Cyano-1-methyl-1H-pyrazol-3-yl)ethoxy]-5-fluorophenyl\}$ ethyl methanesulfonate (**38**). Sodium borohydride (223 mg, 5.9 mmol) was added to a solution of **36** (1.54 g, 5.36 mmol) in MeOH (26.8 mL) cooled to 0 °C. After being stirred for 2 h, the reaction was diluted with EtOAc (25 mL). The organic solution was washed with water (10 mL), brine (10 mL), and dried over  $MgSO_4$ . The reaction was concentrated *in vacuo*, and the residue purified by column chromatography over silica gel (eluting with 0 - 60% EtOAc/heptanes) to afford the intermediate alcohol (1.48 g) as a viscous gum. The alcohol (400 mg, 1.38 mmol) was dissolved in  $CH_2Cl_2$  (6.92 mL), and TEA (289  $\mu$ L, 2.08 mmol) was added. The mixture was cooled to 0 °C using an ice-water bath, and  $MsCl$  (118  $\mu$ L, 1.52 mmol) was added in a drop-wise manner. After 1 h, LC-MS indicated that the starting material had been consumed. The reaction was diluted with EtOAc (15 mL), washed with water (5 mL), brine (5 mL), and dried over  $MgSO_4$ . The reaction was filtered and concentrated *in vacuo* to afford **38** (508 mg, 94% yield over two steps) as a viscous gum, which was used without further purification. LC-MS (APCI),  $m/z$  272.1  $[M - OSO_2Me]^+$ .

1- $\{2-[2-(5-Cyano-1-methyl-1H-pyrazol-3-yl)propoxy]-5-fluorophenyl\}$ ethyl methanesulfonate (**39**). The procedure used to prepare compound **38** was used to prepare compound **39**. LC-MS (APCI),  $m/z$  286.1  $[M - OSO_2Me]^+$ .

3-[2-(2- $\{1-[2-Amino-5-bromopyridin-3-yl]oxy\}$ ethyl)-4-fluorophenoxy)ethyl]-1-methyl-1H-pyrazole-5-carbonitrile (**40**). 2-Amino-3-hydroxy-5-bromopyridine (313 mg, 1.66 mmol), **38**

(507 mg, 1.38 mmol) and cesium carbonate (899 mg, 2.76 mmol) were combined in DMF (6.9 mL), and the reaction mixture heated at 80 °C for 40 h. The reaction was allowed to cool, diluted with EtOAc (15 mL), washed with water (10 mL), brine (5 mL), and dried over MgSO<sub>4</sub>. The reaction was filtered, concentrated *in vacuo*, and the residue purified by column chromatography over silica gel (0 - 50% EtOAc/heptanes) to afford **40** (115 mg, 18% yield) as a brown solid, which was used without further purification. LC-MS (APCI), *m/z* 460.2 [M + H]<sup>+</sup>.

*3-[2-(2-{1-[(2-Amino-5-bromopyridin-3-yl)oxy]propyl}-4-fluorophenoxy)ethyl]-1-methyl-1H-pyrazole-5-carbonitrile (41)*. The procedure used to prepare compound **40** was used to prepare compound **41**. LC-MS (APCI), *m/z* 474.1/476.1 [M + H]<sup>+</sup>.

*(10R)-7-Amino-12-fluoro-2,10-dimethyl-16,17-dihydro-2H,10H-8,4-(metheno)pyrazolo[3,4-d][1,11,8]benzodioxacyclotetradecine-3-carbonitrile (7e)*. Potassium acetate (123 mg, 1.25 mmol), **40** (115 mg, 0.25 mmol), cataCXium A (18.5 mg, 0.05 mmol), Pd(OAc)<sub>2</sub> (5.6 mg, 0.025 mmol) and *t*-amyl alcohol (5 mL) were combined in a microwave vial. Nitrogen was bubbled through the solution for 10 min, and then the vial was sealed and heated in the microwave for 1 h at 140 °C. Additional portions of both cataCXium A (18.5 mg, 0.05 mmol) and Pd(OAc)<sub>2</sub> (5.6 mg, 0.025 mmol) were added, and the vial re-sealed and heated in the microwave at 140 °C for 1 h. LC-MS indicated the starting material had been consumed. The reaction was diluted with EtOAc (20 mL), and the organic phase washed with water (10 mL) and brine (10 mL) before being dried over MgSO<sub>4</sub>. The solution was filtered, and concentrated *in vacuo* with the residue being purified by column chromatography over silica gel (0 - 100% EtOAc/heptanes) to afford **42** (23 mg, 24% yield) as a white solid. LC-MS *m/z* 460.2 [M + H]<sup>+</sup>. Chiral separation was carried out by SFC using an Whelk-O1 (*R,R*) 5 μm column (4.6 x 100 mm) eluting with 30 % MeOH @ 120 bar with a flow rate of 4 mL/min. **7e** was obtained as peak 1 (*R*<sub>t</sub> = 1.36 min).

1  
2  
3  
4  
5  
6  
7  
8  
9  
10  
11  
12  
13  
14  
15  
16  
17  
18  
19  
20  
21  
22  
23  
24  
25  
26  
27  
28  
29  
30  
31  
32  
33  
34  
35  
36  
37  
38  
39  
40  
41  
42  
43  
44  
45  
46  
47  
48  
49  
50  
51  
52  
53  
54  
55  
56  
57  
58  
59  
60

$[\alpha]_D^{20} = + 22.1^\circ$  ( $c = 0.1$ ,  $\text{CHCl}_3$ ); LC-MS (APCI),  $m/z$  380.1 ( $\text{M} + \text{H}$ )<sup>+</sup>; <sup>1</sup>H NMR (400 MHz, 80 °C,  $\text{DMSO-}d_6$ )  $\delta$  7.82 (d,  $J = 1.8$  Hz, 1 H), 7.65 (s, 1 H), 7.43 (dd,  $J = 9.7, 3.1$  Hz, 1 H), 7.10 - 6.95 (m, 2 H), 6.01 - 5.86 (m, 1 H), 5.62 (s, 2 H), 4.62 - 4.47 (m, 1 H), 3.97 (s, 3 H), 3.34 - 3.18 (m,  $J = 16.1$  Hz, 1 H), 2.98 (br s, 2 H), 1.69 (d,  $J = 6.5$  Hz, 3 H). The inactive enantiomer was obtained as peak 2 ( $R_t = 1.60$  min)

*(10R)-7-Amino-12-fluoro-2,10-dimethyl-16,17-dihydro-2H,10H-8,4-(metheno)pyrazolo[3,4-d][1,11,8]benzodioxazacyclotetradecine-3-carbonitrile (7f)*. The procedure used to prepare compound **42** was used to prepare compound **43**. Chiral separation of **43** was carried out by SFC using a Chiralcel OD-H 5  $\mu\text{m}$  column (4.6 x 100 mm) eluting with 30 % MeOH @ 120 bar with a flow rate of 4 mL/min. **7f** was obtained as peak 2 ( $R_t = 1.27$  min).  $[\alpha]_D^{20} = - 18.76^\circ$  ( $c = 0.1$ , MeOH); LC-MS (APCI),  $m/z$  394.2 ( $\text{M} + \text{H}$ )<sup>+</sup>; <sup>1</sup>H NMR (400 MHz, 80 °C,  $\text{DMSO-}d_6$ )  $\delta$  7.82 (d,  $J = 1.8$  Hz, 1 H), 7.65 (s, 1 H), 7.43 (dd,  $J = 9.6, 3.0$  Hz, 1 H), 7.11 - 6.94 (m, 2 H), 6.01 - 5.88 (m, 1 H), 5.62 (s, 2 H), 4.61 - 4.48 (m, 1 H), 3.98 (s, 3 H), 3.26 (br s, 2 H), 2.71 (s, 2 H), 1.69 (d,  $J = 6.3$  Hz, 3 H). The inactive enantiomer was obtained as peak 1 ( $R_t = 1.11$  min).

*Methyl 2-[(1R)-1-{[2-amino-5-(3-{[(tert-butoxycarbonyl)(methyl)amino]methyl}-5-cyano-1-methyl-1H-pyrazol-4-yl)pyridin-3-yl]oxy}ethyl]-4-fluorobenzoate (46)*. Pd(OAc)<sub>2</sub> (53 mg, 0.24 mmol) and cataCXium A (180 mg, 0.5 mmol) were mixed together in toluene (1.5 mL, de-gassed) and the resulting solution was added *via* pipette to a stirred solution of **44** (0.9 g, 2.4 mmol - see Supporting Information), **45** (1.0 g, 3.0 mmol - see Supporting Information) B<sub>2</sub>pin<sub>2</sub> (0.9 g, 3.6 mmol) and CsF (1.9 g, 12.6 mmol) in MeOH/H<sub>2</sub>O (9:1, 12 mL, de-gassed) at 60 °C. The resulting mixture was then stirred at reflux for 3 h. A further portion of Pd(OAc)<sub>2</sub> (26 mg, 0.12 mmol) and cataCXium A (90 mg, 0.25 mmol) in toluene (1.5 mL, de-gassed) was added, and the yellow reaction mixture stirred at 60 °C overnight. After cooling to room temperature,

1  
2  
3 the mixture was diluted with EtOAc (150 mL) and filtered through Celite. The filtrate was  
4  
5 washed with water (100 mL), then brine (100 mL), dried (Na<sub>2</sub>SO<sub>4</sub>) and evaporated. The residue  
6  
7 was purified by flash chromatography over silica gel, which was eluted with 50%  
8  
9 EtOAc/cyclohexane, and gave **46** (570 mg, 43% yield) as a yellow oil. TLC (R<sub>f</sub> = 0.40, 50%  
10  
11 EtOAc/cyclohexane). LC-MS (ESI), *m/z* 539 [M+H]<sup>+</sup>. <sup>1</sup>H NMR (400 MHz, CDCl<sub>3</sub>) δ 8.03 (m, 1  
12  
13 H), 7.65 (s, 1 H), 7.27 (dd, *J* = 9.9, 2.7 Hz, 1 H), 7.01 (m, 1 H), 6.68 (m, 1 H), 6.40 (m, 1 H),  
14  
15 4.90 (br s, 2 H), 4.30 - 4.20 (m, 2 H), 3.96 (s, 3 H), 3.94 (s, 3 H), 2.85 - 2.55 (m, 3 H), 1.68 (d, *J*  
16  
17 = 6.6 Hz, 3 H), 1.24 (s, 9 H).

18  
19  
20  
21  
22 *2-[(1R)-1-{{2-Amino-5-(3-{{(tert-butoxycarbonyl)(methyl)amino}methyl}-5-cyano-1-methyl-*  
23  
24 *1H-pyrazol-4-yl)pyridin-3-yl}oxy}ethyl]-4-fluorobenzoic acid (47)*. To a solution of **46** (69%  
25  
26 purity, 0.95 g, assumed 1.05 mmol) in MeOH (20 mL) was added a solution NaOH (1.0 g, 25  
27  
28 mmol) in water (2 mL). The mixture was stirred at 40 °C for 3.5 h. The reaction was diluted with  
29  
30 water (80 mL), concentrated by 20 mL to remove MeOH on the rotovap, and washed with  
31  
32 TBME (100 mL). The aqueous layer was then acidified carefully with 1 M aq HCl to approx pH  
33  
34 2 (pH paper). Sodium chloride (15 g) was added to the mixture and the mixture was extracted  
35  
36 with EtOAc (100 mL). The organic layer was separated, dried (Na<sub>2</sub>SO<sub>4</sub>) and evaporated to give  
37  
38 **47** (480 mg, 87% yield) as a pale yellow solid. LC-MS (ESI), *m/z* 525 [M+H]<sup>+</sup>; <sup>1</sup>H NMR (400  
39  
40 MHz, CD<sub>3</sub>OD) δ 8.05 (m, 1 H), 7.45 (s, 1 H), 7.37 (dd, *J* = 10.4, 2.8 Hz, 1 H), 7.10 (dt, *J* = 8.5,  
41  
42 2.4 Hz, 1 H), 6.60 - 6.50 (m, 2 H), 4.30 - 4.05 (m, 2 H), 3.99 (s, 3 H), 2.80 - 2.60 (m, 3 H), 1.72  
43  
44 (d, *J* = 6.5 Hz, 3 H).

45  
46  
47  
48  
49  
50  
51 *2-{{(1R)-1-[(2-Amino-5-{{5-cyano-1-methyl-3-[(methylamino)methyl]-1H-pyrazol-4-yl}pyridin-*  
52  
53 *3-yl)oxy}ethyl]-4-fluorobenzoic acid (48)*. A solution of HCl in dioxane (4 M, 6.0 mL) was  
54  
55 added to a solution of **47** (480 mg, 0.91 mmol) in MeOH (6 mL) and the reaction was stirred at  
56  
57  
58  
59  
60

1  
2  
3 40 °C for 2.5 h. The reaction mixture was then concentrated to dryness under reduced pressure.  
4  
5  
6 The residue was taken-up in MeOH (50 mL) and acetonitrile (100 mL) was added and the  
7  
8 mixture was then again evaporated to dryness, to give **48** (400 mg, 87% yield) as an off-white  
9  
10 solid. LC-MS (ESI),  $m/z$  425 [M+H]<sup>+</sup>; <sup>1</sup>H NMR (400 MHz, CD<sub>3</sub>OD) δ 8.07 (dd,  $J$  = 8.9, 5.9 Hz,  
11  
12 1 H), 7.51 (d,  $J$  = 1.7 Hz, 1 H), 7.42 (dd,  $J$  = 9.8, 2.6 Hz, 1 H), 7.23 (d,  $J$  = 1.6 Hz, 1 H), 7.16  
13  
14 (dt,  $J$  = 8.5, 2.7 Hz, 1 H), 6.73 (dd,  $J$  = 11.9, 6.9 Hz, 1 H), 4.22 (d,  $J$  = 14.7 Hz, 1 H), 4.14 (d,  $J$  =  
15  
16 14.7 Hz, 1 H), 4.07 (s, 3 H), 2.75 (s, 3 H), 1.75 (d,  $J$  = 5.5 Hz, 3 H).  
17  
18  
19

20 *(10R)-7-Amino-12-fluoro-2,10,16-trimethyl-15-oxo-10,15,16,17-tetrahydro-2H-8,4-*  
21  
22 *(metheno)pyrazolo[4,3-h][2,5,11]benzoxadiazacyclotetradecine-3-carbonitrile (8k)*. A solution  
23  
24 of **48** (400 mg, assumed 0.91 mmol) as the HCl salt and DIPEA (1.17 g, 9.1 mmol) in DMF (5.0  
25  
26 mL) and THF (0.5 mL) was added drop-wise to a solution of HATU (482 mg, 1.27 mmol) in  
27  
28 DMF (10.0 mL) at 0 °C over 30 min. After complete addition, the mixture was stirred at 0 °C for  
29  
30 a further 30 min. Water (70 mL) was added and the mixture was extracted into EtOAc (2 x 60  
31  
32 mL). The combined organics were washed with saturated aqueous NaHCO<sub>3</sub> (2 x 100 mL), brine  
33  
34 (100 mL), dried over Na<sub>2</sub>SO<sub>4</sub>, and evaporated. The residue was purified by column  
35  
36 chromatography over silica gel, which was eluted with 70% EtOAc/cyclohexane giving 205 mg  
37  
38 of a pale yellow residue (semi-solid). The solids were dissolved in TBME (7 mL) and  
39  
40 cyclohexane (20 mL) was added slowly with good stirring to precipitate the product. After  
41  
42 stirring for 30 min, the mixture was filtered, and **8k** (110 mg, 29% yield) was collected as a  
43  
44 white solid. TLC ( $R_f$  = 0.40, 70% EtOAc in cyclohexane). LC-MS (ESI),  $m/z$  407 [M+H]<sup>+</sup>; <sup>1</sup>H  
45  
46 NMR (400 MHz, CDCl<sub>3</sub>) δ 7.83 (d,  $J$  = 2.0 Hz, 1 H), 7.30 (dd,  $J$  = 9.6, 2.4 Hz, 1 H), 7.21 (dd,  $J$   
47  
48 = 8.4, 5.6 Hz, 1 H), 6.99 (dt,  $J$  = 8.0, 2.8 Hz, 1 H), 6.86 (d,  $J$  = 1.2 Hz, 1 H), 5.75 - 5.71 (m, 1 H),  
49  
50  
51  
52  
53  
54  
55  
56  
57  
58  
59  
60

1  
2  
3 4.84 (s, 2 H), 4.45 (d,  $J = 14.4$  Hz, 1 H), 4.35 (d,  $J = 14.4$  Hz, 1 H), 4.07 (s, 3 H), 3.13 (s, 3 H),  
4  
5  
6 1.79 (d,  $J = 6.4$  Hz, 3 H).  
7

8  
9 *7-Amino-12-fluoro-1,3,10,16-tetramethyl-16,17-dihydro-1H-8,4-(metheno)pyrazolo[4,3-*  
10 *h][2,5,11]benzoxadiazacyclotetradecin-15(10H)-one (8a and 8b)*. Compounds **8a** and **8b** were  
11 prepared in a similar manner to **8k** using **rac-(44)** (see Supporting Information) and *tert*-butyl  
12 [(4-bromo-1,3-dimethyl-1H-pyrazol-5-yl)methyl]methylcarbamate (**70**) (see Supporting  
13 Information) as the reagents in the initial coupling step. Chiral separation was performed on the  
14 final compounds using a Chiralcel OD-3 3  $\mu$ m column (4.6 x 100 mm) eluting with 30% MeOH  
15 @ 120 bar with a flow rate of 5 mL/min. Compound **8a**, peak 1 ( $R_t = 0.75$  min). LC-MS (ESI),  
16  $m/z$  397.0  $[M+H]^+$ ;  $^1H$  NMR (400 MHz, DMSO- $d_6$ )  $\delta$  7.62 (dd,  $J = 10.3, 2.5$  Hz, 1 H), 7.43 -  
17 7.33 (m, 2 H), 7.23 - 7.15 (m, 1 H), 6.76 (d,  $J = 1.5$  Hz, 1 H), 5.81 (s, 2 H), 5.60 (br s, 1 H), 4.62  
18 (d,  $J = 15.1$  Hz, 1 H), 4.08 (d,  $J = 15.1$  Hz, 1 H), 3.88 (s, 3 H), 2.99 (s, 3 H), 2.21 (s, 3 H), 1.65  
19 (d,  $J = 6.0$  Hz, 3 H). Compound **8b**, peak 2 ( $R_t = 1.3$  min). LC-MS (ESI),  $m/z$  397.0  $[M+H]^+$ ;  $^1H$   
20 NMR (400 MHz, DMSO- $d_6$ )  $\delta$  7.65 - 7.57 (m, 1 H), 7.44 - 7.33 (m, 2 H), 7.23 - 7.12 (m, 1 H),  
21 6.76 (s, 1 H), 5.80 (s, 2 H), 5.61 (br s, 1 H), 4.62 (d,  $J = 15.4$  Hz, 1 H), 4.09 (d,  $J = 15.1$  Hz, 1  
22 H), 3.88 (s, 3 H), 2.99 (s, 3 H), 2.21 (s, 3 H), 1.66 (d,  $J = 6.0$  Hz, 3 H).  
23  
24  
25  
26  
27  
28  
29  
30  
31  
32  
33  
34  
35  
36  
37  
38  
39  
40  
41

42 *7-Amino-12-fluoro-1,3,16-trimethyl-16,17-dihydro-1H-8,4-(metheno)pyrazolo[4,3-*  
43 *h][2,5,11]benzoxadiazacyclotetradecin-15(10H)-one (8c)*. Compound **8c** was prepared in a  
44 similar manner to **8k** using methyl 2-{[(2-amino-5-bromopyridin-3-yl)oxy]methyl}-4-  
45 fluorobenzoate (**71**) (see Supporting Information) and *tert*-butyl [(4-bromo-1,3-dimethyl-1H-  
46 pyrazol-5-yl)methyl]methylcarbamate (**70**) (see Supporting Information) as the reagents in the  
47 initial coupling step. LC-MS (ESI),  $m/z$  382  $[M+H]^+$ ;  $^1H$  NMR (400 MHz, DMSO- $d_6$ )  $\delta$  7.56 (dd,  
48  $J = 9.6, 2.4$  Hz, 1 H), 7.44 - 7.38 (m, 2 H), 7.22 (td,  $J = 8.4, 2.8$  Hz, 1 H), 6.73 (d,  $J = 1.6$  Hz, 1  
49 H), 5.80 (s, 2 H), 5.61 (br s, 1 H), 4.62 (d,  $J = 15.4$  Hz, 1 H), 4.09 (d,  $J = 15.1$  Hz, 1  
50 H), 3.88 (s, 3 H), 2.99 (s, 3 H), 2.21 (s, 3 H), 1.66 (d,  $J = 6.0$  Hz, 3 H).  
51  
52  
53  
54  
55  
56  
57  
58  
59  
60

1  
2  
3 H), 5.82 (br s, 2 H), 5.30 (d,  $J = 13.6$  Hz, 1 H), 5.17 (d,  $J = 13.6$  Hz, 1 H), 4.65 (d,  $J = 15.2$  Hz, 1  
4  
5 H), 4.20 (d,  $J = 15.2$  Hz, 1 H), 3.89 (s, 3 H), 2.97 (s, 3 H), 2.54 (s, 1 H), 2.22 (s, 3 H).  
6  
7

8  
9  
10  
11  
12  
13  
14  
15  
16  
17  
18  
19  
20  
21  
22  
23  
24  
25  
26  
27  
28  
29  
30  
31  
32  
33  
34  
35  
36  
37  
38  
39  
40  
41  
42  
43  
44  
45  
46  
47  
48  
49  
50  
51  
52  
53  
54  
55  
56  
57  
58  
59  
60

(5*R*)-7-Amino-12-fluoro-3-methoxy-1,10,16-trimethyl-16,17-dihydro-1*H*-8,4-  
(metheno)pyrazolo[4,3-*h*][2,5,11]benzoxadiazacyclotetradecin-15(10*H*)-one (**8f**). Compound **8f**  
was prepared in a similar manner to **8k** using **44** (see Supporting Information) and *tert*-butyl [(4-  
bromo-3-methoxy-1-methyl-1*H*-pyrazol-5-yl)methyl]methylcarbamate (**72**) (see Supporting  
Information) as the reagents in the initial coupling step. LC-MS (ESI),  $m/z$  412 [M+H]<sup>+</sup>; <sup>1</sup>H  
NMR (400 MHz, CD<sub>3</sub>OD)  $\delta$  7.62 (d,  $J = 1.6$  Hz, 1 H), 7.50 (dd,  $J = 6.4, 2.6$  Hz, 1 H), 7.43 (dd,  $J$   
= 5.6, 3.2 Hz, 1 H), 7.16 - 7.11 (m, 1 H), 6.90 (d,  $J = 1.2$  Hz, 1 H), 5.64 - 5.60 (m, 1 H), 4.84 (d,  
 $J = 15.2$  Hz, 1 H), 4.37 (d,  $J = 15.6$  Hz, 1 H), 3.92 (d,  $J = 9.2$  Hz, 6 H), 3.17 (s, 3 H), 1.78 (d,  $J =$   
6 Hz, 3 H).

(5*R*)-8-Amino-3-fluoro-5,17-dimethyl-13-(methylsulfonyl)-16,17-dihydro-7,11-  
(metheno)dibenzo[*g,l*][1,4,10]oxadiazacyclotetradecin-18(5*H*)-one (**8h**). Compound **8h** was  
prepared in a similar manner to **8k** using **44** (see Supporting Information) and *tert*-butyl [2-  
bromo-4-(methylsulfonyl)benzyl] methylcarbamate (**73**) (see Supporting Information) as the  
reagents in the initial coupling step. LC-MS (ESI),  $m/z$  456 [M+H]<sup>+</sup>. [ $\alpha$ ]<sub>D</sub><sup>22</sup> = + 52.5° (c = 0.52,  
MeOH). <sup>1</sup>H NMR (400 MHz, DMSO-*d*<sub>6</sub>)  $\delta$  7.92 - 7.84 (m, 3 H), 7.69 (dd,  $J = 10.4, 2.8$  Hz, 1 H),  
7.51 (d,  $J = 2.0$  Hz, 1 H), 7.36 (dd,  $J = 8.8, 6.0$  Hz, 1 H), 7.14 (dt,  $J = 8.4, 2.4$  Hz, 1 H), 7.09 (d,  $J$   
= 2.0 Hz, 1 H), 6.13 (s, 2H), 5.71 - 5.67 (m, 1 H), 4.45 (d,  $J = 13.2$  Hz, 1 H), 4.22 (d,  $J = 13.2$   
Hz, 1 H), 3.29 (s, 3 H), 3.01 (s, 3 H), 1.69 (d,  $J = 6.4$  Hz, 3 H).

(5*R*)-7-Amino-3-cyclopropyl-12-fluoro-1,10,16-trimethyl-16,17-dihydro-1*H*-8,4-  
(metheno)pyrazolo[4,3-*h*][2,5,11]benzoxadiazacyclotetradecin-15(10*H*)-one (**8j**). Compound **8j**  
was prepared in a similar manner to **8k** using **44** (see Supporting Information) and *tert*-butyl [(4-

1  
2  
3 bromo-3-cyclopropyl-1-methyl-1*H*-pyrazol-5-yl)methyl]methylcarbamate (**74**) (see Supporting  
4 Information) as the reagents in the initial coupling step. LC-MS (ESI), *m/z* 422 [M+H]<sup>+</sup>; <sup>1</sup>H  
5 NMR (400 MHz, CDCl<sub>3</sub>) δ 7.76 - 7.75 (m, 1 H), 7.25 (dd, *J* = 7.2, 2.8 Hz, 1 H), 7.10 (dd, *J* =  
6 5.6, 2.8 Hz, 1 H), 6.93 - 6.90 (m, 1 H), 6.80 (br s, 1 H), 5.69 (s, 1 H), 4.54 (s, 2 H), 4.40 (d, *J* =  
7 15.2 Hz, 1 H), 4.22 (d, *J* = 15.2 Hz, 1 H), 3.85 (s, 3 H), 3.06 (s, 3 H), 1.85 (m, 1 H), 1.70 (d, *J* =  
8 6.4 Hz, 3 H), 1.02 - 1.01 (m, 1 H), 0.95 - 0.93 (m, 1 H), 0.81 - 0.79 (m, 1 H), 0.63 (m, 1 H).

9  
10  
11  
12  
13  
14  
15  
16  
17  
18  
19  
20  
21  
22  
23  
24  
25  
26  
27  
28  
29  
30  
31  
32  
33  
34  
35  
36  
37  
38  
39  
40  
41  
42  
43  
44  
45  
46  
47  
48  
49  
50  
51  
52  
53  
54  
55  
56  
57  
58  
59  
60  
*(5R)*-8-Amino-3-fluoro-5,14,19-trimethyl-18,19-dihydro-7,11-(metheno)-  
*pyrimido*[2',1':2,3]*imidazo*[4,5-*h*][2,5,11]*benzoxadiazacyclotetradecin*-20(5*H*)-one (**81**).

Compound **81** was prepared in a similar manner to **8k** with the modification that the initial Suzuki coupling was performed utilizing the pre-formed protected boronate **69** (see Supporting Information), as described below.

Nitrogen was bubbled through a suspension of **69** (489 mg, 0.56 mmol - see Supporting Information), *tert*-butyl [(3-bromo-6-methylimidazo[1,2-*a*]pyrimidin-2-yl)methyl]methylcarbamate (**75**) (197 mg, 0.57 mmol - see Supporting Information) and CsF (253 mg, 1.66 mmol) in toluene (3.7 mL) for a period of 10 min. To the mixture was added PdCl<sub>2</sub>.dppf (45.7 mg, 0.06 mmol), and the reaction heated at reflux for 14 h. The reaction was allowed to cool, and diluted with EtOAc (20 mL). The organic phase was washed with water (2 x 5 mL), brine (5 mL), and dried over MgSO<sub>4</sub>. The solution was filtered, and concentrated and the residue purified by column chromatography on silica gel eluting with 0 - 100% EtOAc/heptanes to afford methyl 2-[(1*R*)-1-({3-[bis(*tert*-butoxycarbonyl)amino]-6-(2-{{(*tert*-butoxycarbonyl)(methyl)amino}methyl)}-6-cyanoimidazo[1,2-*a*]pyridin-3-yl)pyrazin-2-yl}oxy)ethyl]-4-fluorobenzoate (288 mg, 66% yield) as a viscous oil. LC-MS (APCI), *m/z* 765.3 [M+H]<sup>+</sup>; <sup>1</sup>H NMR (400 MHz, DMSO-*d*<sub>6</sub>) δ 8.46 (s, 1 H), 8.20 (s, 2 H), 7.97 (dd, *J* = 8.7, 6.2 Hz,

1  
2  
3 1 H), 7.44 - 7.33 (m, 2 H), 7.28 - 7.21 (m, 1 H), 6.41 - 6.30 (m, 1 H), 4.45 - 4.25 (m, 2 H), 3.82  
4  
5 (s, 3 H), 2.74 (s, 3 H), 2.28 (s, 3 H), 1.61 (d,  $J = 6.3$  Hz, 3 H), 1.47 (s, 18 H), 1.30 (br s, 9 H).  
6  
7

8 The ester hydrolysis, exhaustive Boc-deprotection, and HATU-mediated macrolactamization  
9  
10 were performed in a similar manner to **8k** to afford **8l**. LC-MS (APCI)  $m/z$  433  $[M+H]^+$ .  $[\alpha]_D^{22} =$   
11  
12 - 199.2° ( $c = 0.57$ , MeOH).  $^1H$  NMR (400 MHz, DMSO- $d_6$ )  $\delta$  8.79 (dd,  $J = 2.1, 1.2$  Hz, 1 H),  
13  
14 8.45 (d,  $J = 2.2$  Hz, 1 H), 7.82 (d,  $J = 1.7$  Hz, 1 H), 7.66 (dd,  $J = 10.3, 2.6$  Hz, 1 H), 7.47 (dd,  $J =$   
15  
16 8.5, 5.8 Hz, 1 H), 7.17 (dt,  $J = 8.4, 2.7$  Hz, 1 H), 6.88 (d,  $J = 1.6$  Hz, 1 H), 6.22 (s, 2 H), 5.73 -  
17  
18 5.63 (m, 1 H), 4.50 (d,  $J = 13.9$  Hz, 1 H), 4.31 (d,  $J = 13.8$  Hz, 1 H), 3.06 (s, 3 H), 2.31 (s, 3 H),  
19  
20 1.69 (d,  $J = 6.2$  Hz, 3 H).  
21  
22  
23

24  
25 2- $\{1-[3-Amino-6-bromopyrazin-2-yl]oxy\}ethyl\}$ - $N-[4-bromo-1,3-dimethyl-1H-pyrazol-5-$   
26  
27  $yl)methyl]-4-fluoro-N-methylbenzamide$  (**52**). To a solution of **rac-(49)** (266 mg, 0.607 mmol -  
28  
29 see Supporting Information), 1-(4-bromo-1,3-dimethyl-1H-pyrazol-5-yl)- $N$ -methylmethanamine  
30  
31 (**50**) (166 mg, 0.759 mmol - see Supporting Information) and DIEA (211  $\mu$ L, 1.21 mmol) in  
32  
33 toluene (60 mL) was added Pd(P<sup>t</sup>Bu<sub>3</sub>)<sub>2</sub> (32 mg, 0.06 mmol). The reaction mixture was heated at  
34  
35 100 °C under 4 bar CO overnight and then concentrated to afford **52**, which was used without  
36  
37 further purification.  
38  
39

40  
41 2- $\{1-[3-Amino-6-bromopyrazin-2-yl]oxy\}ethyl\}$ - $N-[4-bromo-3-methoxy-1-methyl-1H-$   
42  
43  $pyrazol-5-yl)methyl]-4-fluoro-N-methylbenzamide$  (**53**). The procedure used to prepare  
44  
45 compound **52** was used to prepare compound **53** (from **49** and **51** - see Supporting Information),  
46  
47 which was used without further purification. LC-MS (APCI),  $m/z$  493.0/495.0  $[M+H]^+$ .  
48  
49

50  
51 7-Amino-12-fluoro-1,3,10,16-tetramethyl-16,17-dihydro-1H-8,4-(azeno)-pyrazolo[4,3-  
52  
53  $h][2,5,11]benzoxadiazacyclotetradecin-15(10H)-one$  (**8d** and **8e**). The residue of crude **52** was  
54  
55 taken-up in MeOH (12 mL) and water (1.3 mL) and added to a vial containing B<sub>2</sub>pin<sub>2</sub> (771 mg,  
56  
57  
58  
59  
60

1  
2  
3 3.04 mmol) and CsF (461 mg, 3.04 mmol). The vial was sealed and the reaction mixture was  
4  
5 bubbled with nitrogen before adding a solution of Pd(OAc)<sub>2</sub> (14 mg, 0.06 mmol) and cataCXium  
6  
7 A (45 mg, 0.12 mmol) in toluene (0.5 mL). After heating for 30 min at 60 °C, the temperature  
8  
9 was increased to 90 °C for 6 h. The reaction was allowed to stand at room temperature overnight  
10  
11 then additional Pd(OAc)<sub>2</sub> (14 mg, 0.06 mmol) and cataCXium A (45 mg, 0.12 mmol) in toluene  
12  
13 (0.5 mL) were added. After heating for 2 h at 100 °C, the reaction mixture was cooled to room  
14  
15 temperature and filtered. The mother liquor was diluted with EtOAc (50 mL), washed with water  
16  
17 (2 x 20 mL) and brine (10 mL), dried (MgSO<sub>4</sub>), filtered and concentrated. The crude product was  
18  
19 purified by flash chromatography eluting with MeOH/CH<sub>2</sub>Cl<sub>2</sub> (0 - 8%) followed by a second  
20  
21 column eluting with EtOAc/heptanes (50 - 100%) then MeOH/CH<sub>2</sub>Cl<sub>2</sub> (0 - 6%), and finally  
22  
23 chiral separation by SFC to afford both enantiomers of the title compound. The chiral separation  
24  
25 was performed by SFC on a Chiralcel OD-H 5 μm column (4.6 mm x 250 mm), which was  
26  
27 eluted with 25% MeOH in CO<sub>2</sub> at 140 bar with a flow rate of 3.0 mL/min. Compound **8d**, peak 1  
28  
29 (R<sub>t</sub> = 4.23 min). [α]<sub>D</sub><sup>20</sup> = -77.1° (c = 0.23, MeOH), 14 mg, > 99% ee, 6% yield. LC-MS (ESI),  
30  
31 *m/z* 397 [M+H]<sup>+</sup>; <sup>1</sup>H NMR (400 MHz, DMSO-*d*<sub>6</sub>) δ 7.51 (s, 1 H), 7.51 - 7.46 (m, 1 H), 7.36 (dd,  
32  
33 *J* = 8.3, 5.8 Hz, 1 H), 7.17 (dt, *J* = 8.6, 2.5 Hz, 1 H), 6.29 (s, 2 H), 5.95 - 5.84 (m, 1 H), 4.47 (d, *J*  
34  
35 = 14.7 Hz, 1 H), 4.27 (d, *J* = 14.4 Hz, 1 H), 3.87 (s, 3 H), 2.87 (s, 3 H), 2.26 (s, 3 H), 1.62 (d, *J* =  
36  
37 6.6 Hz, 3 H). Compound **8e**, peak 2 (R<sub>t</sub> = 5.60 min). [α]<sub>D</sub><sup>20</sup> = + 78.6° (c = 0.24, MeOH), 13 mg,  
38  
39 99% ee, 5% yield. LC-MS (ESI), *m/z* 397 [M+H]<sup>+</sup>; <sup>1</sup>H NMR (400 MHz, DMSO-*d*<sub>6</sub>) δ 7.51 (s, 1  
40  
41 H), 7.49 (dd, *J* = 10.2, 2.7 Hz, 1 H), 7.36 (dd, *J* = 8.5, 5.7 Hz, 1 H), 7.17 (dt, *J* = 8.5, 2.5 Hz, 1  
42  
43 H), 6.29 (s, 2 H), 5.95 - 5.82 (m, 1 H), 4.47 (d, *J* = 14.7 Hz, 1 H), 4.27 (d, *J* = 14.4 Hz, 1 H), 3.87  
44  
45 (s, 3 H), 2.87 (s, 3 H), 2.26 (s, 3 H), 1.62 (d, *J* = 6.6 Hz, 3 H).  
46  
47  
48  
49  
50  
51  
52  
53  
54  
55  
56  
57  
58  
59  
60

1  
2  
3  
4  
5  
6  
7  
8  
9  
10  
11  
12  
13  
14  
15  
16  
17  
18  
19  
20  
21  
22  
23  
24  
25  
26  
27  
28  
29  
30  
31  
32  
33  
34  
35  
36  
37  
38  
39  
40  
41  
42  
43  
44  
45  
46  
47  
48  
49  
50  
51  
52  
53  
54  
55  
56  
57  
58  
59  
60

(10*R*)-7-Amino-12-fluoro-3-methoxy-1,10,16-trimethyl-16,17-dihydro-1*H*-8,4-(*azeno*)pyrazolo[4,3-*h*][2,5,11]benzoxadiazacyclotetradecin-15(10*H*)-one (**8g**). KOAc (89.3 mg, 0.91 mmol), pivalic acid (4.6 mg, 0.05 mmol) and **53** (90 mg, 0.018 mmol) were combined in a microwave vial, and DMF (1.82 mL) was added. Nitrogen was bubbled through the solution, followed by the addition of Pd(OAc)<sub>2</sub> (4 mg, 0.018 mmol) and cataCXium A (13.3 mg, 0.036 mmol). The vial was sealed, and heated at 120 °C in the microwave for 1 h. LC-MS indicated no reaction had taken place. Pd(OAc)<sub>2</sub> and cataCXium A were added again, and the vial re-sealed, and heated in the microwave at 150 °C for 1 h. The solution was diluted with EtOAc (10 mL), washed with water (5 mL), brine (5 mL), and dried over MgSO<sub>4</sub>. The solution was filtered, concentrated and purified by reverse phase HPLC (3-Hydroxyphenol column, no additive) to afford **8g** (5.6 mg, 8% yield) as a colorless solid. LC-MS (APCI), *m/z* 413.1 [M+H]<sup>+</sup>; <sup>1</sup>H NMR (400 MHz, DMSO-*d*<sub>6</sub>) δ 7.79 (s, 1 H), 7.44 (dd, *J* = 10.1, 2.5 Hz, 1 H), 7.38 (dd, *J* = 8.6, 5.8 Hz, 1 H), 7.23 - 7.13 (m, 1 H), 6.21 (s, 2 H), 5.83 - 5.68 (m, 1 H), 4.46 (d, *J* = 14.4 Hz, 1 H), 4.29 (d, *J* = 14.4 Hz, 1 H), 3.87 (s, 3 H), 3.81 (s, 3 H), 2.89 (s, 3 H), 1.61 (d, *J* = 6.5 Hz, 3 H).

2-{(1*R*)-1-[(3-Amino-6-bromopyrazin-2-yl)oxy]ethyl}-4-fluorobenzoic acid (**54**). Compound **49** (1.00 g, 2.28 mmol - see Supporting Information) was partially dissolved in MeOH (10 mL), then DIPEA (2.00 mL, 11.41 mmol), DPE-Phos (147 mg, 0.274 mmol) and Pd(OAc)<sub>2</sub> (31 mg, 0.137 mmol) were added. The mixture was then heated at 50 °C under 4 bar of CO pressure for 3 h. After being allowed to cool to room temperature, the mixture was filtered through Celite and eluted with EtOAc (80 mL). The filtrate was concentrated to one third volume (30 mL), then washed with saturated NaHCO<sub>3</sub> solution (2 x 15 mL) and brine (20 mL), dried over MgSO<sub>4</sub> and concentrated. The crude material was purified by flash chromatography on silica gel (1 : 2 EtOAc:heptanes) to give methyl 2-{(1*R*)-1-[(3-amino-6-bromopyrazin-2-yl)oxy]ethyl}-4-

1  
2  
3 fluorobenzoate (0.65 g, 77% yield) as a colorless solid.  $^1\text{H}$  NMR (400 MHz,  $\text{CDCl}_3$ )  $\delta$  7.94 (dd,  
4  
5  $J = 8.7, 5.8$  Hz, 1 H), 7.57 (s, 1 H), 7.24 (dd,  $J = 9.9, 2.7$  Hz, 1 H), 7.00 (ddd,  $J = 8.8, 7.7, 2.7$   
6  
7 Hz, 1 H), 6.89 (qd,  $J = 6.5, 1.4$  Hz, 1 H), 4.89 (s, 2 H), 3.95 (s, 3 H), 1.72 (d,  $J = 6.4$  Hz, 3 H).  
8  
9

10 Methyl 2- $\{(1R)$ -1-[(3-amino-6-bromopyrazin-2-yl)oxy]ethyl}-4-fluorobenzoate (0.65 g, 1.76  
11  
12 mmol) was suspended in MeOH (10 mL) and a solution of NaOH (0.35 g, 8.80 mmol) in  $\text{H}_2\text{O}$  (1  
13  
14 mL) was added. THF (2 mL) was subsequently added to aid solubility and the reaction mixture  
15  
16 stirred at room temperature overnight. The reaction was diluted with  $\text{H}_2\text{O}$  (15 mL) and washed  
17  
18 with TBME (2 x 10 mL). The basic aqueous phase was then acidified to pH  $\sim$ 3 with 2 M HCl  
19  
20 solution and extracted with EtOAc (3 x 10 mL). The combined organic extracts were dried over  
21  
22  $\text{MgSO}_4$  and concentrated to give **54** (0.56 g, 89% yield) as a colorless solid. LC-MS (ESI),  $m/z$   
23  
24 356.0, 357.9  $[\text{M}+\text{H}]^+$ ;  $^1\text{H}$  NMR (400 MHz,  $\text{DMSO}-d_6$ )  $\delta$  7.92 (dd,  $J = 8.7, 6.0$  Hz, 1 H), 7.67 (dd,  
25  
26  $J = 10.5, 2.7$  Hz, 1 H), 7.52 (s, 1 H), 7.19 (td,  $J = 8.4, 2.7$  Hz, 1 H), 6.88 (q,  $J = 6.4$  Hz, 1 H),  
27  
28 6.68 (s, 2 H), 1.57 (d,  $J = 6.3$  Hz, 3 H).  
29  
30  
31  
32  
33

34 2- $\{(1R)$ -1-[(3-Amino-6-bromopyrazin-2-yl)oxy]ethyl}- $N$ -[(6-cyanoimidazo[1,2- $a$ ]pyridin-2-  
35  
36 yl)methyl]-4-fluoro- $N$ -methylbenzamide (**56**). To a mixture of compound **54** (0.217 g, 0.611  
37  
38 mmol), 2-[(methylamino)methyl]imidazo[1,2- $a$ ]pyridine-6-carbonitrile (**55**) (0.15 g, 0.673 mmol  
39  
40 - see Supporting Information) in DMF (20 mL) was added EDCI (0.176 g, 0.916 mmol), HOBT  
41  
42 (0.124 g, 0.916 mmol) and DIPEA (0.531 mL, 3.055 mmol) at  $-35$   $^\circ\text{C}$ . The resulting mixture was  
43  
44 stirred at  $-30$   $^\circ\text{C}$  for 30 min and stirred at room temperature overnight. TLC (petroleum  
45  
46 ether/EtOAc 1 : 1) indicated that the majority of the starting material had been consumed. The  
47  
48 mixture was diluted with EtOAc (50 mL) and  $\text{H}_2\text{O}$  (10 mL). The organic layer was separated and  
49  
50 the aqueous layer was extracted with EtOAc (2 x 20 mL). The organic layers were combined,  
51  
52 washed with brine (5 x 10 mL), dried over  $\text{Na}_2\text{SO}_4$ , filtered and concentrated *in vacuo* to give the  
53  
54  
55  
56  
57  
58  
59  
60

1  
2  
3 crude product, which was purified by prep. TLC to obtain **56** (150 mg, 46% yield) as a white  
4  
5 solid, which was used without further purification. LC-MS (APCI),  $m/z$  524/526  $[M+1]^+$ .  
6  
7

8 *(5R)-8-Amino-3-fluoro-5,19-dimethyl-20-oxo-5,18,19,20-tetrahydro-7,11-*

9  
10 *(azeno)pyrido[2',1':2,3]imidazo[4,5-h][2,5,11]benzoxadiazacyclotetradecine-14-carbonitrile*

11  
12 **(8m)**. To a mixture of **56** (0.15 g, 0.29 mmol), cataCXium A (22 mg, 0.058 mmol), *t*-AmOH (6  
13 mg, 0.06 mmol) and KOAc (140 mg, 1.43 mmol) in freshly distilled DMA (15 mL) was added  
14 Pd(OAc)<sub>2</sub> (7 mg, 0.029 mmol) at room temperature under a nitrogen atmosphere. The resulting  
15 mixture was sealed and heated at 110 °C for 12 h. LC-MS showed the reaction was complete.  
16  
17 The mixture was diluted with EtOAc (50 mL) and then washed with brine (4 x 10 mL). The  
18 organic layer was separated and dried over Na<sub>2</sub>SO<sub>4</sub>, filtered and concentrated *in vacuo* to give  
19 the crude product, which was purified by prep. TLC and then re-purified by reverse phase  
20 preparative HPLC to obtain **8m** (15.4 mg, 12% yield) as a yellow solid. LC-MS (APCI),  $m/z$  444  
21  
22  $[M+H]^+$ .  $[\alpha]_D^{23} = -177.0^\circ$  ( $c = 0.5$ , MeOH). <sup>1</sup>H NMR (400 MHz, DMSO-*d*<sub>6</sub>)  $\delta$  9.28 (s, 1 H), 8.03  
23 (s, 1 H), 7.79 (d,  $J = 9.3$  Hz, 1 H), 7.61 - 7.49 (m, 2 H), 7.42 (dd,  $J = 8.6, 5.8$  Hz, 1 H), 7.17 (dt,  $J$   
24 = 8.5, 2.6 Hz, 1 H), 6.80 (s, 2 H), 6.10 - 5.99 (m, 1 H), 4.51 - 4.32 (m, 2 H), 2.95 (s, 3 H), 1.67  
25 (d,  $J = 6.5$  Hz, 3 H).  
26  
27  
28  
29  
30  
31  
32  
33  
34  
35  
36  
37  
38  
39

40  
41 *2-{\(1R)-1-[3-Amino-6-bromopyrazin-2-yl]oxy\}ethyl\}-N-[2-bromo-4-(methylsulfonyl)benzyl]-*  
42  
43 *4-fluoro-N-methylbenzamide (58)*. To a mixture of compound **54** (0.300 g, 0.842 mmol), 1-[2-  
44 bromo-4-(methylsulfonyl)phenyl]-*N*-methylmethanamine (**57**) (0.291 g, 0.926 mmol - see  
45 Supporting Information) in DMF (5.61 mL) was added HATU (0.363 g, 0.926 mmol), followed  
46 by DIPEA (0.586 mL, 3.37 mmol) at room temperature. The mixture was stirred for 12 h, then  
47 diluted with EtOAc (50 mL), and washed with saturated Na<sub>2</sub>CO<sub>3</sub> solution (2 x 20 mL), and brine  
48 (20 mL). The organic layers were dried over Na<sub>2</sub>SO<sub>4</sub>, filtered and concentrated *in vacuo* to give  
49  
50  
51  
52  
53  
54  
55  
56  
57  
58  
59  
60

1  
2  
3 the crude product, which was purified by column chromatography on silica gel (0 – 75 %  
4 EtOAc/heptanes to afford **58** (487 mg, 94% yield) as a cream solid, which was used without  
5 further purification. LC-MS (APCI),  $m/z$  614.9/616.9/618.9 [M+H]<sup>+</sup>.  
6  
7

8  
9  
10 *(5R)-8-Amino-3-fluoro-5,17-dimethyl-13-(methylsulfonyl)-16,17-dihydro-7,11-*  
11 *(azeno)dibenzo[g,l][1,4,10]oxadiazacyclotetradecin-18(5H)-one (8i)*. Compound **58** (485 mg,  
12 0.787 mmol) was taken-up in THF (15.7 mL), and added to a vial containing B<sub>2</sub>pin<sub>2</sub> (600 mg,  
13 2.36 mmol) and K<sub>2</sub>CO<sub>3</sub> (544 mg, 3.94 mmol). The vial was sealed and the reaction mixture was  
14 bubbled with nitrogen before adding Pd(OAc)<sub>2</sub> (17.7 mg, 0.08 mmol) and cataCXium A (58 mg,  
15 0.157 mmol), and the reaction was heated to 80 °C for 6 h. The reaction was diluted with EtOAc  
16 (100 mL), washed with saturated NH<sub>4</sub>Cl solution (40 mL) and brine (40 mL), dried (MgSO<sub>4</sub>),  
17 filtered and concentrated. The crude product was purified twice by flash chromatography on  
18 silica gel eluting with EtOAc/heptanes (0 – 100 %) to afford **8i** (28 mg, 8% yield) as a white  
19 solid. LC-MS (APCI),  $m/z$  457.1 [M+H]<sup>+</sup>. <sup>1</sup>H NMR (400 MHz, DMSO-*d*<sub>6</sub>) δ 7.96 (s, 1 H), 7.93 -  
20 7.81 (m, 2 H), 7.77 (s, 1 H), 7.57 (d, *J* = 10.6 Hz, 1 H), 7.35 (dd, *J* = 8.1, 5.8 Hz, 1 H), 7.22 -  
21 7.10 (m, 1 H), 6.71 (br s, 2 H), 6.05 - 5.91 (m, *J* = 6.3 Hz, 1 H), 4.47 (d, *J* = 12.3 Hz, 1 H), 4.32  
22 (d, *J* = 12.3 Hz, 1 H), 3.29 (br s, 3 H), 2.87 (s, 3H), 1.66 (d, *J* = 6.0 Hz, 3 H).  
23  
24  
25  
26  
27  
28  
29  
30  
31  
32  
33  
34  
35  
36  
37  
38  
39  
40

41 *2-{(1R)-1-[(2-Aminopyridin-3-yl)oxy]ethyl}-N-[(5-cyano-1-methyl-1H-pyrazol-3-yl)methyl]-*  
42 *4-fluoro-N-methylbenzamide (61)*. To a solution of **59** (1 g, 2.8 mmol - see Supporting  
43 Information), **60** (573 mg, 3.07 mmol - see Supporting Information) and DIPEA (1.94 mL, 11.2  
44 mmol) in toluene (28 mL) was added Pd(P<sup>t</sup>Bu<sub>3</sub>)<sub>2</sub> (146 mg, 0.28 mmol). The reaction mixture was  
45 heated at 85 °C under 4 bar CO for 18 h, and then concentrated. The residue was taken-up in  
46 EtOAc, and the organic solution was washed with water and brine before being dried over  
47 MgSO<sub>4</sub>. The solution was filtered, concentrated, and the residue purified by column  
48  
49  
50  
51  
52  
53  
54  
55  
56  
57  
58  
59  
60

1  
2  
3 chromatography on silica gel (0 - 5% MeOH/ CH<sub>2</sub>Cl<sub>2</sub>) to afford **61** (1.08 g, 95% yield) as a  
4  
5 yellow gummy solid, which was used without further purification (contains *ca.* 15% *tert*-butyl  
6  
7 phosphine oxide by NMR). LC-MS (APCI), *m/z* 409.2 [M+H]<sup>+</sup>.  
8  
9

10  
11 *2-[(1R)-1-[(2-Amino-5-bromopyridin-3-yl)oxy]ethyl]-N-[(5-cyano-1-methyl-1H-pyrazol-3-*  
12  
13 *yl)methyl]-4-fluoro-N-methylbenzamide (62)*. To a -10 °C (ice-salt bath) solution of **61** (4.6 g, 11  
14  
15 mmol) in THF (115 mL) was added a solution of NBS (2 g, 11 mmol) in THF (35 mL). The  
16  
17 reaction was stirred for 1 h with the reaction temperature being maintained below 0 °C. LC-MS  
18  
19 indicated that ~35% of **61** remained. Solid NBS (682 mg, 3.83 mmol) was added in a portion-  
20  
21 wise manner with the reaction temperature being maintained below 0 °C. After being stirred for  
22  
23 15 min, LC-MS indicated that the reaction was complete. The reaction was diluted with EtOAc  
24  
25 (250 mL), washed with 1 M Na<sub>2</sub>CO<sub>3</sub> (2 x 100 mL) and brine (100 mL), dried over MgSO<sub>4</sub>,  
26  
27 filtered and concentrated. The residue was purified by column chromatography over silica gel  
28  
29 (eluting with 25 - 75% EtOAc/heptanes) to afford **62** as a slightly yellow solid, which was used  
30  
31 without any further purification. LC-MS (APCI), *m/z* 487.0/489.0 [M+H]<sup>+</sup>.  
32  
33  
34  
35

36  
37 *2-[(1R)-1-[[5-Bromo-2-(diacetylamino)pyridin-3-yl]oxy]ethyl]-N-[(5-cyano-1-methyl-1H-*  
38  
39 *pyrazol-3-yl)methyl]-4-fluoro-N-methylbenzamide (63)*. Compound **62** (6.38 g, 13.1 mmol) was  
40  
41 taken up in acetic anhydride (26.2 mL), and heated at 100 °C for 24 h. The reaction was allowed  
42  
43 to cool, and the solvent evaporated. The residue was azeotroped with toluene (2 x 100 mL)  
44  
45 followed by being dried in the vacuum oven to afford **63** (7.48 g, 100%) as a gummy solid,  
46  
47 which was used without any further purification. LC-MS (APCI), *m/z* 571.0/573.0 [M+H]<sup>+</sup>.  
48  
49

50  
51 *(10R)-7-Amino-12-fluoro-2,10,16-trimethyl-15-oxo-10,15,16,17-tetrahydro-2H-8,4-*  
52  
53 *(metheno)pyrazolo[4,3-*h*][2,5,11]benzoxadiazacyclotetradecine-3-carbonitrile (8k)*. KOAc  
54  
55 (6.43 g, 65.5 mmol) and **63** (7.48 g, 13.1 mmol) were combined in a 500 mL Parr vessel, and *t*-  
56  
57  
58  
59  
60

1  
2  
3 AmOH (1.82 mL) was added. Nitrogen was bubbled through the solution, followed by the  
4  
5 addition of Pd(OAc)<sub>2</sub> (294 mg, 1.31 mmol) and cataCXium A (968 mg, 2.62 mmol). The vessel  
6  
7 was sealed, and heated at 130 °C for 14 h. The solution was diluted with EtOAc (500 mL),  
8  
9 washed with water (2 x 250 mL) and brine (250 mL), and dried over MgSO<sub>4</sub>. The solution was  
10  
11 filtered, concentrated and the residue dissolved in MeOH (100 mL), and HCl (4 M in dioxane,  
12  
13 32.8 mL) added. The reaction was heated at 60 °C for 18 h. The solution was diluted with EtOAc  
14  
15 (250 mL), washed with saturated NaHCO<sub>3</sub> solution (3 x 100 mL) and brine (100 mL), and dried  
16  
17 over MgSO<sub>4</sub>. The solution was filtered, concentrated and the residue purified by column  
18  
19 chromatography over silica gel eluting with 15 - 100% EtOAc/heptanes to afford 2.3 g of a light  
20  
21 foamy solid. This solid was slurried in MeOH/water for 1 h. The solid was isolated by filtration,  
22  
23 and dried overnight in the vacuum oven to afford **8k** (2.25 g, 42% yield) as a colorless powder.  
24  
25  
26  
27  
28  
29 LC-MS (ESI) *m/z* 407 [M+H]<sup>+</sup>; <sup>1</sup>H NMR (400 MHz, CDCl<sub>3</sub>) δ 7.83 (d, *J* = 2.0 Hz, 1 H), 7.30  
30  
31 (dd, *J* = 9.6, 2.4 Hz, 1 H), 7.21 (dd, *J* = 8.4, 5.6 Hz, 1 H), 6.99 (dt, *J* = 8.0, 2.8 Hz, 1 H), 6.86 (d,  
32  
33 *J* = 1.2 Hz, 1 H), 5.75 - 5.71 (m, 1 H), 4.84 (s, 2 H), 4.45 (d, *J* = 14.4 Hz, 1 H), 4.35 (d, *J* = 14.4  
34  
35 Hz, 1 H), 4.07 (s, 3 H), 3.13 (s, 3 H), 1.79 (d, *J* = 6.4 Hz, 3 H); <sup>13</sup>C NMR (101 MHz, DMSO-*d*<sub>6</sub>)  
36  
37 δ 168.26, 163.09, 149.73, 144.18, 143.45, 138.97, 137.43, 132.13, 128.26, 127.51, 118.42,  
38  
39 115.42, 114.69, 114.55, 112.35, 110.66, 71.64, 47.56, 38.94, 31.66, 22.47; <sup>19</sup>F NMR (377 MHz,  
40  
41 DMSO-*d*<sub>6</sub>) δ -110.12 (note that it is negative relative to the reference CFCl<sub>3</sub> at 0 ppm for <sup>19</sup>F). ~  
42  
43 99.5% ee. [α]<sub>D</sub><sup>20</sup> = - 90.8° (c = 0.58, MeOH). Chiral analysis by SFC on a Whelk O-1 (*R,R*) 5  
44  
45 μm column (4.6 mm x 250 mm), which was eluted with 30% MeOH in CO<sub>2</sub> at 140 bar with a  
46  
47 flow rate of 3.0 mL/min. **8k** was eluted as peak 1 (R<sub>t</sub> = 2.99 min). Under these conditions, the  
48  
49 enantiomer elutes as peak 2 (R<sub>t</sub> = 4.33 min).  
50  
51  
52  
53  
54  
55  
56  
57  
58  
59  
60

1  
2  
3  
4  
5  
6  
7  
8  
9  
10  
11  
12  
13  
14  
15  
16  
17  
18  
19  
20  
21  
22  
23  
24  
25  
26  
27  
28  
29  
30  
31  
32  
33  
34  
35  
36  
37  
38  
39  
40  
41  
42  
43  
44  
45  
46  
47  
48  
49  
50  
51  
52  
53  
54  
55  
56  
57  
58  
59  
60

*Co-crystal Structures.* The co-crystal structures described for the first time here have been deposited to the Protein Data Bank (wwPDB) and the details of the methods used can be found under accession codes: 4CNH (wt ALK+**6b**, 1.84 Å), 4CMO (wt ALK+**6h**, 1.83 Å), 4CMT (wt ALK+**6i**, 1.73 Å), 4CMU (wt ALK+**8a**, 1.80 Å), 4CTC (wt ALK+**8j**, 2.14 Å), 4CLI (wt ALK+**8k**, 2.05 Å), 4CLJ (L1196M ALK+**8k**, 1.66 Å), 4CTB (wt ALK+**8m**, 1.79 Å). Non-phosphorylated human wt and L1196M mutant ALK kinase domain proteins (amino acids 1093-1411) were crystallized by the hanging drop vapor diffusion method at 13 °C by mixing equal volumes of a purified protein (11-15 mg/mL)-inhibitor (0.001 M) complex solution with a crystallization solution containing 0.15 M ammonium sulfate, 9 - 10.5% (w/v) monomethylether polyethylene glycol (MW 5 K) and 0.1 M MES buffer in a pH range of 5.3-5.6 for wt ALK, or 0.2 M lithium sulfate, 18% (w/v) polyethylene glycol (MW 5 K) and 0.1 M Tris at pH 8.5 for L1196M ALK.

31  
32  
33  
34  
35  
36  
37  
38  
39  
40  
41  
42  
43  
44  
45  
46  
47  
48  
49  
50  
51  
52  
53  
54  
55  
56  
57  
58  
59  
60

*Modeling Methods.* Compound **8a** was built from the crystal structure of compound **6h** using in house software. The resulting ligand was minimized in the rigid protein structure of co-crystal **6h** using the OPLS2001 force field.<sup>59</sup> The strain calculations were based on three calculations. A restrained minimization was performed for the given conformation where torsion angles were fixed with a force constant of 500 kJ/mol while bond lengths and angles were relaxed (energy A). Second, the given conformation was minimized to the nearest local minimum (energy B). Third, the given conformation was subjected to a Monte Carlo conformational search followed by minimization to locate the global energy minima (energy C). The minimization and searches were performed with BatchMin MCMM search routine using the OPLS2001 force field.<sup>60</sup> The local strain energy was reported as the difference of energies A and B, and the global strain energy was reported as the difference between energies A and C.

1  
2  
3 *Biochemical Kinase Assays.* Recombinant human wild-type and mutant ALK kinase domain  
4 proteins (amino acids 1093-1411) were produced in house using baculoviral expression, pre-  
5 activated *via* auto-phosphorylation with MgATP, and assayed for kinase activity using a  
6 microfluidic mobility shift assay, essentially as previously reported.<sup>24a,30</sup> The reactions contained  
7 1.3 nM wild-type ALK or 0.5 nM mutant ALK (appropriate to produce 15 - 20%  
8 phosphorylation of peptide substrate after 1 h reaction), 3  $\mu$ M 5-FAM-KKSRGDYMTMQIG-  
9 CONH<sub>2</sub>), 5 mM MgCl<sub>2</sub> and the K<sub>m</sub>-level of ATP in 25 mM Hepes, pH 7.1. The inhibitors were  
10 shown to be ATP-competitive from kinetic and crystallographic studies. The K<sub>i</sub> values were  
11 calculated by fitting the % conversion to a competitive inhibition equation (GraphPad Prism,  
12 GraphPad Software, San Diego, CA). ROS1 enzyme was assayed as described above for ALK,  
13 except using 0.25 nM recombinant human ROS1 catalytic domain (amino acids 1883-2347)  
14 (Invitrogen Inc., Carlsbad, CA). Kinase inhibitor selectivity was evaluated using a 206-kinase  
15 Invitrogen panel (Carlsbad, CA).  
16  
17  
18  
19  
20  
21  
22  
23  
24  
25  
26  
27  
28  
29  
30  
31  
32  
33

34 *Kinase selectivity enzyme assays.* The experiments were conducted at Invitrogen Inc.  
35 (Carlsbad, CA) at their Madison, WI, facility. Most of the kinase panel assays were the FRET-  
36 based Z'-LYTE® assays that employ a fluorescence-based, coupled-enzyme format, taking  
37 advantage of the differential sensitivity of phosphorylated and non-phosphorylated peptides to  
38 proteolytic cleavage. Other assays were the TR-FRET-based Adapta® assay format that employs  
39 an Alexa Fluor® 647 labeled ADP tracer and Eu-labeled anti-ADP antibody. The assays of the  
40 above two formats were normally conducted with ATP near the K<sub>M,app</sub>. Another assay format  
41 used were the TR-FRET-based LanthaScreen® binding assays utilizing an Alexa Fluor® tracer  
42 and Eu-labeled anti-tag antibody that binds to the respective affinity tag of the target kinase.  
43  
44  
45  
46  
47  
48  
49  
50  
51  
52  
53  
54  
55  
56  
57  
58  
59  
60

1  
2  
3 Details of these assay procedures are described on the vendor's website  
4  
5 (https://www.lifetechnologies.com/us/en/home/brands/invitrogen.html).  
6  
7

8 *Cell-based Phospho-ALK ELISA Assay.* Cells were seeded at 20,000 cells/well in a 96-well  
9  
10 plate in growth media with 0.5% serum and incubated overnight. Compounds were diluted in  
11  
12 media without serum, added to the cells, incubated for one hour, and then removed by aspirating  
13  
14 the media by vacuum suction. Cell lysates were generated and the phospho-ALK (Tyr1604)  
15  
16 levels were determined by using the PathScan® Phospho-ALK (Tyr1604) Chemiluminescent  
17  
18 Sandwich ELISA Kit (Cell Signaling, Cat#: 7020) or PathScan® Total ALK Chemiluminescent  
19  
20 Sandwich ELISA Kit (Cell Signaling, Cat#: 7084) as described in the manufacturer's protocol.  
21  
22 The IC<sub>50</sub> values were calculated by concentration-response curve fitting utilizing a four-  
23  
24 parameter analytical method.  
25  
26  
27  
28  
29  
30

### 31 ASSOCIATED CONTENT

32  
33  
34 **Supporting Information.** X-ray data and 207-member panel kinase selectivity data for  
35  
36 compound **8k**, and experimental data for compounds **6e, 6f, 6h, 9, 10, 17, 20, 21, 30, 31, 44, 45,**  
37  
38 **49, 50, 51, 55, 57, 59, 60, 69 – 75** not explicitly shown in Schemes. This material is available  
39  
40 free of charge *via* the Internet at <http://pubs.acs.org>.  
41  
42  
43  
44

### 45 AUTHOR INFORMATION

#### 46 **Corresponding Author**

47  
48  
49 \*e-mail: [ted.w.johnson@pfizer.com](mailto:ted.w.johnson@pfizer.com). phone: (858) 526-4683.  
50  
51

52  
53 \*e-mail: [paul.f.richardson@pfizer.com](mailto:paul.f.richardson@pfizer.com). phone: (858) 526-4290.  
54  
55  
56  
57  
58  
59  
60

## ACKNOWLEDGMENT

We are grateful to Kevin N. Dack, Patrick S. Johnson, Nick Puhalo and Andrew S. Cook for helpful discussion and synthesis of compounds **6b** and **6c**, Klaus Dress for data management and visualization, Curtis Moore (UCSD) and Alex Yanovsky for small molecule X-ray of **8k**, and Jeff Elleraas and Loanne Chung for purification work.

## ABBREVIATIONS

ABC, ATP-binding cassette; ADME, absorption, distribution, metabolism, and excretion; ALCL, anaplastic large cell lymphoma; ALK, anaplastic lymphoma kinase; ATP, adenosine triphosphate; BBB, blood-brain-barrier; BCRP, breast cancer resistance protein; BM, brain metastases; CAN, ceric ammonium nitrate; c-MET, mesenchymal epithelial transition factor; C<sub>eff</sub>, efficacious concentration; Cl<sub>u</sub>, unbound clearance; CNS, central nervous system; C<sub>tox</sub>, toxic concentration; CSF, cerebrospinal fluid; DIAD, diisopropyl azodicarboxylate; DIPEA, *N,N*-diisopropylethylamine (Hunig's base); DLBCL, diffuse large B-cell lymphoma; EDCI, 1-ethyl-3-(3-dimethylaminopropyl)carbodiimide; ER, efflux ratio; EML4, echinoderm microtubule associated protein-like 4; F, % bioavailability; FDA, Food and Drug Administration; G-loop, glycine loop; HACNT, heavy atom count; HATU, *O*-(7-azabenzotriazole-1-yl)-1,1,3,3-tetramethyluronium hexafluorophosphate; HBD, hydrogen bond donors; HLM, human liver microsome; HOBt, 1-hydroxybenzotriazole; HPLC, high-performance liquid chromatography; IC<sub>50</sub>, 50% inhibitory concentration; IMHB, intramolecular hydrogen bond; LipE, lipophilic efficiency; log D, octanol:buffer (pH 7.4) distribution coefficient; IMT, inflammatory myofibroblastic tumor; IR, insulin receptor; MDR, multiple drug resistance; MPO, multiple parameter optimization; MsCl, methanesulfonyl chloride; MW, molecular weight; NBS, *N*-

1  
2  
3 bromosuccinimide; NPM, nucleophosmin; NSCLC, non-small-cell lung carcinoma; pALK, Pgp,  
4 p-glycoprotein 1, phospho-ALK; PFS, progression-free survival; PK, pharmacokinetic; ROS1, c-  
5 ros oncogene 1; RTK, receptor tyrosine kinase; SASA, solvent accessible surface area; SBDD,  
6 structure based drug design; SFC, supercritical fluid chromatography; SOC, standard of care; wt,  
7 wild-type; TFAA, trifluoroacetic anhydride; wt, wild-type.  
8  
9  
10  
11  
12  
13  
14  
15  
16  
17

## 18 REFERENCES

- 19  
20 1. Morris, S. W.; Naeve, C.; Mathew, P.; James, P. L.; Kirstein, M. N.; Cui, X.; Witte, D. P.  
21 ALK, the chromosome 2 gene locus altered by the t(2;5) in non-Hodgkin's lymphoma, encodes a  
22 novel neural receptor tyrosine kinase that is highly related to leukocyte tyrosine kinase (LTK).  
23 *Oncogene* **1997**, *14* (18), 2175-2188.  
24  
25 2. Bilsland, J. G.; Wheeldon, A.; Mead, A.; Znamenskiy, P.; Almond, S.; Waters, K. A.;  
26 Thakur, M.; Beaumont, V.; Bonnert, T. P.; Heavens, R.; Whiting, P.; McAllister, G.; Munoz-  
27 Sanjuan, I. Behavioral and neurochemical alterations in mice deficient in anaplastic lymphoma  
28 kinase suggest therapeutic potential for psychiatric indications. *Neuropsychopharmacology* **2008**,  
29 *33* (3), 685-700.  
30  
31 3. Le Beau, M. M.; Bitter, M. A.; Larson, R. A.; Doane, L. A.; Ellis, E. D.; Franklin, W. A.;  
32 Rubin, C. M.; Kadin, M. E.; Vardiman, J. W. The t(2;5)(p23;q35): a recurring chromosomal  
33 abnormality in Ki-1-positive anaplastic large cell lymphoma. *Leukemia* **1989**, *3* (12), 866-870.  
34  
35 4. Morris, S. W.; Kirstein, M. N.; Valentine, M. B.; Dittmer, K. G.; Shapiro, D. N.;  
36 Saltman, D. L.; Look, A. T. Fusion of a kinase gene, ALK, to a nucleolar protein gene, NPM, in  
37 non-Hodgkin's lymphoma. *Science* **1994**, *263* (5151), 1281-1284.  
38  
39  
40  
41  
42  
43  
44  
45  
46  
47  
48  
49  
50  
51  
52  
53  
54  
55  
56  
57  
58  
59  
60

- 1  
2  
3  
4  
5  
6  
7  
8  
9  
10  
11  
12  
13  
14  
15  
16  
17  
18  
19  
20  
21  
22  
23  
24  
25  
26  
27  
28  
29  
30  
31  
32  
33  
34  
35  
36  
37  
38  
39  
40  
41  
42  
43  
44  
45  
46  
47  
48  
49  
50  
51  
52  
53  
54  
55  
56  
57  
58  
59  
60
5. Yu, H.; Huang, J. X.; Wang, C. F.; Shi, D. R. ALK-positive large B-cell lymphoma: report of a case. *Zhonghua Bing Li Xue Za Zhi* **2011**, *40* (8), 561-562.
6. Griffin, C. A.; Hawkins, A. L.; Dvorak, C.; Henkle, C.; Ellingham, T.; Perlman, E. J. Recurrent involvement of 2p23 in inflammatory myofibroblastic tumors. *Cancer Res.* **1999**, *59* (12), 2776-2780.
7. (a) Mano, H. Non-solid oncogenes in solid tumors: EML4-ALK fusion genes in lung cancer. *Cancer Sci.* **2008**, *99* (12), 2349-2355; (b) Shaw, A. T.; Solomon, B. Targeting anaplastic lymphoma kinase in lung cancer. *Clin. Cancer Res.* **2011**, *17* (8), 2081-2086; (c) Soda, M.; Choi, Y. L.; Enomoto, M.; Takada, S.; Yamashita, Y.; Ishikawa, S.; Fujiwara, S.; Watanabe, H.; Kurashina, K.; Hatanaka, H.; Bando, M.; Ohno, S.; Ishikawa, Y.; Aburatani, H.; Niki, T.; Sohara, Y.; Sugiyama, Y.; Mano, H. Identification of the transforming EML4-ALK fusion gene in non-small-cell lung cancer. *Nature* **2007**, *448* (7153), 561-566; (d) Kinoshita, K.; Oikawa, N.; Tsukuda, T. Anaplastic lymphoma kinase inhibitors for the treatment of ALK-positive cancers. *Annu. Rep. Med. Chem.* **2012**, *47*, 281-293.
8. (a) Azarova, A. M.; Gautam, G.; George, R. E. Emerging importance of ALK in neuroblastoma. *Semin. Cancer. Biol.* **2011**, *21* (4), 267-275; (b) Caren, H.; Abel, F.; Kogner, P.; Martinsson, T. High incidence of DNA mutations and gene amplifications of the ALK gene in advanced sporadic neuroblastoma tumours. *Biochem. J.* **2008**, *416* (2), 153-159; (c) Chen, Y.; Takita, J.; Choi, Y. L.; Kato, M.; Ohira, M.; Sanada, M.; Wang, L.; Soda, M.; Kikuchi, A.; Igarashi, T.; Nakagawara, A.; Hayashi, Y.; Mano, H.; Ogawa, S. Oncogenic mutations of ALK kinase in neuroblastoma. *Nature* **2008**, *455* (7215), 971-974; (d) George, R. E.; Sanda, T.; Hanna, M.; Frohling, S.; Luther, W.; Zhang, J.; Ahn, Y.; Zhou, W.; London, W. B.; McGrady, P.; Xue, L.; Zozulya, S.; Gregor, V. E.; Webb, T. R.; Gray, N. S.; Gilliland, D. G.; Diller, L.;

1  
2  
3 Greulich, H.; Morris, S. W.; Meyerson, M.; Look, A. T. Activating mutations in ALK provide a  
4 therapeutic target in neuroblastoma. *Nature* **2008**, *455* (7215), 975-978; (e) Janoueix-Lerosey, I.;  
5 Lequin, D.; Brugieres, L.; Ribeiro, A.; de Pontual, L.; Combaret, V.; Raynal, V.; Puisieux, A.;  
6 Schleiermacher, G.; Pierron, G.; Valteau-Couanet, D.; Frebourg, T.; Michon, J.; Lyonnet, S.;  
7 Amiel, J.; Delattre, O. Somatic and germline activating mutations of the ALK kinase receptor in  
8 neuroblastoma. *Nature* **2008**, *455* (7215), 967-970; (f) Mosse, Y. P.; Laudenslager, M.; Longo,  
9 L.; Cole, K. A.; Wood, A.; Attiyeh, E. F.; Laquaglia, M. J.; Sennett, R.; Lynch, J. E.; Perri, P.;  
10 Laureys, G.; Speleman, F.; Kim, C.; Hou, C.; Hakonarson, H.; Torkamani, A.; Schork, N. J.;  
11 Brodeur, G. M.; Tonini, G. P.; Rappaport, E.; Devoto, M.; Maris, J. M. Identification of ALK as  
12 a major familial neuroblastoma predisposition gene. *Nature* **2008**, *455* (7215), 930-935.  
13  
14  
15  
16  
17  
18  
19  
20  
21  
22  
23  
24  
25

26  
27 9. Tuma, R. S. ALK gene amplified in most inflammatory breast cancers. *J. Natl. Cancer*  
28 *Inst.* **2012**, *104* (2), 87-88.  
29

30  
31 10. Ren, H.; Tan, Z. P.; Zhu, X.; Crosby, K.; Haack, H.; Ren, J. M.; Beausoleil, S.; Moritz,  
32 A.; Innocenti, G.; Rush, J.; Zhang, Y.; Zhou, X. M.; Gu, T. L.; Yang, Y. F.; Comb, M. J.  
33 Identification of anaplastic lymphoma kinase as a potential therapeutic target in ovarian cancer.  
34 *Cancer Res.* **2012**, *72* (13), 3312-3323.  
35  
36  
37  
38

39  
40 11. (a) Bergethon, K.; Shaw, A. T.; Ou, S. H.; Katayama, R.; Lovly, C. M.; McDonald, N. T.;  
41 Massion, P. P.; Siwak-Tapp, C.; Gonzalez, A.; Fang, R.; Mark, E. J.; Batten, J. M.; Chen, H.;  
42 Wilner, K. D.; Kwak, E. L.; Clark, J. W.; Carbone, D. P.; Ji, H.; Engelman, J. A.; Mino-  
43 Kenudson, M.; Pao, W.; Iafrate, A. J. ROS1 rearrangements define a unique molecular class of  
44 lung cancers. *J. Clin. Oncol.* **2012**, *30* (8), 863-870; (b) Gainor, J. F.; Shaw, A. T. Novel targets  
45 in non-small cell lung cancer: ROS1 and RET fusions. *Oncologist* **2013**, *18* (7), 865-875.  
46  
47  
48  
49  
50  
51  
52  
53  
54  
55  
56  
57  
58  
59  
60

- 1  
2  
3  
4  
5  
6  
7  
8  
9  
10  
11  
12  
13  
14  
15  
16  
17  
18  
19  
20  
21  
22  
23  
24  
25  
26  
27  
28  
29  
30  
31  
32  
33  
34  
35  
36  
37  
38  
39  
40  
41  
42  
43  
44  
45  
46  
47  
48  
49  
50  
51  
52  
53  
54  
55  
56  
57  
58  
59  
60
12. (a) Cui, J. J.; Tran-Dube, M.; Shen, H.; Nambu, M.; Kung, P. P.; Pairish, M.; Jia, L.; Meng, J.; Funk, L.; Botrous, I.; McTigue, M.; Grodsky, N.; Ryan, K.; Padrique, E.; Alton, G.; Timofeevski, S.; Yamazaki, S.; Li, Q.; Zou, H.; Christensen, J.; Mroczkowski, B.; Bender, S.; Kania, R. S.; Edwards, M. P. Structure based drug design of crizotinib (PF-02341066), a potent and selective dual inhibitor of mesenchymal-epithelial transition factor (c-MET) kinase and anaplastic lymphoma kinase (ALK). *J. Med. Chem.* **2011**, *54* (18), 6342-6363; (b) Cui, J. J.; McTigue, M.; Kania, R.; Edwards, M. Case history : Xalkori<sup>TM</sup> (Crizotinib), a potent and selective dual inhibitor of mesenchymal epithelial transition (MET) and anaplastic lymphoma kinase (ALK) for cancer treatment. *Annu. Rep. Med. Chem.* **2013**, *48*, 421-434.
13. (a) Christensen, J. G.; Zou, H. Y.; Arango, M. E.; Li, Q.; Lee, J. H.; McDonnell, S. R.; Yamazaki, S.; Alton, G. R.; Mroczkowski, B.; Los, G. Cytoreductive antitumor activity of PF-2341066, a novel inhibitor of anaplastic lymphoma kinase and c-Met, in experimental models of anaplastic large-cell lymphoma. *Mol. Cancer Ther.* **2007**, *6* (12 Pt 1), 3314-3322; (b) Zou, H. Y.; Li, Q.; Lee, J. H.; Arango, M. E.; McDonnell, S. R.; Yamazaki, S.; Koudriakova, T. B.; Alton, G.; Cui, J. J.; Kung, P. P.; Nambu, M. D.; Los, G.; Bender, S. L.; Mroczkowski, B.; Christensen, J. G. An orally available small-molecule inhibitor of c-Met, PF-2341066, exhibits cyto-reductive antitumor efficacy through antiproliferative and antiangiogenic mechanisms. *Cancer Res.* **2007**, *67* (9), 4408-4417.
14. (a) Kwak, E. L.; Bang, Y. J.; Camidge, D. R.; Shaw, A. T.; Solomon, B.; Maki, R. G.; Ou, S. H.; Dezube, B. J.; Janne, P. A.; Costa, D. B.; Varella-Garcia, M.; Kim, W. H.; Lynch, T. J.; Fidias, P.; Stubbs, H.; Engelman, J. A.; Sequist, L. V.; Tan, W.; Gandhi, L.; Mino-Kenudson, M.; Wei, G. C.; Shreeve, S. M.; Ratain, M. J.; Settleman, J.; Christensen, J. G.; Haber, D. A.; Wilner, K.; Salgia, R.; Shapiro, G. I.; Clark, J. W.; Iafrate, A. J. Anaplastic lymphoma kinase

- 1  
2  
3 inhibition in non-small-cell lung cancer. *N. Engl. J. Med.* **2010**, *363* (18), 1693-703; (b) Shaw, A.  
4  
5 T.; Yeap, B. Y.; Solomon, B. J.; Riely, G. J.; Gainor, J.; Engelman, J. A.; Shapiro, G. I.; Costa,  
6  
7 D. B.; Ou, S. H.; Butaney, M.; Salgia, R.; Maki, R. G.; Varella-Garcia, M.; Doebele, R. C.;  
8  
9 Bang, Y. J.; Kulig, K.; Selaru, P.; Tang, Y.; Wilner, K. D.; Kwak, E. L.; Clark, J. W.; Iafrate, A.  
10  
11 J.; Camidge, D. R. Effect of crizotinib on overall survival in patients with advanced non-small-  
12  
13 cell lung cancer harbouring ALK gene rearrangement: a retrospective analysis. *Lancet Oncol.*  
14  
15 **2011**, *12* (11), 1004-1012.  
16  
17  
18  
19  
20 15. Pao, W.; Chmielecki, J. Rational, biologically based treatment of EGFR-mutant non-  
21  
22 small-cell lung cancer. *Nat. Rev. Cancer* **2010**, *10* (11), 760-774.  
23  
24  
25 16. Costa, D. B.; Kobayashi, S.; Pandya, S. S.; Yeo, W. L.; Shen, Z.; Tan, W.; Wilner, K. D.  
26  
27 CSF concentration of the anaplastic lymphoma kinase inhibitor crizotinib. *J. Clin. Oncol.* **2011**,  
28  
29 *29* (15), e443-445.  
30  
31  
32 17. Steeg, P. S.; Camphausen, K. A.; Smith, Q. R. Brain metastases as preventive and  
33  
34 therapeutic targets. *Nat. Rev. Cancer* **2011**, *11* (5), 352-363.  
35  
36  
37 18. Yamanaka, R. Management of refractory or relapsed primary central nervous system  
38  
39 lymphoma (Review). *Mol. Med. Rep.* **2009**, *2* (6), 879-885.  
40  
41  
42 19. Nguyen, T. D.; DeAngelis, L. M. Brain metastases. *Neurol. Clin.* **2007**, *25* (4), 1173-  
43  
44 1192, x-xi.  
45  
46  
47 20. Katayama, R.; Khan, T. M.; Benes, C.; Lifshits, E.; Ebi, H.; Rivera, V. M.; Shakespeare,  
48  
49 W. C.; Iafrate, A. J.; Engelman, J. A.; Shaw, A. T. Therapeutic strategies to overcome crizotinib  
50  
51 resistance in non-small cell lung cancers harboring the fusion oncogene EML4-ALK. *Proc. Natl.*  
52  
53 *Acad. Sci. U.S.A.* **2011**, *108* (18), 7535-7540.  
54  
55  
56  
57  
58  
59  
60

- 1  
2  
3  
4  
5  
6  
7  
8  
9  
10  
11  
12  
13  
14  
15  
16  
17  
18  
19  
20  
21  
22  
23  
24  
25  
26  
27  
28  
29  
30  
31  
32  
33  
34  
35  
36  
37  
38  
39  
40  
41  
42  
43  
44  
45  
46  
47  
48  
49  
50  
51  
52  
53  
54  
55  
56  
57  
58  
59  
60
21. (a) Kinoshita, K.; Kobayashi, T.; Asoh, K.; Furuichi, N.; Ito, T.; Kawada, H.; Hara, S.; Ohwada, J.; Hattori, K.; Miyagi, T.; Hong, W. S.; Park, M. J.; Takanashi, K.; Tsukaguchi, T.; Sakamoto, H.; Tsukuda, T.; Oikawa, N. 9-substituted 6,6-dimethyl-11-oxo-6,11-dihydro-5H-benzo[b]carbazoles as highly selective and potent anaplastic lymphoma kinase inhibitors. *J. Med. Chem.* **2011**, *54* (18), 6286-6294; (b) Kinoshita, K.; Ono, Y.; Emura, T.; Asoh, K.; Furuichi, N.; Ito, T.; Kawada, H.; Tanaka, S.; Morikami, K.; Tsukaguchi, T.; Sakamoto, H.; Tsukuda, T.; Oikawa, N. Discovery of novel tetracyclic compounds as anaplastic lymphoma kinase inhibitors. *Bioorg. Med. Chem. Lett.* **2011**, *21* (12), 3788-93; (c) Sakamoto, H.; Tsukaguchi, T.; Hiroshima, S.; Kodama, T.; Kobayashi, T.; Fukami, T. A.; Oikawa, N.; Tsukuda, T.; Ishii, N.; Aoki, Y. CH5424802, a selective ALK inhibitor capable of blocking the resistant gatekeeper mutant. *Cancer Cell* **2011**, *19* (5), 679-690.
22. Kuromitsu, S.; Mori, M.; Shimada, I.; Kondoh, Y.; Shindoh, N.; Soga, T.; Furutani, T.; Konagai, S.; Sakagami, H.; Nakata, M.; Ueno, Y.; Saito, R.; Sasamata, M.; Kudou, M. Anti-tumor activity of ASP3026. A novel and selective ALK inhibitor of anaplastic lymphoma kinase (ALK). In *Annual Meeting of the American Association for Cancer Research (AACR)*, Orlando, FL, 2011.
23. (a) Galkin, A. V.; Melnick, J. S.; Kim, S.; Hood, T. L.; Li, N.; Li, L.; Xia, G.; Steensma, R.; Chopiuk, G.; Jiang, J.; Wan, Y.; Ding, P.; Liu, Y.; Sun, F.; Schultz, P. G.; Gray, N. S.; Warmuth, M. Identification of NVP-TAE684, a potent, selective, and efficacious inhibitor of NPM-ALK. *Proc. Natl. Acad. Sci. U.S.A.* **2007**, *104* (1), 270-275; (b) Marsilje, T. H.; Pei, W.; Chen, B.; Lu, W.; Uno, T.; Jin, Y.; Jiang, T.; Kim, S.; Li, N.; Warmuth, M.; Sarkisova, Y.; Sun, F.; Steffy, A.; Pferdekamper, A. C.; Li, A. G.; Joseph, S. B.; Kim, Y.; Liu, B.; Tuntland, T.; Cui, X.; Gray, N. S.; Steensma, R.; Wan, Y.; Jiang, J.; Chopiuk, G.; Li, J.; Gordon, W. P.; Richmond,

1  
2  
3 W.; Johnson, K.; Chang, J.; Groessl, T.; He, Y. Q.; Phimister, A.; Aycinena, A.; Lee, C. C.;  
4  
5 Bursulaya, B.; Karanewsky, D. S.; Seidel, H. M.; Harris, J. L.; Michellys, P. Y. Synthesis,  
6  
7 structure-activity relationships, and in vivo efficacy of the novel potent and selective anaplastic  
8  
9 lymphoma kinase (ALK) inhibitor 5-Chloro-N2-(2-isopropoxy-5-methyl-4-(piperidin-4-  
10  
11 yl)phenyl)-N4-(2-(isopropylsulfonyl)phenyl)pyrimidine-2,4-diamine (LDK378) currently in  
12  
13 phase 1 and phase 2 clinical trials. *J. Med. Chem.* **2013**, *56* (14), 5675-5690.

14  
15  
16  
17 24. (a) Huang, Q.; Johnson, T. W.; Bailey, S.; Brooun, A.; Bunker, K. D.; Burke, B. J.;  
18  
19 Collins, M. R.; Cook, A. S.; Cui, J. J.; Dack, K. D.; Deal, J. G.; Deng, Y.-L.; Dinh, D.; Engstrom,  
20  
21 L. D.; He, M.; Hoffman, J.; Hoffman, R. L.; Johnson, P. S.; Kania, R. S.; Lam, H.; Lam, J. L.;  
22  
23 Le, P. T.; Li, Q.; Lingardo, L.; Liu, W.; Lu, M. W.; McTigue, M.; Palmer, C. L.; Richardson, P.  
24  
25 F.; Sach, N. W.; Shen, H.; Smeal, T.; Smith, G. L.; Stewart, A. E.; Timofeevski, S.; Tsaparikos,  
26  
27 K.; Wang, H.; Zhu, H.; Zhu, J.; Zou, H. Y.; Edwards, M. P. Design of potent and selective  
28  
29 inhibitors to overcome clinical anaplastic lymphoma kinase mutations resistant to crizotinib. *J.*  
30  
31 *Med. Chem.* **2014**, *57* (4), 1170-1187; (b) Johnson, T. W.; Bailey, S.; Burke, B. J.; Collins, M.  
32  
33 R.; Cui, J.J.; Deal, J.; Deng, Y.; Edwards, M. P.; He, M.; Hoffman, J.; Hoffman, R. L.; Huang,  
34  
35 Q.; Kania, R. S.; Le, P.; McTigue, M.; Palmer, C. L.; Richardson, P. F.; Sach, N. W.; Smith, G.  
36  
37 L.; Engstrom, L.; Hu, W.; Lam, H.; Lam, J. L.; Smeal, S.; Zou, H. Y. Is CNS availability for  
38  
39 oncology a no-brainer? Discovery of PF-06463922, a novel small molecule inhibitor of  
40  
41 ALK/ROS1 with preclinical brain availability and broad spectrum potency against ALK-resistant  
42  
43 mutations. In *Proceedings of the AACR-NCI-EORTC International Conference: Molecular*  
44  
45 *Targets and Cancer Therapeutics*, Boston, MA, 2013 Oct 19-23; AACR; Mol Cancer Abstract  
46  
47 nr PR10; (c) Zou, H. Y.; Engstrom, L. R.; Li, Q.; West-Lu, M.; Tang, R. W.; Wang, H.;  
48  
49 Tsaparikos, K.; Timofeevski, S.; Lam, J.; Yamazaki, S.; Hu, W.; Gukasyan, H.; Lee, N.;

1  
2  
3 Johnson, T. W.; Fantin, V.; Smeal, T. PF-06463922, a novel ROS1/ALK inhibitor, demonstrates  
4 sub-nanomolar potency against oncogenic ROS1 fusions and capable of blocking the resistant  
5 ROS1-G2032R mutant in preclinical tumor models. In *Proceedings of the AACR-NCI-EORTC*  
6  
7  
8  
9  
10  
11  
12  
13  
14  
15  
16  
17  
18  
19  
20  
21  
22  
23  
24  
25  
26  
27  
28  
29  
30  
31  
32  
33  
34  
35  
36  
37  
38  
39  
40  
41  
42  
43  
44  
45  
46  
47  
48  
49  
50  
51  
52  
53  
54  
55  
56  
57  
58  
59  
60

Johnson, T. W.; Fantin, V.; Smeal, T. PF-06463922, a novel brain-penetrating small molecule  
inhibitor of ALK/ROS1 with potent activity against a broad spectrum of ALK resistant mutations  
in preclinical models in vitro and in vivo. In *Proceedings of the AACR-NCI-EORTC*  
*International Conference: Molecular Targets and Cancer Therapeutics*; Boston, MA, 2013 Oct  
19-23; AACR; Mol Cancer Abstract nr C253.

25. Edwards, M. P.; Price, D. A. Role of physicochemical properties and lipophilic ligand  
efficiency (LipE or LLE) in addressing drug safety risks. *Annu. Rep. Med. Chem.* **2010**, *45*, 381-  
391.

26. (a) Freeman-Cook, K. D.; Hoffman, R. L.; Johnson, T. W. Lipophilic efficiency: the most  
important efficiency metric in medicinal chemistry. *Future Med. Chem.* **2013**, *5* (2), 113-115; (b)  
Ryckmans, T.; Edwards, M. P.; Horne, V. A.; Correia, A. M.; Owen, D. R.; Thompson, L. R.;  
Tran, I.; Tutt, M. F.; Young, T. Rapid assessment of a novel series of selective CB(2) agonists  
using parallel synthesis protocols: A lipophilic efficiency (LipE) analysis. *Bioorg. Med. Chem.*  
*Lett.* **2009**, *19* (15), 4406-4409.

27. Johnson, T. W.; Dress, K. R.; Edwards, M. Using the golden triangle to optimize  
clearance and oral absorption. *Bioorg. Med. Chem. Lett.* **2009**, *19* (19), 5560-5564.

- 1  
2  
3 28. Dose is proportional to (Ceff)(Clu)/F  
4  
5  
6 29. Gleeson, M. P. Generation of a set of simple, interpretable ADMET rules of thumb. *J.*  
7  
8 *Med. Chem.* **2008**, *51* (4), 817-834.  
9  
10 30. Bunnage, M. E.; Cook, A. S.; Cui, J. J.; Dack, K. N.; Deal, J. G.; Gu, D.; He, M.;  
11  
12 Johnson, P. S.; Johnson, T. W.; Le, P. T.; Palmer, C. L.; Shen, H. Heterocyclic derivatives for  
13  
14 the treatment of diseases. WO 2011/138751 A2, 2011.  
15  
16  
17 31. Feng, B.; Mills, J. B.; Davidson, R. E.; Mireles, R. J.; Janiszewski, J. S.; Troutman, M.  
18  
19 D.; de Morais, S. M. In vitro P-glycoprotein assays to predict the in vivo interactions of P-  
20  
21 glycoprotein with drugs in the central nervous system. *Drug Metab. Dispos.* **2008**, *36* (2), 268-  
22  
23 275.  
24  
25  
26  
27 32. Macrocycles in drug discovery have been defined as a ring system consisting of 12 or  
28  
29 more atoms.  
30  
31  
32 33. (a) Driggers, E. M.; Hale, S. P.; Lee, J.; Terrett, N. K. The exploration of macrocycles for  
33  
34 drug discovery--an underexploited structural class. *Nat. Rev. Drug Discov.* **2008**, *7* (7), 608-624;  
35  
36 (b) Giordanetto, F.; Kihlberg, J. Macrocyclic drugs and clinical candidates: what can medicinal  
37  
38 chemists learn from their properties? *J. Med. Chem.* **2014**, *57* (2), 278-295; (c) Marsault, E.;  
39  
40 Peterson, M. L. Macrocycles are great cycles: applications, opportunities, and challenges of  
41  
42 synthetic macrocycles in drug discovery. *J. Med. Chem.* **2011**, *54* (7), 1961-2004; (d) Vendeville,  
43  
44 S.; Cummings, M. D. Synthetic macrocycles in small-molecule drug discovery, *Annu. Rep. Med.*  
45  
46 *Chem.* **2013**, *48*, 371-386; (e) Breslin, H. J.; Lane, B. M.; Ott, G. R.; Ghoshe, A. K.; Angeles, T.  
47  
48 S.; Albom, M. S.; Cheng, M.; Wan, W.; Haltiwanger, R. C.; Wells-Knecht, K. J.; Dorsey, B. D.  
49  
50 Design, synthesis, and anaplastic lymphoma kinase (ALK) inhibitory activity for a novel series  
51  
52  
53  
54  
55  
56  
57  
58  
59  
60

1  
2  
3 of 2,4,8,22-tetraazatetracyclo[14.3.1.1<sup>3,7</sup>.1<sup>9,13</sup>]docosa-1(20),3(22),4,6,9(21),10,12,16,18-nonaene  
4  
5 macrocycles. *J. Med. Chem.* **2011**, 55 (1), 449-464.

6  
7  
8 34. Bertrand, T.; Kothe, M.; Liu, J.; Dupuy, A.; Rak, A.; Berne, P. F.; Davis, S.; Gladysheva,  
9  
10 T.; Valtre, C.; Crenne, J. Y.; Mathieu, M. The crystal structures of TrkA and TrkB suggest key  
11  
12 regions for achieving selective inhibition. *J. Mol. Biol.* **2012**, 423 (3), 439-453.

13  
14  
15 35. (a) He, H.; Lyons, K. A.; Shen, X.; Yao, Z.; Bleasby, K.; Chan, G.; Hafey, M.; Li, X.;  
16  
17 Xu, S.; Salituro, G. M.; Cohen, L. H.; Tang, W. Utility of unbound plasma drug levels and P-  
18  
19 glycoprotein transport data in prediction of central nervous system exposure. *Xenobiotica* **2009**,  
20  
21 39 (9), 687-693; (b) Kodaira, H.; Kusuhara, H.; Fujita, T.; Ushiki, J.; Fuse, E.; Sugiyama, Y.  
22  
23 Quantitative evaluation of the impact of active efflux by p-glycoprotein and breast cancer  
24  
25 resistance protein at the blood-brain barrier on the predictability of the unbound concentrations  
26  
27 of drugs in the brain using cerebrospinal fluid concentration as a surrogate. *J. Pharmacol. Exp.*  
28  
29 *Ther.* **2011**, 339 (3), 935-944; (c) Ohe, T.; Sato, M.; Tanaka, S.; Fujino, N.; Hata, M.; Shibata,  
30  
31 Y.; Kanatani, A.; Fukami, T.; Yamazaki, M.; Chiba, M.; Ishii, Y. Effect of P-glycoprotein-  
32  
33 mediated efflux on cerebrospinal fluid/plasma concentration ratio. *Drug Metab. Dispos.* **2003**, 31  
34  
35 (10), 1251-1254; (d) Redzic, Z. Molecular biology of the blood-brain and the blood-  
36  
37 cerebrospinal fluid barriers: similarities and differences. *Fluids Barriers CNS* **2011**, 8 (1), 3.

38  
39  
40  
41  
42  
43 36. Compounds with low intrinsic permeability (MDR BA <2.5) were removed from the  
44  
45 dataset to eliminate low MDR BA/AB false positives.

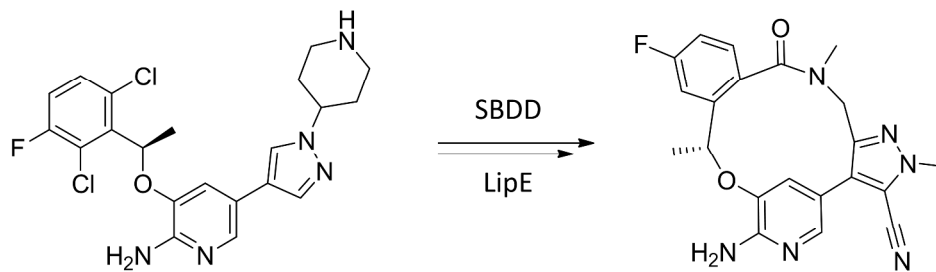
46  
47  
48 37. Wager, T. T.; Hou, X.; Verhoest, P. R.; Villalobos, A. Moving beyond rules: the  
49  
50 development of a central nervous system multiparameter optimization (CNS MPO) approach to  
51  
52 enable alignment of druglike properties. *ACS Chem. Neurosci.* **2010**, 1 (6), 435-449.

- 1  
2  
3 38. Kuhn, B.; Mohr, P.; Stahl, M. Intramolecular hydrogen bonding in medicinal chemistry.  
4  
5 *J. Med. Chem.* **2010**, *53* (6), 2601-2611.  
6  
7  
8 39. Solvent Accessible Surface Area values were calculated using Pipeline Pilot 8.5 "3D  
9  
10 Coords" and "Surface Area and Volume 3D" protocols.  
11  
12 40. Di, L.; Umland, J. P.; Chang, G.; Huang, Y.; Lin, Z.; Scott, D. O.; Troutman, M. D.;  
13  
14 Liston, T. E. Species independence in brain tissue binding using brain homogenates. *Drug*  
15  
16 *Metab. Dispos.* **2011**, *39* (7), 1270-1277.  
17  
18  
19 41. (a) Illuminati, G.; Mandolini, L. Ring closure reactions of bifunctional chain molecules.  
20  
21 *Acc. Chem. Res.* **1981**, *14* (4), 95-102; (b) Wessjohann, L. A.; Ruitjer, E.; Garcia-Rivera, D.;  
22  
23 Brandt, W. What can a chemist learn from nature's macrocycles ? - A brief, conceptual view.  
24  
25 *Mol. Divers.* **2005**, *9*, 171-186.  
26  
27  
28 42. Blankenstein, J.; Zhu, J. Conformation-directed macrocyclization reactions. *Eur. J. Org.*  
29  
30 *Chem.* **2005** (10), 1949-1964.  
31  
32  
33 43. Cheung, K. M. J.; Reynisson, J.; McDonald, E. A facile synthesis of pyrazoles with  
34  
35 multi-point structural diversity by 1,3-dipolar cycloaddition. *Tetrahedron Lett.* **2010**, *51* (45),  
36  
37 5915-5918.  
38  
39  
40 44. Campagna, F.; Carotti, A.; Casini, G. A convenient synthesis of nitriles from primary  
41  
42 amides under mild conditions. *Tetrahedron Lett.* **1977**, *18* (21), 1813-1815.  
43  
44  
45 45. Swamy, K. C. K.; Kumar, N. N. B.; Balaraman, E.; Kumar, K. V. P. Mitsunobu and  
46  
47 related reactions : Advances and applications. *Chem. Rev.* **2009**, *109* (6), 2551-2651.  
48  
49  
50 46. Merkul, E.; Schäfer, E.; Müller, T. J. J. Rapid synthesis of bis(hetero)aryls by one-pot  
51  
52 Masuda borylation-Suzuki coupling sequence, and its application to concise total syntheses of  
53  
54 meridianins A and G. *Org. Biomol. Chem.* **2011**, *9*, 3139-3141.  
55  
56  
57  
58  
59  
60

- 1  
2  
3  
4  
5  
6  
7  
8  
9  
10  
11  
12  
13  
14  
15  
16  
17  
18  
19  
20  
21  
22  
23  
24  
25  
26  
27  
28  
29  
30  
31  
32  
33  
34  
35  
36  
37  
38  
39  
40  
41  
42  
43  
44  
45  
46  
47  
48  
49  
50  
51  
52  
53  
54  
55  
56  
57  
58  
59  
60
47. Han, G.; Tamaki, M.; Hruby, V. J. Fast, efficient and selective deprotection of the tert-butoxycarbonyl (Boc) group using HCl/dioxane (4M), *J. Pept. Res.* **2001**, *58* (4), 338-341.
48. Chinchilla, R.; Nájera, C. Recent advances in Sonogashira reactions. *Chem. Soc. Rev.* **2011**, *40*, 5084-5121.
49. Sach, N. W.; Richter, D. T.; Cripps, S.; Tran-Dube, M.; Zhu, H.; Huang, B.; Cui, J.; Sutton, S. C. Synthesis of aryl ethers *via* a sulfonyl transfer reaction. *Org. Lett.* **2012**, *14* (15), 3886-3889.
50. Ackermann, L.; Vicente, R.; Kapdi, A. R. Transition metal-catalyzed direct arylation of (hetero)arenes by C-H bond cleavage. *Angew. Chem. Int. Ed.* **2009**, *48* (52), 9792-9826.
51. Kaur, H.; Heapy, A. M.; Brimble, M. A. Synthesis of the all-L cyclopentapeptides versicoloritides A, B, and C. *Synlett* **2012**, *23*, 2284-2288.
52. Hoffmann, R. W. Allylic 1,3-strain as a controlling factor in stereoselective transformations. *Chem. Rev.* **1989**, *89* (8), 1841-1860.
53. (a) LaPlante, S. R.; Edwards, P. J.; Fader, L. D.; Jakalian, A.; Hucke, O. Revealing atropisomer axial chirality in drug discovery. *ChemMedChem.* **2011**, *6* (3), 505-513; (b) Clayden, J.; Moran, W. J.; Edwards, P. J.; LaPlante, S. R. The challenge of atropisomerism in drug discovery. *Angew. Chem. Int. Ed.* **2009**, *48* (35), 6398-6401; (c) Van den Berge, E.; Pospíšil, J.; Trieu-Van, T.; Collard, L.; Robiette, R. Planar chirality of imidazole-containing macrocycles - Understanding and tuning atropisomerism. *Eur. J. Org. Chem.* **2011**, *33*, 6649-6655.
54. Carbonelle, A-C.; Zhu, J. A novel synthesis of biaryl-containing macrocycles by a domino Miyaura arylboronate formation: Intramolecular Suzuki reaction. *Org. Lett.* **2000**, *2* (22), 3377-3380.

- 1  
2  
3  
4  
5  
6  
7  
8  
9  
10  
11  
12  
13  
14  
15  
16  
17  
18  
19  
20  
21  
22  
23  
24  
25  
26  
27  
28  
29  
30  
31  
32  
33  
34  
35  
36  
37  
38  
39  
40  
41  
42  
43  
44  
45  
46  
47  
48  
49  
50  
51  
52  
53  
54  
55  
56  
57  
58  
59  
60
55. Brennführer, A.; Neumann, H.; Beller, M. Palladium-catalyzed carbonylation reactions of aryl halides and related compounds. *Angew. Chem. Int. Ed.* **2009**, *48* (23), 4114-4133.
56. Bensaid, S.; Laidaoui, N.; El Abed, D.; Kacimi, S.; Doucet, H. Palladium-catalysed direct arylations of heteroaromatics using more eco-compatible solvents pentan-1-ol or 3-methylbutan-1-ol. *Tetrahedron Lett.* **2011**, *52* (12), 1383-1387.
57. (a) Du, B.; Jiang, X.; Sun, P. Palladium-catalyzed highly selective *ortho*-halogenation (I, Br, Cl) of aryl nitriles *via* sp<sup>2</sup> C-H bond activation using cyano as directing group. *J. Org. Chem.* **2013**, *78* (6), 2786-2791; (b) Li, W.; Xu, Z.; Sun, P.; Jiang, X.; Fang, M. Synthesis of biphenyl-2-carbonitrile derivatives *via* a palladium-catalyzed sp<sup>2</sup> C-H bond activation using cyano as a directing group. *Org. Lett.* **2011**, *13* (6), 1286-1289.
58. (a) Lafrance, M.; Lapointe, D.; Fagnou, K. Mild and efficient palladium-catalyzed intramolecular direct arylation reactions. *Tetrahedron* **2008**, *64* (26), 6015-6020; (b) Lafrance, M.; Fagnou, K. Palladium-catalyzed benzene arylation: Incorporation of catalytic pivalic acid as a proton shuttle and a key element in catalyst design. *J. Am. Chem. Soc.* **2006**, *128* (51), 16496-16497.
59. Kaminski, G. A.; Friesner, R. A.; Tirado-Rives, J.; Jorgensen, W. L. Evaluation and Reparametrization of the OPLS-AA force field for proteins *via* comparison with accurate quantum chemical calculations on peptides, *J. Phys. Chem. B.* **2001**, *105*, 6474-6487.
60. Mohamadi, F., Richards, N. G. J., Guida, W. C., Liskamp, R., Lipton, M., Caufield, C., Chang, G., Hendrickson, T., Still, W. C. MacroModel - an integrated software system for modeling organic and bioorganic molecules using molecular mechanics, *J. Comput. Chem.* **1990**, *11*, 440-467.

## TABLE OF CONTENTS GRAPHIC



|                                  | crizotinib (1) | 8k     |
|----------------------------------|----------------|--------|
| ALK cell IC <sub>50</sub>        | 80 nM          | 1.3 nM |
| ALK-L1196M cell IC <sub>50</sub> | 843 nM         | 21 nM  |
| MDR BA/AB                        | 45             | 1.5    |